CHALMERS

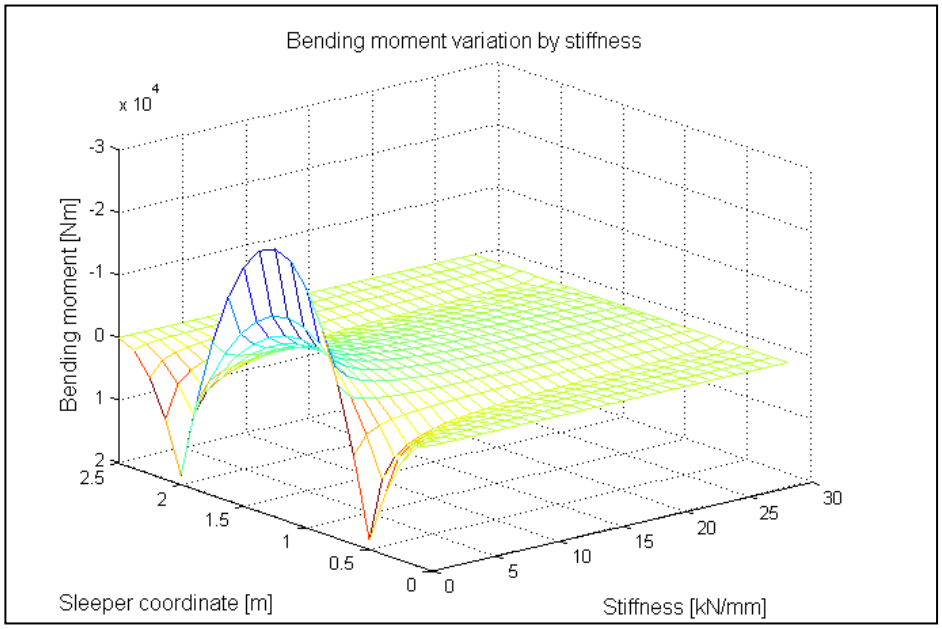

The Influence of Stiffness Variations in Railway Tracks

A study on design, construction, monitoring and maintenance procedures to obtain suitable support conditions for railway sleepers

Bachelor thesis in Civil Engineering

ALEXANDER ANDERSSON
HANNA BERGLUND
JOHAN BLOMBERG
OSCAR YMAN

Department of Applied Mechanics
Division of Dynamics
CHALMERS UNIVERSITY OF TECHNOLOGY
Göteborg, Sweden, 2013
Bachelor thesis 2013:02

..

BACHELOR THESIS 2013:02

The Influence of Stiffness Variation in Railway Track

A study on design, construction, monitoring and maintenance procedures to obtain suitable support conditions for railway sleepers

Bachelor thesis in Civil Engineering

ALEXANDER ANDERSSON
HANNA BERGLUND
JOHAN BLOMBERG
OSCAR YMAN

Department of Applied Mechanics
Division of Dynamics
CHALMERS UNIVERSITY OF TECHNOLOGY
Göteborg, Sweden 2013

The Influence of Stiffness Variation on Railway Track
A study on design, construction, monitoring and maintenance procedures to obtain suitable support conditions for railway sleepers
Bachelor thesis in Civil Engineering
ALEXANDER ANDERSSON
HANNA BERGLUND
JOHAN BLOMBERG
OSCAR YMAN

Bachelor thesis 2013:02
ISSN 1654-4676
Department of Applied Mechanics
Division of Dynamics
Chalmers University of Technology
SE-412 96 Göteborg
Sweden
Phone: + 46 (0)31-772 1000

Department of Applied Mechanics
Göteborg, Sweden 2013

.

Abstract

The railway is one of society's most important transportation systems today. It is effective in moving people and cargo long distances and is better for the environment than most other transportation alternatives available.

The focus of this report is on track support conditions. The report looks into how the awareness of variation in stiffness and support conditions can be used to plan and improve the track maintenance. The aim is to provide a better understanding of the problems with railway maintenance, how maintenance is performed today, why it is needed and how it is measured.

A literature review is made and interviews performed with representatives from the railway industry. These indicate that the maintenance performed today is mostly tamping and track lining and the maintenance mostly addresses acute problems and preventative measures, e.g. ballast- and shoulder cleaning, are not regularly performed. Due to the current short-term contract form, with maintenance entrepreneurs, the whole lifespan of the railway track is not considered when maintenance is planned.

Further the study shows that variations in support condition and differences in ballast stiffness influence the risk of damage on track and train. There are several ways to measure vertical stiffness. However this is not regularly performed in Sweden, neither at newly constructed railways nor at existing ones. If stiffness was evaluated for a track, it could be used as a parameter to optimize the maintenance by identifying local weaknesses along the track and detect hanging sleepers.

Simulations are made on a concrete sleeper, modelled as an Euler-Bernoulli beam on an elastic foundation, using MATLAB and CALFEM. Bending moments and vertical displacements are calculated for different support conditions and varying support stiffness. According to the simulations track stiffness has a large influence on sleeper bending moments and displacements. It can therefore be concluded that track stiffness is an important parameter regarding track durability.

Conclusions made from this research are that additional preventive maintenance should be performed to reduce the need of tamping and track lining and to raise the quality of the track. Stiffness measurements should be performed regularly and used as a tool when maintenance is planned.

Keywords: Railway sleeper, ballast, maintenance, track stiffness, stiffness variation, support condition

Sammanfattning

Järnvägen är idag ett av samhällets viktigaste transportsystem. Det är ett effektivt sätt att transportera människor och gods över långa avstånd och är miljömässigt bättre än många andra tillgängliga alternativ.

Fokus för denna rapport är på spårets upplagsförhållande. Rapporten ger en inblick i hur uppföljningen av styvhetsvariationer och upplagsförhållanden kan användas till att planera och förbättra spårunderhåll. Syftet är även att ge en ökad förståelse för de problem som finns inom järnvägsunderhåll, hur underhåll genomförs idag, varför det behövs och hur det mäts.

En litteraturstudie och intervjuer med representanter från företag i järnvägsbranschen har utförts. Dessa visar att det underhåll som utförs på järnvägen idag till största delen består av spårriktning. Vidare är den största delen av det underhåll som genomförs idag relaterat till brådskande problem. Förebyggande underhåll som till exempel ballastrening och bankettrensning, utförs inte regelbundet. På grund av de kortsiktiga kontraktsformer - med underhållsentreprenörer - som används idag tas normalt inte hela spårets livscykel i beaktande då underhåll planeras.

Studien visar även att variationer i upplagsförhållanden och ballaststyvhet ökar risken för skador på banor och tåg. Det finns flera sätt att mäta vertikal styvhet i spår. Emellertid används inte dessa regelbundet i Sverige, varken på nybyggda eller befintliga spår. Om styvhetsmätningar utfördes så skulle resultaten kunna användas för att optimera underhållet av järnvägar, till exempel genom att upptäcka lokala svagheter och hängande slipers i spåret.

Simuleringar på en betongsliper har gjorts i MATLAB och CALFEM där slipern är modellerad som en Euler-Bernoulli balk på ett fjädrande underlag. Böjande momentet och förskjutning beräknas med varierande styvhetsvärden för olika upplagsförhållanden. Enligt beräkningarna har styvheten stort inflytande på böjande moment och förskjutning hos en sliper. Därmed kan det konstateras att styvheten är en viktig parameter som påverkar hållbarheten av järnvägsspåret.

De slutsatser som kan dras och de rekommendationer som kan ges utifrån denna undersökning är att mer förebyggande underhåll bör utföras för att minska behovet av spårriktning och höja kvaliteten på spåret. Styvhetsmätningar bör göras regelbundet och kan då användas som ett verktyg vid planering av underhåll.

Contents

Figures

Tables

1 Introduction

Railway transport is currently one of the most important transportation systems. It is highly efficient in moving people and cargo long distances, and has better environmental features than most other available transportation alternatives.

Trafikverkets – The Swedish Transport Administration's – vision of travelling is that "all passengers will arrive easily, environmentally, friendly and safely (Trafikverket, 2012a)." Good construction and maintenance strategies relates to all three of these parameters. Failure to maintain good track geometry will increase wear of trains and tracks, which will lead to an increased deterioration, resulting in higher risks of accidents and delayed or cancelled trains. This will make Trafikverket unable to reach their vision of travelling.

In order to have a working railway, regular maintenance is required. In 2011 Trafikverket spent 3 billion SEK on railway maintenance compared to 6.7 billion SEK spent on road maintenance (Trafikverket, 2012a). These are large amounts and there is an interest in knowing how to spend this money on more efficient measures.

1.1 Project objectives

The intent of the report is to examine the support conditions below the rails, in particular below the sleepers, in form of vertical track stiffness. The report also looks into how an awareness of variations in stiffness and support conditions can be used to plan and improve track maintenance. A further aim is to provide a better understanding of some problems with maintenance of railway tracks, how maintenance is performed today, why it is needed and how the status is measured. To answer this, the report also covers how the railway and included components are designed.

The research will consist of a literature study and interviews with representatives mainly from Trafikverket, Abetong and Infranord. It also includes a computer model that analyses bending moments and displacements of a pre-stressed monoblock concrete sleeper subjected to different support conditions and varying track stiffness values.

1.2 Structure of a railway track

The main type of track used in Sweden is the ballasted railway track. It may be divided into two parts, substructure and superstructure.

1.2.1 Substructure

The substructure mainly consists of three layers; ballast, sub-ballast and sub-grade. They rest on the subsoil, normally the natural ground. The structure is shown in Figure 1.

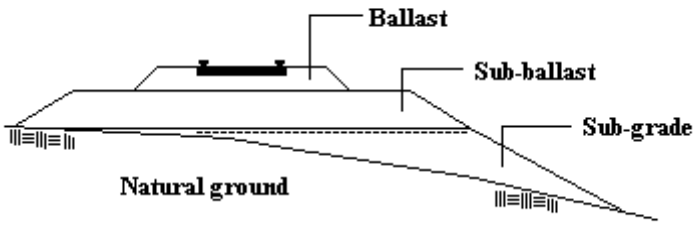

Figure 1 Substructure of a ballasted railway track

1.2.1.1 Ballast

The main functions of ballast are to secure track stability in all directions, prevent excessive sleeper movement, absorb static and dynamic loads and provide good drainage of water (Andersson and Berg, 2007). To secure these functions, high quality ballast in terms of good vertical and horizontal load bearing capacity is required (Banverket, 2002). Further, wear resistance, good elastic characteristics and a good drainage capacity are important. To meet these demands it is important to fill the ballast embankment. It is also important to use hard stone materials that carry large pore volumes and are angular. The angularity provides high friction between the grains.

In Sweden, ballast with a particle size of 32 – 64 mm is used to meet these requirements (Andersson och Berg, 2007). More finely grained ballast, 11 – 32 mm, is used in railway yards and sometimes at switches and crossings to get a more level surface. The stone material generally available as ballast in Sweden is hard, e.g. granite.

The ballast layer should be at least 300 mm thick below a sleeper and the layer on bridges should be at least 400 mm (Banverket, 2002). The ballast layer should not cover the sleeper surface in order to minimize the risk of ballast spray. It is also important for the sleeper ends to be surrounded with a sufficient amount of ballast to secure the sleeper's lateral stability.

1.2.1.2 Sub-ballast

The main purpose of the sub-ballast is to support the ballast and distribute traffic loads further down in the structure (Banverket, 2002). It also aids in draining the track and prevents small particles from the sub-grade to mix with the ballast. This requires a material with good properties regarding bearing capacity, stiffness and drainage. The employed material is usually sand or gravel with a particle size of 0 – 150 mm that should be frost resistant.

The sub-ballast layers depth depends on the frost depth in the ground, which means that it should be sufficiently thick to keep the underlying subgrade free from frost (Banverket, 2002). A minimum thickness of the sub-ballast layer is 800 mm, but it can be extended if the frost extends deeper. If the track is built on bedrock, 500 mm depth of sub-ballast layer is acceptable.

1.2.1.3 Sub-grade

The purpose of the sub-grade is to create a smooth foundation for the layers above. It usually contains filling materials like moraine or blasted stones. The requirements on the sub-grade are to resist settlements and softening, which can cause penetration of ballast, and to resist frost heave. The sub-grade should be located below the frost affected zone (Banverket, 2002).

1.2.2 Track superstructure

The superstructure consists of rail, railpad, fastening system and sleeper. All components interact and have different functions in the structure. The track superstructure is shown in Figure 2.

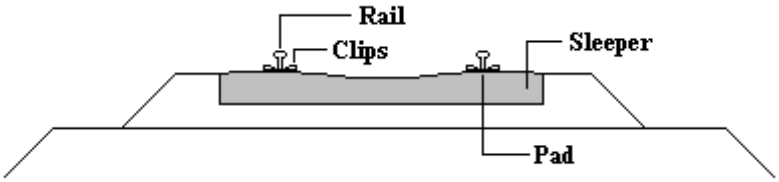

Figure 2 Track superstructure

1.2.2.1 Rail

The functions of the rails are to: distribute dynamic and static loads from vehicle to sleeper, function as a level surface for the wheel to minimize vibrations, offer sufficiently low friction in wheel/rail interaction, and resist thermal expansion (Andersson and Berg, 2007).

To secure the functions, there are high demands on the rails in the form of material hardness, with a high ultimate stress limit (Andersson and Berg, 2007). It should further have a good resistant to wear and good welding abilities. To meet these demands steel is used.

1.2.2.2 Sleeper

Four different types of sleeper materials are available: wood, steel, concrete and polymer. Mainly wood and concrete are used in Sweden.

The functions of a sleeper are to: transfer and distribute forces from the rails to the ballast, fix the track gauge, maintain adequate rail inclination, resist rail movements in all directions (horizontal, vertical and longitudinal).

It is important that the sleepers have a sufficiently regular spacing. Otherwise high stresses arise in the rails and an uneven load distribution to the ballast is created. This will cause faster degradation of the track. Main tracks in Europe usually have a distance of 600 to 650 mm between sleepers, but shorter distances exist (Andersson and Berg, 2007). One example is a

part of Malmbanan in northern Sweden that has a sleeper spacing of 500 mm. This is because it is dimensioned for the heavy traffic of the mining industry.

Recommended standard values for sleeper design is a length of 2500 or 2600 mm, a width of maximum 300 mm and height 200 – 230 mm at the rail seat (UIC, 2004). This is for standard gauge tracks and with the aim to reach requirements of acceptable ballast pressure and lateral stability. A standard sleeper should have a minimum weight of 240 kg and the recommended concrete strength class is C50/60 MPa.

1.2.2.3 Rail pads

The rail pad is a rubber or polymer pad that is located between sleeper and rail. Its function is to protect the sleeper from wear and dynamic loads from the rails by absorbing shocks and vibrations (Åström, 2011). It also prevents abrasion of the rail and the sleeper, resists lateral movements of the rail and electrically insulates the rails from each other. The rail pad is shown as the black part in the left picture of Figure 3.

Figure 3 Railpad and clips of type Pandrol FASTCLIP

1.2.2.4 Fastener system

The fastener system has different designs depending on type of sleeper. Example of concrete sleeper fastenings are Pandrol clips, type FASTCLIP, which are fastened to a steel plate (Åström, 2011). The steel plate is fixed to the sleeper in the casting process. See Figure 3.

The purpose of the fastener system is to secure the rail position. Desired properties are that the system should be elastic and able to absorb shocks and vibrations from the dynamic loads (Åström, 2011). It should also resist lateral, longitudinal and vertical movements of the rail. It is important that the system is easy to maintain.

2 Track stiffness and support conditions

The function of a sleeper depends on the support conditions and these are directly related to the track stiffness. Thus, track stiffness is an important track property. It is constituted from the properties of the substructure and superstructure.

Track stiffness, k [N/m], is generally defined as the quota of vertical force, Q [N], exerted on top of one rail and the vertical track displacement, y [m], see equation 1, (Li and Berggren, 2010). However, the track stiffness is not linear in that the track usually gets stiffer with increased loading (Oscarsson and Dahlberg, 1998).

$$k = \frac{Q}{y} \tag{1}$$

Relatively high track stiffness is desired to provide adequate track resistance to the applied loads and to limit the track deflection. This will in turn, reduce the track deterioration (Li and Berggren, 2010). Too high track stiffness and especially variations in stiffness on a stiff track can cause increased dynamic forces on sleepers, ballast and in the wheel-rail interface. This can lead to wear and fatigue damage on track components. Low track stiffness leads to large rail displacements and high bending moments in the rails. On the other hand, low track stiffness leads to better load distribution between sleepers and lowers train/track interaction forces (Berggren, 2009).

If the ballast, sub-ballast or subgrade is very soft the global track stiffness will be low (Li and Berggren, 2010). High global track stiffness generally corresponds to stiff ballast, sub-ballast, subgrade and rail pads. Conditions between these extremes are desired. Further, stiffness variations along the track should be avoided. Typical places along the track where variations in stiffness occur are in transition areas between bridges and embankment, at pile decks and at switches and turnouts (Dahlberg 2010). Measurements made in Sweden show that the stiffness can vary as much as 100 kN/mm in 25 meters of track.

In an effort to establish optimum global stiffness of track, researches on high-speed lines Madrid-Sevilla and Paris-Lyon have been done. Considerations regarding maintenance and dissipated energy from trains show that the optimum stiffness lies between 70 and 80 kN/mm per half sleeper (Lopez Pita et al, 2004). Calculations have been made by Li and Berggren (2010) using two different computer models, Zimmerman's and DIFF, to find the optimum global track stiffness. Three different values of global stiffness have been tested: 31.6, 78 and 171.5 kN/mm (per half sleeper). The result shows that 78 kN/mm gives a good compromise between rail displacements and strains in sleepers. This correlates well to the results mentioned above. Caution should be made to interpret these values to strict as different conditions appear, depending on the type of traffic or soil conditions etc.

2.1 Track settlement

Different support conditions along a railway track appear due to differences along the line in settlement rates of the ballast, the sub-ballast and the soil in and under the embankment. This is a natural process during the years directly after construction of a new railway and is induced by the weight of the structure. Later in the track life cycle, additional track settlements mostly appear due to the weight of passing trains, but it can also be an effect of

ballast fouling and the resulting frost sensitivity (Berggren, 2009). The mechanisms of ballast fouling are explained in section 3.3.1 of this report.

Due to uneven settlement of the substructure, support conditions will differ between sleepers along the track but also along a single sleeper. Here, settlement differences result in gaps and pockets of loosely packed ballast under a sleeper.

The settlement rate is influenced by the drainage capacity of the track. Poor drainage capacity increases the risk of damage due to frost, and water filled ballast will affect the stability of the track. Uncontrolled water flowing through the track will lead to increased erosion.

How to maintain track to ensure a good track standard is described in Chapter 3.

3 Maintenance of track and ballast bed

There are several different methods to perform maintenance of track and ballast bed. The purpose of the maintenance is to retain a stable ballast bed that provides a good support for the sleepers and consequently for the rails. A track that is regularly maintained should provide rather constant support conditions. By keeping a constant vertical level along the track, there will be less damage to the track and the passengers will experience a more comfortable journey. To this end, supporting materials must be properly arranged and compacted. The most common method to arrange the ballast is by tamping. This chapter will cover the main parts of how maintenance is performed.

3.1 Maintenance structure

The maintenance is planned according to two types of inspections which are regularly performed, safety- and maintenance inspections. Safety inspections are carried out several times a year and focus on safety related and more acute issues. A maintenance inspection is a part of a more long-term maintenance plan. How often inspections are made depends on the category of the track as discussed in section 3.4.3.

3.2 Types of maintenance

The following sub-chapters covers the most common maintenance methods used.

3.2.1 Track lining / Tamping

Track lining is the process of correcting the rail position in the track. Tamping is the most commonly used method for track lining and is usually performed by a maintenance train (Plasser & Theurer, 2012). The tamping machine has sensitive instruments to decide the position of the track. This data gives directives to the machine that will lift the track to correct the location, vertically and horizontally. The last step is to tamp the ballast underneath the sleepers to stabilize it. This is done by tamping tines that penetrate the ballast bed and compact the ballast under the sleepers using a squeezing movement, see Figure 4. Both tamping tines work with the same pressure and vibrate at a frequency of 35 Hz.

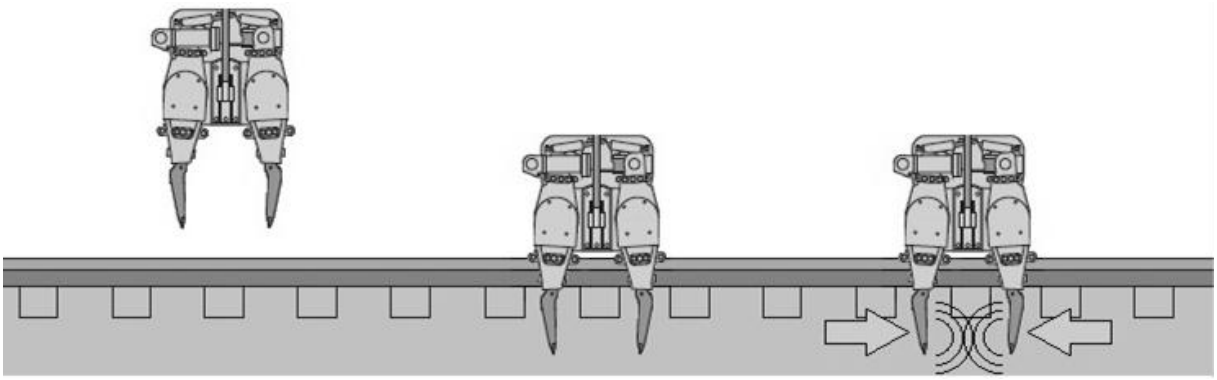

Figure 4 The tamping process (Lander and Pettersson, 2012)

It is often necessary to add more ballast to the embankment after tamping (Åhström, 2011). Directly after tamping the stability of the track is lowered since the ballast is less compacted

and the friction between the ballast stones are lower. The stability is restored after some time owing to the loading of passing train. A machine that vibrates the track in a manner similar to a train is sometimes employed to speed up this process.

3.2.2 Stoneblowing

An alternative method to tamping is stoneblowing[1]. Regular tamping compacts the existing ballast to get rid of voids under sleepers and to provide a correct track lining. The stoneblowing technique instead fills the gaps with new material to obtain the same results.

The stoneblowing machine performs a measurement run over the track distance where maintenance is needed[2]. During the measurement run the machines evaluates how much ballast that is required to add at each sleeper along the track. It then lifts the rails and sleepers 40 mm and injects the computed amount of single ballast; see Figure 5. The amount of ballast injected ranges from 0.5 to 22 kg per sleeper and side. The grain fraction used is 14 – 22 mm single ballast. After the injection, sleepers and rails are lowered and should now be at the desired level. The procedure is applicable everywhere, but specific values given above are employed in United Kingdom.

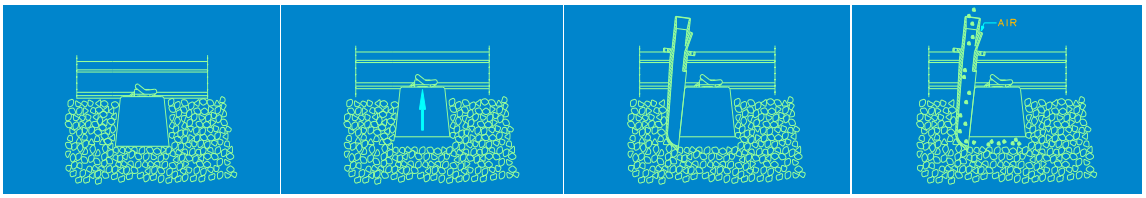

Figure 5 The stoneblowing process (Harsco Rail)

This technology was invented by the British Rail in the 1970s and developed during the following decades. It is in use in the UK since 1997 (Fair, 2003) and in Australia (Newman and Zarembski, 2008). The motivation for the invention was to overcome problems with a phenomenon called ballast memory (Fair, 2003). Problems with ballast memory can arise when maintenance with regular tamping is performed. With traffic loading the ballast returns to the same geometry it had before tamping. The ballast memory effect is stemming from a natural settlement process that can be quite fast, Figure 6 shows a measurement performed along a track and illustrates how an effect is measurable already after five days and how the ballast can return to its pre-maintained state within nine weeks.

[1] Personal communication: Roland Bång (Infranord) 2013-02-25
[2] Personal communication: Roland Bång (Infranord) 2013-02-25

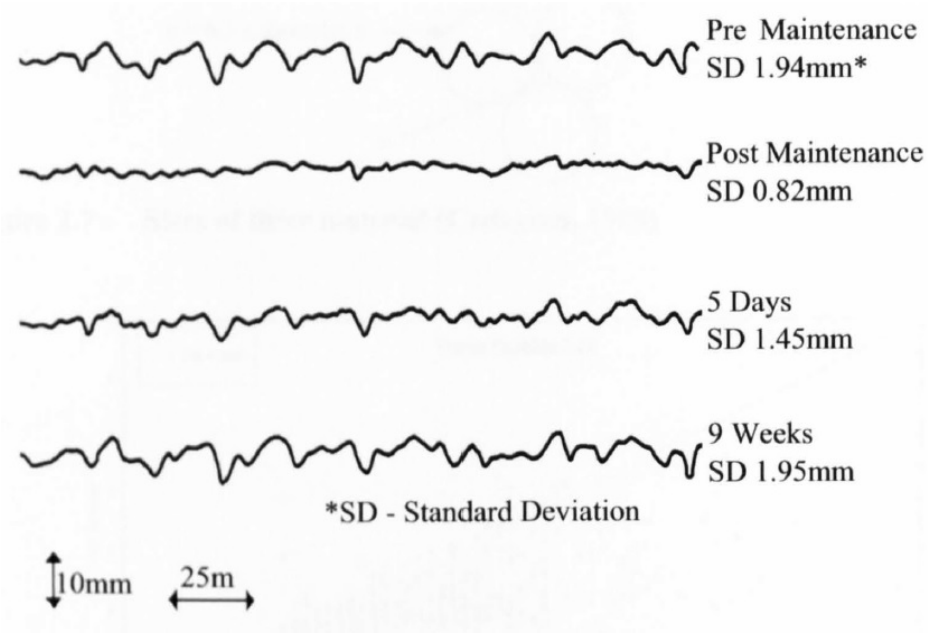

Figure 6 Examples of measurements along a track showing the phenomenon of ballast memory (Fair, 2003)

Ballast memory is not a problem when stoneblowing is used since it does not disturb the natural order among the ballast grains. Measurements done by Fair (2003) show that the positive effect on track geometry is longer-lasting when stoneblowing is used as compared to tamping. These measurements also show that results from stoneblowing are considerably worse at the beginning and end of the maintained sections.

Criticism against stoneblowing brings forth potential problem of adding so small fractions to the ballast. Normal criteria of ballast prescribe stone sizes between 32 – 64 mm. The concern is that the smaller stones may migrate into the ballast, block voids and due to this decrease the drainage capacity of the track. Research performed by Kay (1998) shows that there is no evidence of migration of stones of the size of 14 – 20 mm (Fair, 2003). The stones do not filter through the ballast layer since the voids between the ballast grains are smaller than 14 mm.

Another disadvantage with this maintenance method is that it cannot be used at switches and crossings if using track based machines (Fair, 2003). The maintenance can however be carried out manually at these locations.

3.2.3 Ballast cleaning

The purpose of ballast cleaning is to remove finer materials from the ballast (Hedström, 2002). The ballast cleaner picks up the top layer of the ballast to separate class one macadam (32 – 64 mm) from other material. The process used to separate the grain fractions is dry sieving. The ballast cleaner normally operates on a width of 4.2 m and down to 0.3 m below the sleepers. With different equipment the operating width can be adjusted between 3.7 m and 4.5 m. When the grain fractions are separated, the class one macadam is returned to the track while the other materials (0 – 32 mm) is transported away. The amount of fine material extracted varies from 0.3 to 1.0 m^3 per track meter. A daily production of about 1 km, produces about 500 – 1000 m^3 waste material. Figure 7 shows a ballast cleaner in action.

Figure 7 Ballast cleaner "Mud Mantis" in action (Infranord)

3.2.4 Shoulder cleaning

This type of maintenance is performed to increase the track's drainage ability (Hedström, 2002). Vegetation growing near the track will absorb large amounts of water, which will be stored in the track bed. When the ground freezes the water expands and may cause settlements during thawing. By removing the vegetation and finer grain fractions from the shoulder, the amount of water bound to the track bed is reduced. This will increase the track stability and load carrying capacity.

A shoulder cleaner remove additional railway embankment material, starting about 1 m from the rails and moving outwards (Hedström, 2002). The aim is to restore the normal section and remove some of the extra weight on the track bed. Shoulder cleaning is done mechanically and no chemicals are used. Figure 8 below shows the results.

Figure 8 Left: Before shoulder cleaning, right: after shoulder cleaning (Hedström, 2002)

3.2.5 Mechanical vegetation removal

The method used in mechanical vegetation removal is the same as in shoulder cleaning (Hedström, 2002). What separates them is that mechanical vegetation removal only removes the vegetation layer. The procedure does not require any brushwood removal to be performed.

The benefit is that it prevents regrowth of vegetation for a longer period than standard brushwood removal. This also improves the track's draining ability.

3.2.6 Ballast supplementing

When a track is short of ballast it is very important to refill it, otherwise the track may lose its lateral and longitudinal support (Infranord, 2012). This could be dangerous as it may e.g. cause sun kinks that might lead to derailments.

Ballast supplementing is often performed after track adjustments, track replacements and on newly constructed tracks. Since this method requires large amounts of macadam, special trains have been developed. One example is the QBX-train with ten wagons, each able to load 370 m^3 of material. The QBX-train is shown in Figure 9.

Figure 9 QBX-train at Infranord, (Infranord)

3.3 Deterioration of ballast and sleepers

Deterioration of ballast and sleepers is caused by exterior factors, such as vegetation and trainloads but also by maintenance actions. This part will cover some of these problems.

3.3.1 Deterioration caused by operational factors

Damage to the ballast bed is mostly caused by infiltration of smaller particles in-between ballast grains. These particles contaminate the ballast, which reduces the capacity of the ballast. This process is mostly known as "ballast fouling" (Sundvall, 2005). Five main causes as to why these particles are formed are: ballast breakdown, infiltration from the ballast surface, sleeper wear, infiltration from underlying granular layers and subgrade infiltration (Aursudkij, 2007). An example from North America is presented in Figure 10 to provide an overview of the relative influence of each of the five causes for ballast fouling.

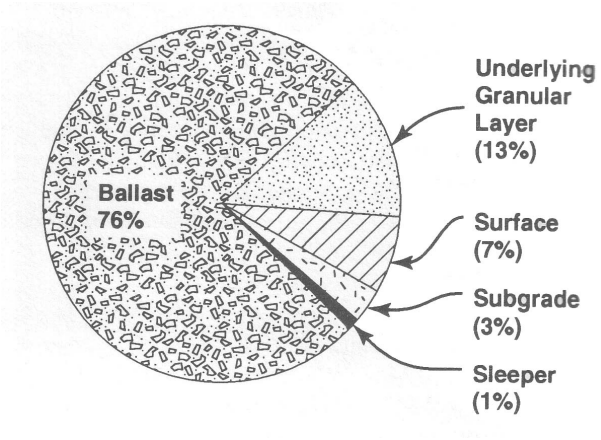

Figure 10 Sources of ballast fouling (Aursudkij, 2007)

The majority of the fouling is, according to Figure 10, due to the physical breakdown of the ballast, which is mainly caused by freeze thaw damages, chemical erosion and traffic loads (Aursudkij, 2007). Infiltration from the subgrade implies that e.g. clay is pushed upwards by the applied force from operational track. Infiltration from the ballast surface is debris brought by air, water and also generated by passing trains.

3.3.2 Deterioration caused by maintenance

Damage to the sleepers is more likely to come from lack of maintenance than by the tamping itself. The only damage that may occur is if the tines accidentally hit the sleepers or when ballast grains by accident are crushed between the tamping tines and sleeper[3].

Maintenance cause approximately 20 per cent of the total damage to the ballast, the major cause is the tamping procedure (Aursudkij, 2007). How maintenance is performed is very important to decrease ballast degradation.

The tamping procedure may damage the ballast due to the high force used when the tines are pushed into the ballast, and then vibrates the ballast. This may cause ballast stones to fracture which consequently will result in smaller particles (Aursudkij, 2007). Dust created by such a process can absorb water and reduce the water eduction. Finally it should be mentioned that both tamping and stoneblowing cause ballast breakage, Figure 11 shows the difference in produced particles.

[3] Personal communication: Roland Bång (Infranord) Meeting 2013-02-25

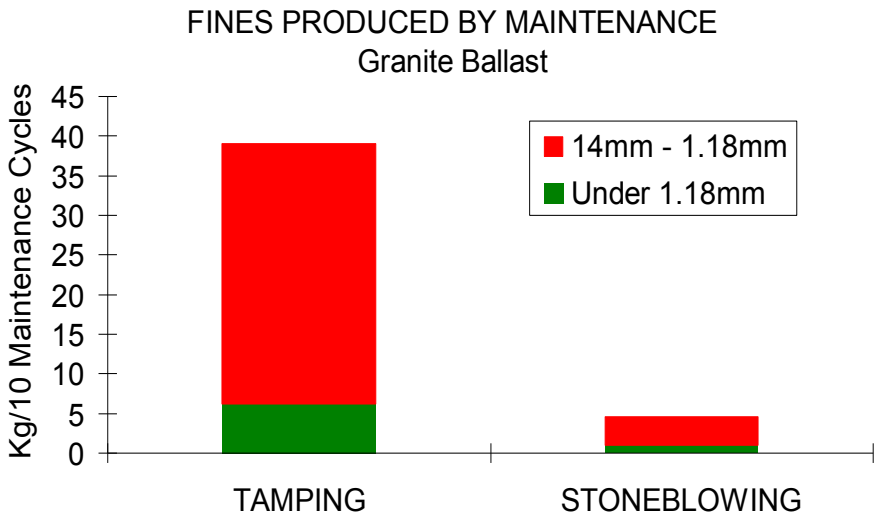

Figure 11 Comparison of damage to the ballast caused by Tamping and Stoneblowing (Harsco Rail)

3.4 Inspections and control of maintenance

This part will explain how the safety inspection procedures are carried out and how often they are performed. Trafikverket states "the target level for different tracks, regarding their technical status, should be determined by the amount of traffic but also by socio-economical aspects and demands from train operators" (Trafikverket, 2012a).

The purpose of safety surveys is to ensure that there are no defects on the track and the related equipment (Trafikverket, 2012b). Controls should detect the errors and prevent successive degradation of railway facilities.

3.4.1 Survey classes

To prescribe the amount of surveys and measurements Trafikverket uses five different survey classes (Trafikverket, 2012b). These classes are defined by several important factors. These factors are train speed, traffic load, type of traffic (e.g dangerous goods), climate- and environmental conditions, geotechnical conditions, technical structure, built-in function safety, age and quality of the track. The survey classes are denoted B1 to B5. Table 1 shows the survey classes and which operational conditions they correspond to.

Table 1 Trafikverkets survey classes (modified from Trafikverket, 2012b)

Survey class	Applied for:
B1	Speed: v ≤ 40 km/h
B2	Speed: 40 km/h < v ≤ 80 km/h Traffic load: ≤ 8 MGT/year (Million Gross Ton/year)
B3	Speed: 40 km/h < v ≤ 80 km/h Traffic load: > 8 MGT/year Speed: 80 km/h < v ≤ 140 km/h Traffic load: ≤ 8 MGT/year
B4	Speed: 80 km/h < v ≤ 140 km/h Traffic load: > 8 MGT/year Speed: v > 140 km/h Traffic load: ≤ 8 MGT/year
B5	Speed: v > 140 km/h Traffic load: > 8 MGT/year

Figure 12 provides a graphical description of the survey classes. The most important factors are train speed and traffic load, as manifested in Table 1.

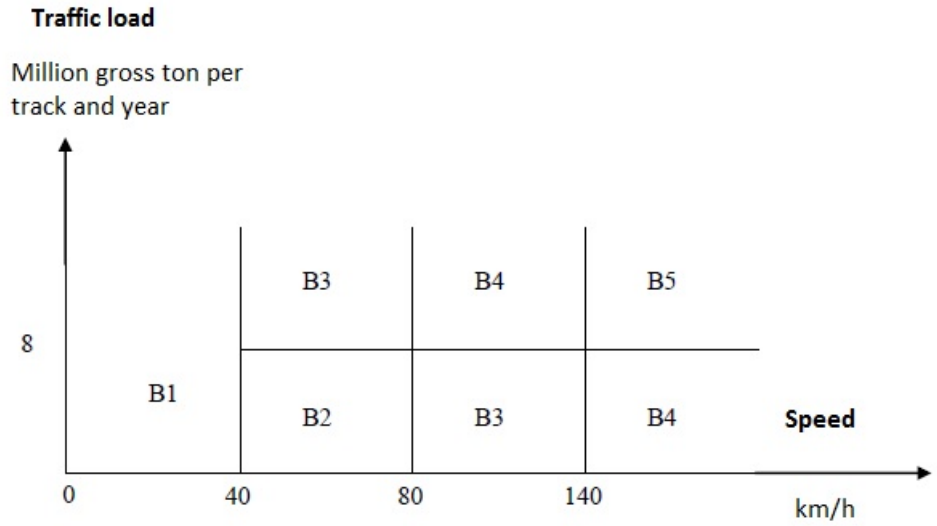

Figure 12 Survey classes diagram (modified from Trafikverket, 2012b)

3.4.2 Priority alternatives

In Sweden there are four different priority alternatives used when conducting safety surveys (Trafikverket, 2012b). These are used to determine how urgent the need for mitigating actions is. The alternatives provide a time indication and a specific time period when maintenance is to be carried out. The priority alternatives are:

A – This priority is the most urgent. A facility or equipment in this state result in an immediate risk of accidents or train disturbance. These remarks require immediate maintenance actions to be performed, otherwise the train traffic may have to be cancelled.

V – Remarks carrying this priority have to be corrected within two weeks.

M – Remarks of this priority have to be corrected within three months.

B – Remarks of this priority have to be corrected until the next safety inspection.

3.4.3 Number of inspections

The number of inspections per year varies between different survey classes and also depends on the equipment controlled. Table 2 shows the number of required safety inspections per year for components relevant to this study.

Table 2 Number of safety inspections per year for different track components (modified from Trafikverket, 2012b)

Type of facility	Number of safety inspections per year				
	B1	B2	B3	B4	B5
Track	1	2	3	3	3
Rail	1/4	1/3	1/2	1	1
Track switch – Track position	1	3	4	6	6
Embankment	1	2	2	2	2
Sub-ballast	1	2	3	3	3
Drainage and ditches	1	2	3	3	3

3.4.4 Inspection points for different components

3.4.4.1 Track/rail

The position of the track is examined and width, height- and side coordinates of the track are measured (Trafikverket, 2012b). The inspection can be performed manually or with an inspection wagon. Faults that must be dealt with immediately are such that might cause derailment.

The rail is inspected through ultrasonic testing (UT) to detect cracks (Trafikverket, 2012b). These tests are performed with either a machine-controlled UT-train or manually with a wagon mounted test equipment driven by hand. A visual survey of the rail profile is also performed to follow up on previous errors.

Sleepers are examined to locate cracks and sleepers out of position, which may affect the width and side position of the track (Trafikverket, 2012b). Lines with damaged concrete sleepers – DEF-sleepers – are examined through DEF-inspections to locate and monitor critical positions along the track.

The ballast is also inspected to ensure a correct ballast profile in accordance to current standards (Trafikverket, 2012b). Figure 13-15 shows minimum allowed dimensions of the ballast bed.

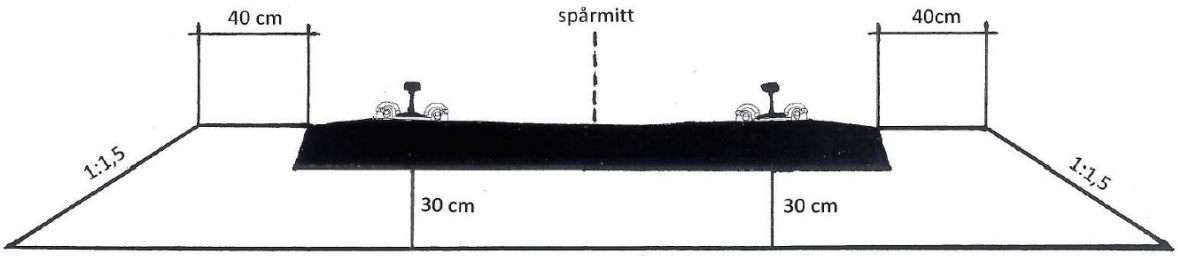

Figure 13 Ballast profile for radius - R ≥ 500m (Trafikverket, 2012b)

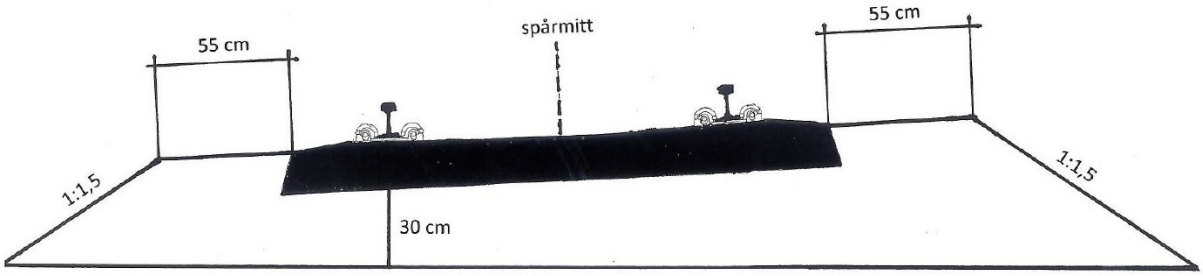

Figure 14 Ballast profile for radius - 400m ≤ R < 500m (Trafikverket, 2012b)

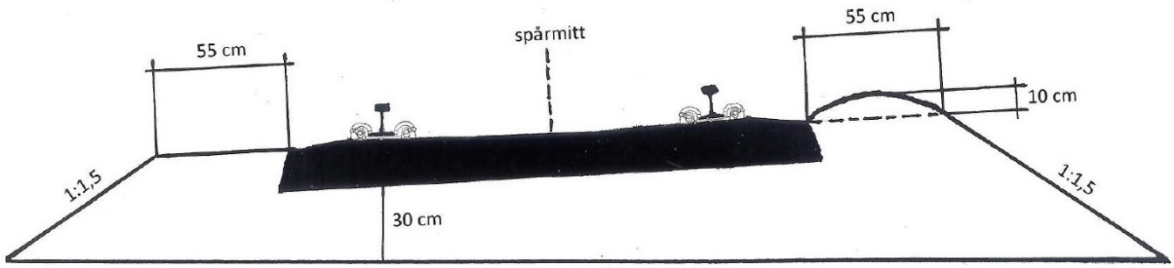

Figure 15 Ballast profile for radius - R < 400m (Trafikverket, 2012b)

3.4.4.2 Embankment

Embankments are inspected for erosion and cracks (Trafikverket, 2012b). Uncontrolled water leaks from the slopes are examined as well as movements and damage on any reinforcements along the embankment.

3.4.4.3 Sub-ballast

Settlements and movements from thawing are inspected (Trafikverket, 2012b). Erosion and other effects should not have affected the geometry of the track bed.

3.4.4.4 Drainage and ditches

If there are bodies of water or water flowing uncontrolled through the construction an examination is required to make sure the water does not cause stability issues and erosion damage to the embankment and nearby slopes (Trafikverket, 2012b).

3.4.5 Responsibility distribution

Trafikverket's guiding documents clearly states that the entrepreneur is responsible to correct inspection remarks of priorities A and V (Trafikverket, 2012b). M and B remarks are not included in the contract and should be handled by separate procurement or appended to the existing contract.

3.5 Stiffness measurements

Vertical track stiffness can be measured either at standstill in intervals or through rolling measurements (Berggren et al., 2005). Measurement information may be used to verify the quality of newly built or maintained track, show weak or variable spots when planning track upgrades regarding speed/axle load, or to plan maintenance.

3.5.1 Measurement of vertical stiffness at standstill

There are several methods to measure the vertical track stiffness at standstill. Four common methods in use are; instrumentation, impact hammer, falling weight deflectometer (FWD) and a track-loading vehicle TLV (Berggren, 2009).

Instrumentation is a method where the sleeper, or sleepers and rails, are instrumented with displacement devises or accelerometers to measure the effect of passing trains (Berggren, 2009). With a known axle load of a passing train, the stiffness can be evaluated. Results from this type of measurements are usually shown in load-deflection diagrams.

The impact hammer is a hand-held tool that is used to hit either the sleeper or the rails in a controlled manner. The head of the hammer is equipped with a device to measure the impulse load and the sleeper or rail is equipped with an accelerometer. The impulse of the hammer and the acceleration of the sleeper or rail are then evaluated. The method is suitable for investigations of noise, vibrations and interaction forces between wheel and rail (Berggren, 2009).

FWD is a method that often is used in the road industry to measure vertical stiffness. However with small modifications it can also be used in the railway industry (Brough et al., 2003). The principle of this method is to drop a known mass onto a plate. The deflection under the center of the plate is recorded automatically by sensors at various distances from the plate. The sensor directly under the plate measures the total deflection and the external sensors measure deflections in different layers (Hon, 2010).

The method of a TLV is to create a load on the track from the weight of the vehicle with help of hydraulic jacks. Most commonly the railheads are loaded. Alternatively the sleeper can be loaded with the rail decoupled (Berggren, 2009).

3.5.2 Rolling measurements of vertical stiffness

Rolling measurements has huge potential compared to standstill measurements as the railway track does not need to be closed and the measurements take less time due to the continuous measurement (Berggren, 2009). There are several types of rolling measurement vehicles around the world. The development has been done by rail organisations/authorities for example in China (CARS), USA (TTCI) and Sweden (Trafikverket). The vehicles are all unique with different design and systems to calculate the vertical stiffness.

Eurobalt II was a European research project for optimising ballasted tracks that was active 1997 – 2000. Several rail administrations, rail industries and universities were involved. In Eurobalt II, a prototype for rolling measurement was developed by Banverket, now Trafikverket (Berggren, 2009). The prototype showed a good potential and 2003 – 2004 a new vehicle, RSMV (Rolling Stiffness Measurement Vehicle), was constructed from a rebuilt freight wagon see Figure 16.

Figure 16 Rolling Stiffness Measurement Vehicle RSMV (Gomersson, 2012)

A common technique to evaluate the vertical stiffness with a rolling measurement vehicle is to measure the vertical displacement at one or two axles of the vehicle, where the static axle load is known (Berggren et al., 2005). The RSMV uses another measurement technique that is based on dynamic excitation of track through a single axle, see Figure 17. An advantage with this method is that static and dynamic measurements at low frequencies are possible. Low frequency measurements give values for the whole track system accounting all different layers in the soil, where as higher frequency measurements only consider the upper layers. The RSMV vehicle has a static axle load of 180 kN and a dynamic axle load of 60 kN, and can measure vertical stiffness in speeds up to 50 km/h (Berggren, 2009).

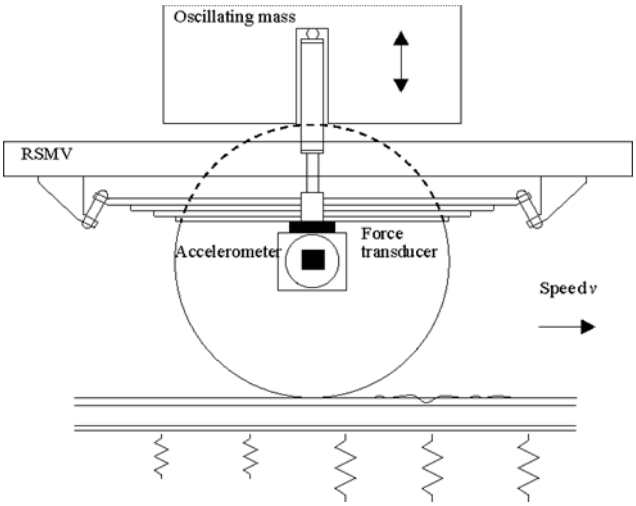

Figure 17 Overview of the RSMV technique (Gomersson, 2012)

The railway company Infranord manages the RSMV vehicle today and they are the only ones in Sweden to measure vertical stiffness when rolling[4]. The RSMV has so far mainly been used for research purpose and in projects related to increase axle load or speed on a railway line[5]. It is also possible to measure stiffness when rolling with a method called EVS (Eber Vertical Stiffness). This method can be used by Infranords track measurement vehicles IMV100.

[4] Personal communication: Jan Gomersson (Infranord) 2013-05-06
[5] Personal communication: Eric Berggren (Eber Dynamics) 2013-05-05

3.6 Discussion

This subchapter will discuss interesting topics within the maintenance chapter regarding tamping, stoneblowing, issues within the maintenance system and ways to maintain optimum support conditions regarding stiffness.

3.6.1 Comparison between tamping and stoneblowing

The purpose of tamping and stoneblowing is to create and maintain correct support conditions. In this analysis some of the benefits and disadvantages of these methods will be discussed.

Stoneblowing has been stated to double the life span of ballast[6]. Tamping break ballast grains and increases the need for ballast cleaning. Stoneblowing does not damage the ballast to the same extent, see Figure 11, but add grains of smaller size. An interesting question is how ballast cleaning works in combination with stoneblowing since ballast cleaning removes grain fractions between 0 – 32 mm and stoneblowing uses 14 – 22 mm grains. This may be a subject for further research.

The contact surface between the ballast and the sleeper increase with the smaller grains added by stoneblowing. The load distribution should improve with a larger contact surface. The friction between ballast and sleeper is increased but how the interaction and friction between the larger and the smaller grains is, as compared to the original ballast bed, is unknown. Loads on individual grains decreases as the contact surface increases but there are more relative movements between smaller grains. How this affects the damage rate of the ballast is unknown.

The stiffness of the track should be higher after stoneblowing than after tamping. With stoneblowing the natural compaction remains and more material is added but with tamping the ballast order is disturbed. The natural compaction is lost and the ballast is more loosely packed than before tamping.

The maintenance cost per mile is higher for the stoneblower than for tamping. However, considering the fact that stoneblowing is stated to give better results and maintenance can be performed less often, stoneblowing is cheaper (Newman and Zarembski, 2008).

This report cannot give any qualified advice as whether to recommend tamping or stoneblowing. The material regarding stoneblowing has been largely influenced by the corporations that provided the information. To draw further conclusions regarding the matter, more objective information is needed such as independent tests of stoneblowing in Sweden. A stoneblower can be rented and tested for a reasonable cost[7]. This should be compared to the total annual cost of railway maintenance of 3 billion SEK. It may be a reasonable investment since it may give more solid facts as how to improve maintenance and lower costs.

3.6.2 Issues within the maintenance system

A highly used track is today expected to have a technical life span of 40 years. The maintenance contracts usually last for five years. Most of the contractors are privately owned and driven by profit, which in the extent could lead to a loss of long-term perspective on track

[6] Personal communication: Roland Bång (Infranord) 2013-02-25
[7] Personal communication: Roland Bång (Infranord) 2013-02-25

maintenance. Contracts are specified to provide a functional track during the contract time and the entrepreneur should use preventive maintenance to keep the track in, at least, as good shape as at the start of the contract period. Such contracts are hard to formulate and follow up[8]. For this reason Trafikverket are planning to implement adjustable amounts in the contracts. This is in order to give the client more freedom to decide when and where to use specific maintenance measures.

When it comes to what type of, and when, maintenance is performed the various interviews with representatives from Infranord and Trafikverket provides a picture which is mostly similar from both entrepreneur and client side. The most common maintenance is tamping and track lining. Other types, such as ballast cleaning and shoulder cleaning, are rarely performed. It is logical to provide most resources to track lining since it has such big impact on the overall technical status of the track. However, this report has found that preventative measures, e.g. shoulder cleaning, also have a high impact on the track quality. This may render many of the issues that require track lining and thus reduce needed resources.

Regarding survey remarks the interviews, with Infranord and Trafikverket, provided some support to the initial concern that only the more urgent remarks where adjusted. According to Bång[9] Infranord's priorities mainly concern track lining and measures which make the day-to-day traffic possible. Their recourses are limited and the long-term preventive measures are simply not carried out. Cedergårdh[10] states that the system has developed towards correcting errors when safety tolerances are exceeded rather than correcting them at the maintenance limit. The maintenance limits are constructed to make the recourses used to maintenance more effectively spent. However, it has proven difficult in practice.

Today there are several ways to measure vertical stiffness, both at standstill and with a rolling vehicle. However this is not regularly performed in Sweden, neither at newly constructed railways nor at existing ones. This is despite stiffness being a very important parameter considering loads and strains on the track, and also regarding passenger comfort. There are no sets of regulations regarding required track stiffness today.

Other parameters that could be interesting to look into when planning maintenance are e.g maximum deflection and bending moments of sleepers and rails. In Chapter 5 these parameters are examined. According to Berggren[11] this might be considered as new parameters in future editions of railway regulations.

3.6.3 Ways to maintain optimum support conditions regarding stiffness

The best support condition today regarding stiffness is not clarified. It is stated 70-80 kN/mm is a favourable stiffness, this however is for a specific high speed track (Lopez Pita et al, 2004). The method should be applicable with modifications to Swedish conditions. This could in the extent generate guideline values for Swedish tracks. However the values might not be similar to those in Lopez Pita et al (2004) due to the differences in e.g. ballast quality, climate and axle load.

If an optimal stiffness value is acquired for a track, the best way to maintain it is to conduct stiffness measurements to obtain the overall stiffness status of the track. This data can be used

[8] Personal communication: Dan Cedergårdh (Trafikverket) 2013-04-29
[9] Personal communication: Roland Bång (Infranord) 2013-02-25
[10] Personal communication: Dan Cedergårdh (Trafikverket) 2013-04-29
[11] Personal communication: Eric Berggren (Eber Dynamics) 2013-05-05

to optimize the maintenance, partly by identifying specific locations of local weaknesses along the track – e.g. hanging sleepers – but also which type of measure is required to correct them.

Today's maintenance procedures affect the track stiffness but the connection is still not regarded. This report has presented several different maintenance procedures. It would be interesting to know more about how these affect the track stiffness and how the results look after some time, e.g. some weeks after tamping when the ballast probably has settled.

4 Effects of track stiffness variations

This chapter will explain and discuss how the track and track components are affected by stiffness variations and varying support conditions.

4.1 Effects of unsupported sleepers

Unsupported sleepers have a negative influence on the track deformation, which can have a significant effect on contact forces between wheel and rail (Recuero, Escalona and Shabana, 2011). They also cause increasing track damage and high stresses in some of the train component. Several unsupported sleepers in a region violate the safety requirements, e.g. due to an increased risk of sun kinks thus increasing the risk of derailment. They are also a source of variation in wheel acceleration, which influences passenger comfort (Li and Berggren 2010).

An interesting parameter related to track maintenance routines, and safety requirements, is how fast settlements occur and develop. One example of measurements performed in 1999 by Banverket, now Trafikverket, is presented in Figure 18. These measurements show that a gap under a sleeper can be amplified by 150 per cent in six months.

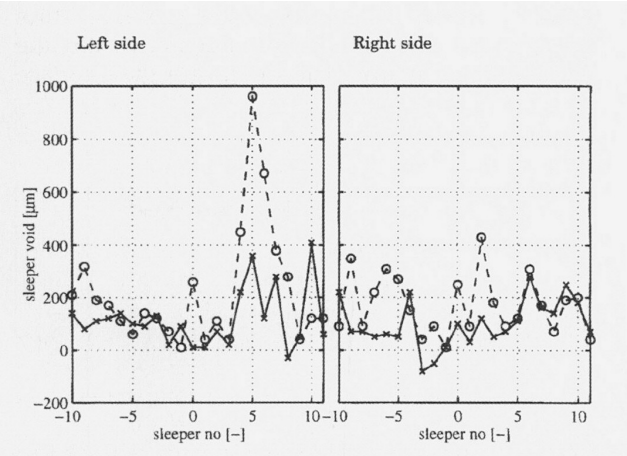

Figure 18 Size of gaps under sleepers, measured by Banverket in 1999. The solid line represents measurements preformed in January and the dashed line measurements preformed in August. (Olsson and Zackrisson, 2002)

4.2 Effects of support variations along the track

Studies of support variations along the track examine the effects of one or more completely unsupported sleepers on the immediate surrounding track and on the unsupported sleeper.

If one sleeper is totally unsupported – in this report also called voided or hanging sleeper – the surrounding sleepers need to carry a higher load. This corresponds to a higher quasi static load from passing trains and also an additional dynamic load due to the change in track stiffness caused by the hanging sleeper (Lundqvist and Dahlberg, 2005). This makes a sleeper close to a hanging sleeper likely to crack e.g. due to forces induced by wheel irregularities, such as wheel flats. A cracked sleeper does not significantly influence the general dynamic behaviour of the track, but it may have a reduced lifetime (Kumaran, Menon and Nair Krishnan, 2003).

The contact force between an unsupported sleeper and the ballast is close to zero when not loaded. However, the deflection of a voided sleeper is large (Lundqvist and Dahlberg, 2005). The stresses in the surrounding sleepers are higher than if all sleepers were well supported. The result in Lundqvist and Dahlberg (2005) shows that the effect of one hanging sleeper on the sleepers closest to it differs with the size of the gap between the sleeper and the ballast. When the gap is 1 mm, the effect on the supported sleeper before the unsupported one is that the contact force towards the ballast is stretched out in time since that sleeper needs to carry the load of the wheel longer and the displacements increase.

The sleeper after a hanging one is subjected to an increased dynamic load. For the case studied in Lundqvist and Dahlberg (2005), the sleeper/ballast contact force increased by 70 per cent at a speed of 90 m/s. There is also a significantly higher contact force between the rail and the wheel at the sleeper following the hanging one. This impact is caused by the imposed upward movement of the wheel when it has passed the deflection at the unsupported sleeper.

A track with hanging sleepers will also experience large bending moments in the rail, e.g. if the train has wheel flats (Innotrack, 2006). The dynamic effect caused by the impact from the wheel flat on the hanging sleeper gives high tension stresses in the rail. This can lead to rail breaks, especially if the rail has cracks.

It is also found in Lundqvist and Dahlberg (2005) that when the stiffness of the sleeper support differs, higher speeds will cause higher contact forces, larger deflections and higher levels of vibration. Vibrating sleepers may cause wear and degradation of the supporting ballast grains.

4.3 Effects of support variation along one sleeper

Interesting parameters to study is how the eigenfrequencies, vertical displacements, reaction forces and bending moment distributions are affected by the sleeper's support conditions. An example of stiffness variations under a sleeper can be seen in Figure 19. The black and white parts have different stiffness.

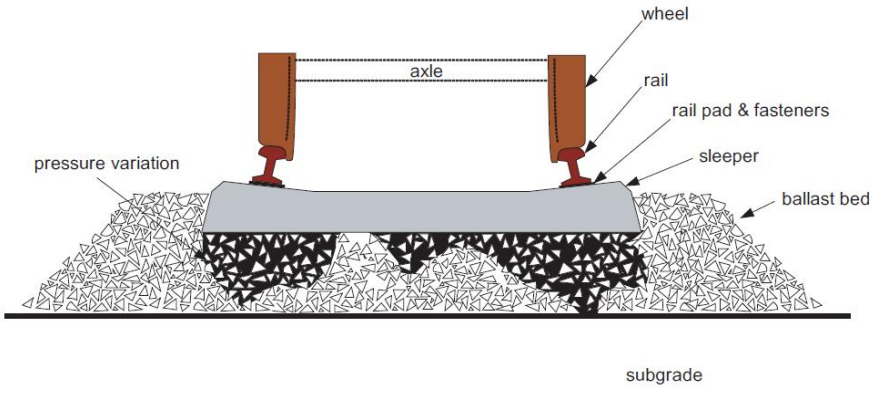

Figure 19 Example of variation in stiffness under a sleeper (Kaewunruen and Remennikov, 2007)

4.3.1 Vertical displacements, reaction forces and bending moments

In research by Li (2012) a static and a dynamic analysis on a single sleeper is performed. Four cases are considered. The first is a fully supported sleeper, the following two correspond to a

central void as described in section 5.3, Figure 22. Case two with low stiffness and case three with no support in the mid-section. The last case studied corresponds to the double side-central void see Figure 22.

The result of the static analysis shows that, of these four cases, the case with double side-central void is the worst-case scenario (Li, 2012). The most severe consequence of this support condition is that it induces tensile stresses in parts of the sleeper where the reinforcement is insufficient. Thereby the risk for cracking and tensile failure increases.

The dynamic analysis also singles out the double side-central void case as a worst-case scenario with longer lasting reaction forces, larger vertical displacement and significantly higher stresses (Li, 2012). For the case studied, the tensile stress in the mid-section of the sleeper is estimated to 10 MPa which is a much higher than the tensile capacity of concrete (3 MPa). That means that a sleeper experiencing such a support condition is likely to have damage caused by tensile stresses.

Notable is that Li (2012) did not study the case of a double hanging sleeper (see Figure 22). In research by Bolmsvik and Nielsen (2006) this case is studied. They state that stiffness variations under a sleeper have a negligible influence on the wheel/rail contact force, as long as the total ballast stiffness under the sleeper is constant. Bolmsvik and Nielsen (2006) also showed that very high bending moments arise in the mid-section of the sleeper when the sleeper is subjected to a support condition corresponding to double hanging.

It is stated by Lilja (2006) that variations in ballast stiffness is the second main parameter that influence variation in bending moment for the sleeper.

4.3.2 Eigenfrequencies of a sleeper

When a railway track is designed, eigenfrequencies of the whole system - train, super- and substructure - should be taken into account. If the eigenfrequencies of one of the components, and thereby the whole system, are changed due to variation in support conditions a situation can arise where the system is exposed to vibrations at the altered eigenfrequency. This can lead to increased deterioration of track and operating trains.

According to Kaewunruen and Remennikov (2007) a concrete railway sleeper mainly cracks when it vibrates at one of its eigenfrequencies. To know the eigenvalues and eigenmodes of a single railway sleeper and how they are affected by variation in support conditions is thus of interest.

An example of vibration modes for an in situ concrete sleeper can be seen in Figure 20 where (a) shows translation, (b) rotation, (c) the first bending mode, (d) the second bending mode, (e) the third bending mode, (f) the fourth bending mode and (g) the fifth bending mode.

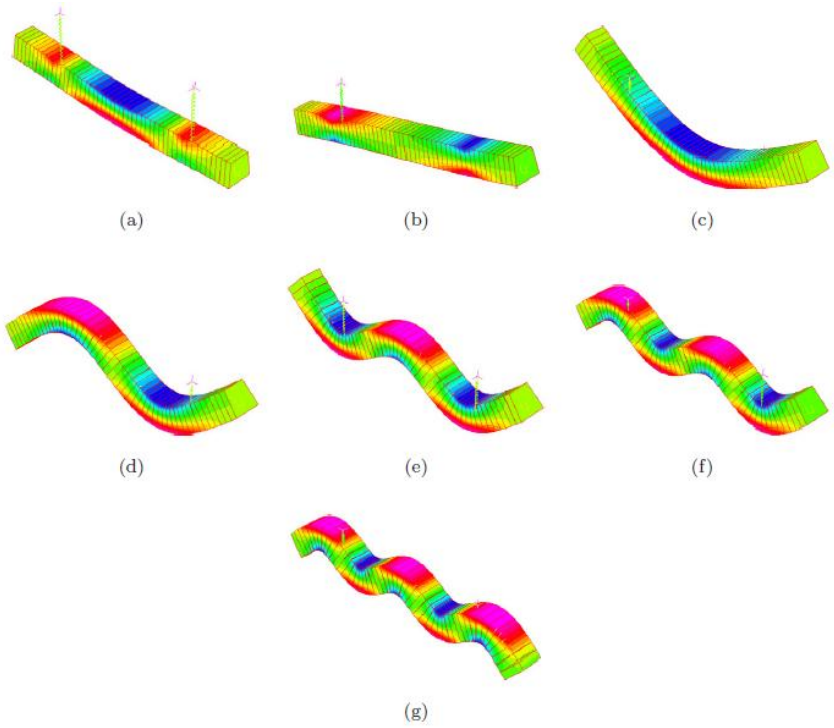

Figure 20 Eigenmodes of an ideal in situ concrete sleeper. (a) translation (b) rotation (c) 1st bending mode (d) 2nd bending mode (e) 3rd bending mode (f) 4th bending mode (g) 5th bending mod (Kaewunruen and Remennikov, 2007).

Rezaei and Dahlberg (2010) studied the case of a sleeper with support at both sides and a void in the middle. This support condition is preferred in practice since it minimizes the risk of having the detrimental case of a sleeper that is only supported in the middle. A simulation is made with different lengths of the gap. The results show that the vibration modes for this case are either translational or rotational and no combinations exist. The first eigenfrequency, associated to the translational mode shape, decreases when the length of the void increases. The first eigenfrequency decreases from 81.9 Hz, when fully supported, down to 58.6 Hz when the sleeper is completely hanging. The second eigenfrequency, associated to the rotational mode shape, also decreases when the length of the void increases but not as much as the first. There is a significant drop in the second eigenfrequency when the sleeper is almost hanging as compared with the case where it is totally voided. This difference is around 7.3 Hz.

The second case studied by Rezaei and Dahlberg (2010) is of a sleeper with lack of support at one end. In this case the vibrations are a combination of translation and rotation. Both the first and the second eigenfrequency decrease as the length of the voided pocket at the rail end widens.

The influence of the ballast stiffness on the first two eigenfrequencies of a railway sleeper is up to thirty per cent (Rezaei and Dahlberg 2010). Conclusions are made by Rezaei (2010) that the lower the eigenvalue, the more sensitive the bending mode is to variations in support conditions. Evaluations show that bending modes up to the fifth are sensitive to the size of the void between the ballast and the sleeper. Changes for higher modes are not significant.

4.4 Summary

It can be concluded from the study above that variation in support conditions influence the risk of damage on track and train. The problems with variation in support conditions can be

solved by proper maintenance. It is important that such maintenance is performed regularly since damage to the track that has become too severe requires larger and more expensive actions. It is also concluded that track stiffness is a part of the support conditions. Currently Trafikverket does not regularly consider track stiffness during construction or maintenance.

5 Computer simulations of a concrete sleeper

The most common computer models used to analyse the influence of differing support conditions on sleepers consists of a series of springs, and sometimes also dampers. They are distributed under the sleeper acting as the ballast bed and discrete springs at top of the sleeper at the positions of the rails. The sleeper itself can be modelled as different types of beams, a rigid body, three-dimensional elastic body, Euler-Bernoulli beam or a Rayleigh-Timoshenko beam, normally depending on the range of the frequency of the dynamic loads that is studied.

There also exist a number of different models, in which there, for example, is possible to see the effects of a moving train on unsupported sleepers and their surroundings.

5.1 Purpose

The purpose of this model is to show the bending moments and displacements given by different stiffness values. Those are chosen from previous studies made within the area. The bending moments and displacements are then used in an analysis. The results will determine which ballast stiffness distribution and support condition that affects the track the most during a train passage with a known pre-specified axle load.

5.2 Method

In this study a pre-stressed monoblock concrete sleeper with dimensions according to Table 3 is investigated. Since only the vertical displacement of the sleeper is investigated, the sleeper is modelled as a 2D Euler-Bernoulli beam on an elastic foundation, a Winkler bed, using MATLAB and its help tool CALFEM. The scripts are presented in Appendix 2, 3, 4 and 5. A schematic figure of the model is displayed in Figure 21.

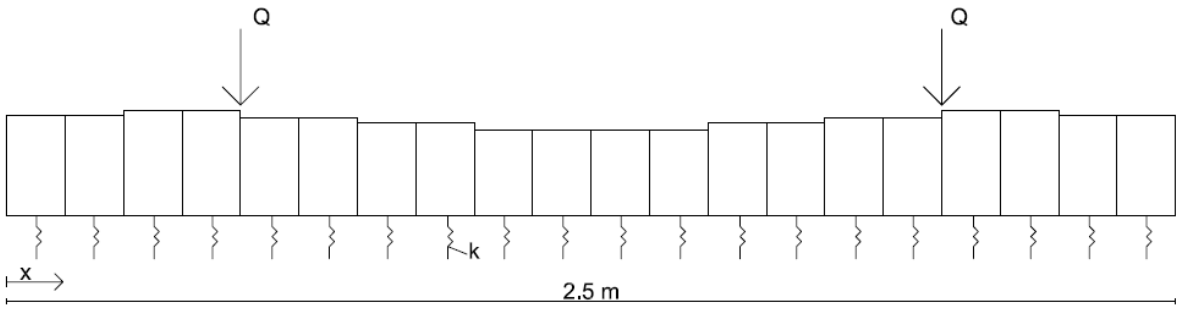

Figure 21 Schematic picture of the computer model

The model has restrained horizontal translation, since only vertical loading is considered in the analysis. The sleeper model is symmetric around the centre section and each half is divided into five sections with two elements in each section. The parameters used in the model can be seen in Table 3 (Kabo, 2004).

The module of elasticity, combined from reinforcement and concrete, is set to 40 GPa (Kabo, 2004). The length of the beam is set to 2.5 m based on the dimension of a standard pre-stressed concrete sleeper used in Sweden.

Table 3 Material and cross section properties (Kabo, 2004)

	Section 1	**Section 2**	**Section 3**	**Section 4**	**Section 5**
Module of elasticity, E (GPa)	40	40	40	40	40
Density, ρ (kg/m^3)	2400	2400	2400	2400	2400
Cross section area, A (m^2)	4.71×10^{-2}	4.83×10^{-2}	4.46×10^{-2}	3.78×10^{-2}	3.32×10^{-2}
Moment of inertia, I (m^4)	2.54×10^{-4}	2.75×10^{-4}	2.16×10^{-4}	1.31×10^{-4}	8.92×10^{-5}

The weight of the sleeper is considered as a uniform distributed load. The force from a train is modelled as two point loads, Q see equation (2), at the position of the rails see Figure 21.

$$Q = \frac{q*\varphi*g}{2} \qquad (2)$$

q – Static axle load
φ – Dynamic factor
g – Gravitational acceleration

The static axle load is set to 25 ton since it is the highest load allowed on standard tracks in Sweden. The dynamic load factor is set to 1.5 since speeds below 200 km/h is assumed (Bolmsvik and Nielsen, 2006). The gravitational acceleration is set to 9.81 m/s^2.

120, 186 and 252 kN/mm is used as stiffness values for a half sleeper. Those are realistic values according to Oscarsson (1998) and Lilja (2006). The stiffness values 78 and 40 kN/mm (for a half sleeper) are also investigated (Li and Berggren, 2010). The three first values are based on field measurements, where 186 kN/mm is the mean value and the other two values are calculated based on the realizations, which are three times the standard deviation far from the nominal value. The last two are based on a report by Li and Berggren (2010), where 78 kN/mm is considered ideal, and therefore interesting to test.

The connection between the stiffness underneath one element and the stiffness beneath the whole sleeper can be calculated as the total stiffness divided by the number of elements in the model. CALFEM calculates the bending moment at the nodes of each beam element, considering this, the sleeper is divided into 20 elements in the calculations to be accurate.

The different support conditions shown in Figure 22 are tested with the five different stiffness values discussed above distributed in the model according to Table 4. This is done to examine which one of the cases that can be considered the most severe. A second type of simulation is made where the sleeper at start is fully supported underneath and then the ballast stiffness is declining towards zero with a start value of 280 kN/mm. This is also done for the cases of double hanging sleeper and sleeper with a central void. The intention is to give an overview of the correlation between stiffness changes and bending moment and also to see if there is a notable change in stiffness when the stiffness is close to zero. The third type of simulation performed is made with a sleeper subjected to support conditions corresponding to double hanging and central void. The support stiffness in the void is set to zero and the remaining support stiffness is varied from soft to stiff, 10 kN/mm to 280 kN/mm. This is done to investigate what influence the stiffness of the supported part of the sleeper has in the case of a partially supported sleeper.

To calculate how the eigenfrequency varies with a decreasing stiffness the eigenvalue problem in equation 4, is solved in MATLAB for the general differential equation of motion in equation 5.

$$|\mathbf{K} - \lambda\mathbf{M}| = \mathbf{0} \tag{4}$$

$$[\mathbf{M}]\{\ddot{D}\} + [\mathbf{K}]\{D\} = \mathbf{0} \tag{5}$$

M – Mass matrix
K – Stiffness matrix
f – Load vector
D – Displacement vector
$\ddot{D}$ – Acceleration vector

5.3 Support conditions

The variation in ballast stiffness beneath one sleeper is generally stochastic. In some studies the sleepers are modelled as having stochastic support conditions but most studies focus on four to five situations generally considered being the most common. The ones that are used in these calculations can be seen in Figure 22 and are:

a) Centre void – the void is located in the middle of the sleeper and symmetrically expands to the sides.

b) Single hanging – the gap is at one end of the sleeper and expands towards the other end.

c) Double hanging – the sleeper is unsupported at both ends.

d) Side-central voids – the gaps are located both in the middle and at one side

e) Double side-central void – the sleeper is unsupported in the middle and at both sides.

f) Full support

These cases are examined considering varying stiffness. Other parameters that can differ but are not taken into account in this model are for example rail-pad stiffness, axle load and dynamic effects. However a dynamic load factor is accounted for.

A centre void, is to some extent (with the reservation that the centre void should ideally be supporting but with a lower stiffness than the remaining sleeper), desirable and is aimed at during construction and maintenance e.g. tamping.

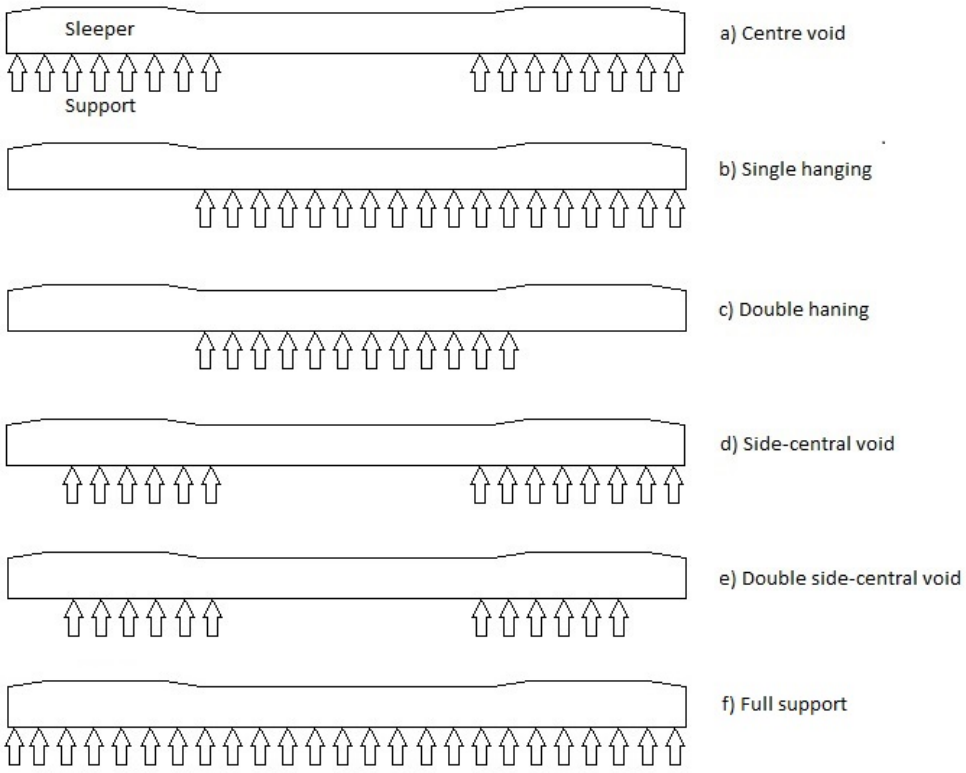

Figure 22 Different support conditions for sleepers used in the computer simulations

If a sleeper is partly hanging with a small gap, the loading of a passing train could cause the sleeper deflection to be larger than the gap size. That means that the sleeper will at first be hanging but with loading and subsequent deflection the sleeper will gradually gain support (Innotrack, 2006). It would be interesting to know the effects of this on the response from the track (in terms of stress evolution in the sleeper). However this is not taken into account in the computer analysis of this report.

The studied stiffness distribution and how the specific elements are supported for the various support conditions are presented in Table 4.

Table 4 Supported elements for each support condition

Support condition	1	2	3	4	5	6	7	8	9	10	11	12	13	14	15	16	17	18	19	20
a) Central void	■	■	■	■	■	■	■							■	■	■	■	■	■	■
b) Single hanging							■	■	■	■	■	■	■	■	■	■	■	■	■	■
c) Double hanging							■	■	■	■	■	■	■	■						
d) Side-central void			■	■	■	■	■							■	■	■	■	■	■	■
e) Double side-central void			■	■	■	■	■							■	■	■	■	■		
f) Full support	■	■	■	■	■	■	■	■	■	■	■	■	■	■	■	■	■	■	■	■

■ Supported element

5.4 Results

The results from the simulations are presented in the following sub-chapter.

5.4.1 Results from analyses of different support conditions

Calculated maximum bending moments are shown in Table 5 where the rail seats are located at 0.5 and 2 m from the left end of the 2.5 m long sleeper. The bending moment distribution for the six different cases when the stiffness is 78 kN/mm is shown in Figure 24 – 29. For further moment distributions and vertical displacements see Appendix 3.

Table 5 Maximum moment and position (see Figure 21) of maximum moment for the different support conditions and stiffness values.

Stiffness	40 kN/mm		78 kN/mm		120 kN/mm		186 kN/mm		252 kN/mm	
Support condition	Maximum moment [kNm]	Position [m]	Maximum moment [kNm]	Position [m]	Maximum moment [kNm]	Position [m]	Maximum moment [kNm]	Position [m]	Maximum moment [kNm]	Position [m]
a) Central void	29.5	0.5, 2	29.2	0.5, 2	28.9	0.5, 2	28.4	0.5, 2	28.0	0.5, 2
b) Single hanging	83.9	1.25	83.1	1.125	82.5	1.125	81.6	1.125	80.7	1.125
c) Double hanging	92.2	1.25	92.0	1.25	91.7	1.25	91.3	1.25	90.9	1.25
d) Side-central void	22.0	0.5, 2	22.0	0.5, 2	22.0	0.5, 2	21.9	0.5, 2	21.9	0.5, 2
e) Double side-central void	11.4	0.875	11.3	1.625	11.2	0.875	11.0	1.625	10.8	0.5, 2
f) Full support	21.9	1.25	21.0	1.25	20.1	1.25	19.8	2	20.2	0.5, 2

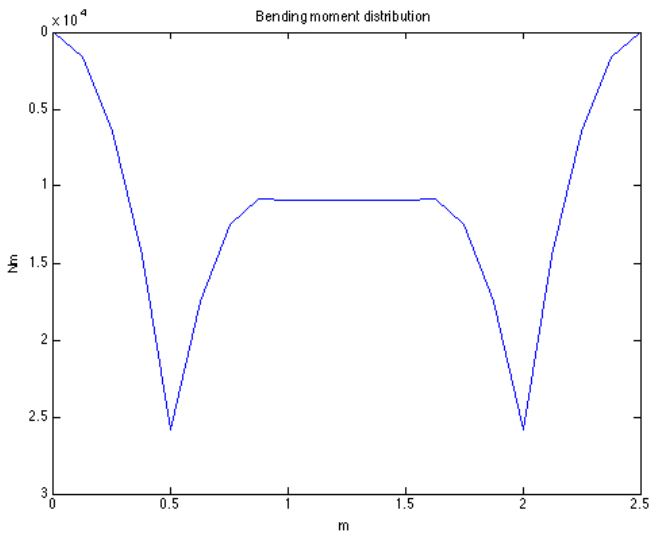

Figure 23 Bending moment distribution for case a) Central void with element support stiffness k=7.8 kN/mm

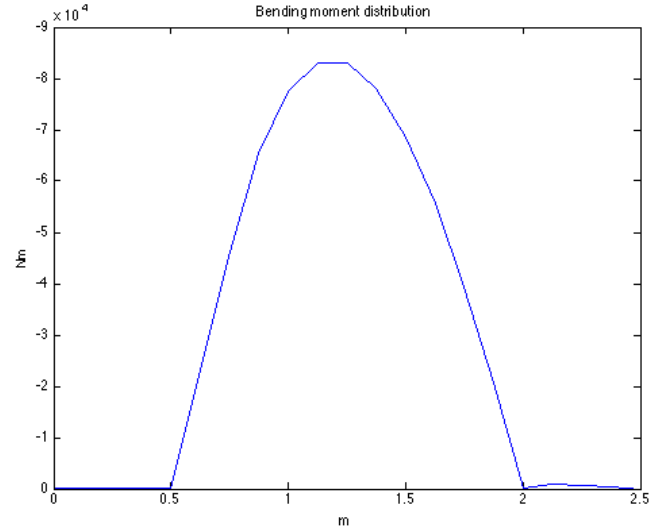

Figure 24 Bending moment distribution for case b) Single hanging with element support stiffness k=7.8 kN/mm

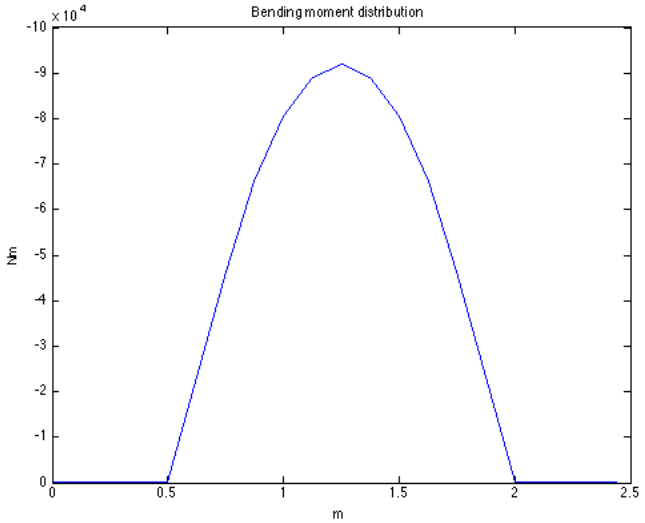

Figure 25 Bending moment distribution for case c) Double hanging with element support stiffness k=7.8 kN/mm

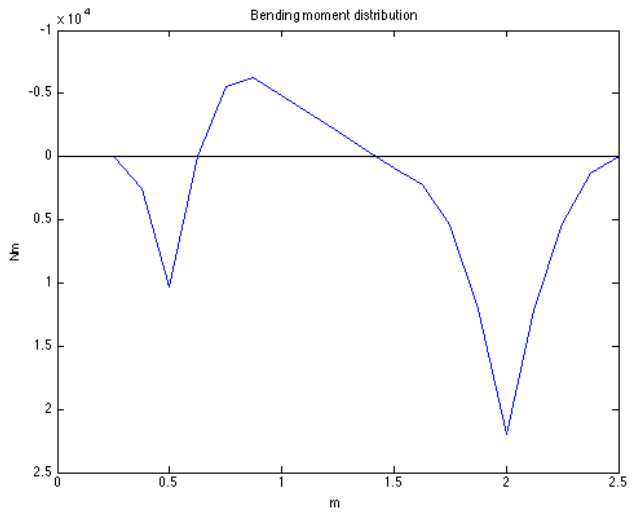

Figure 26 Bending moment distribution for case d) Side- central void with stiffness element support stiffness k=7.8 kN/mm

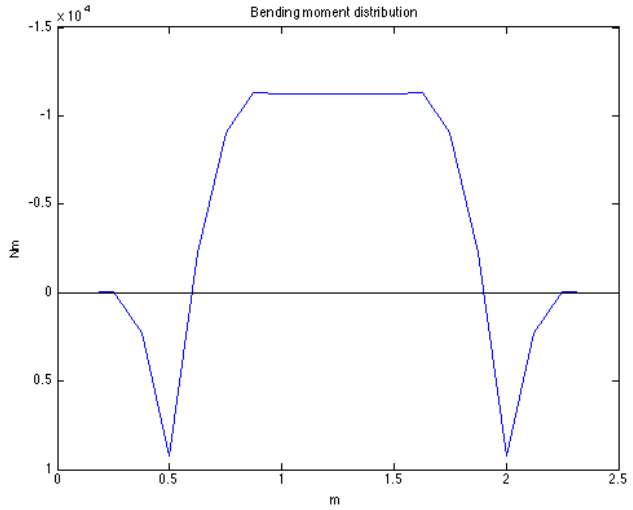

Figure 27 Bending moment distribution for case e) Double side- central void with element support stiffness k=7.8 kN/mm

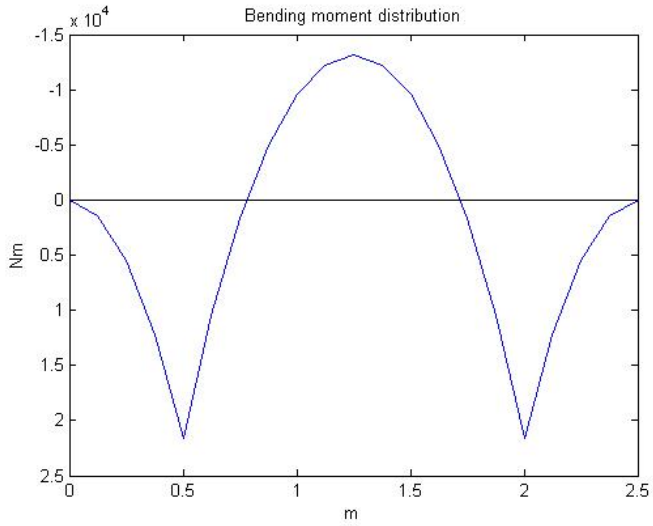

Figure 28 Bending moment distribution for case f) fully supported with element support stiffness k=7.8 kN/mm

5.4.2 The impact of stiffness on bending moments and displacements

The bending moment variation for a sleeper with different stiffness values going from central void to full support is displayed in Figure 29. The stiffness for each element in the voided area varies from 0 to 28 kN/mm with steps of 2 kN/mm. The lowest stiffness in the void gives the highest bending moments. The variation in displacement for the same case can be seen in Figure 30.

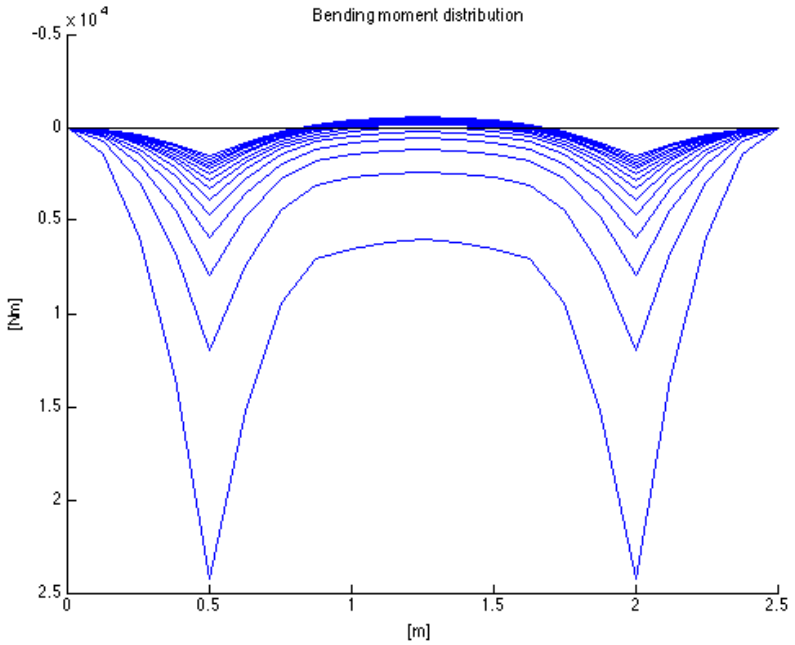

Figure 29 Bending moment variation for different stiffness values in the central void area. The Stiffness per element varies from 0 to 28 kN/mm with steps of 2 kN/mm. The lowest stiffness gives the highest bending moments.

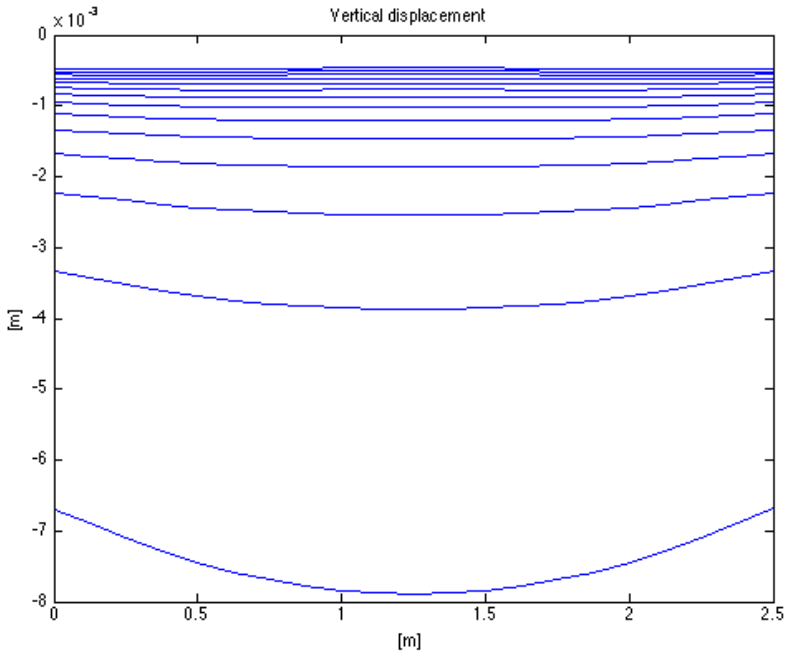

Figure 30 Vertical displacement variation for different stiffness values for Central Void to Full Support. The Stiffness per element varies from 0 to 28 kN/mm with steps of 2 kN/mm.

The bending moment variation for a sleeper with different stiffness values going from double hanging to fully supported in the hanging areas is presented in Figure 31. The support stiffness per element varies from 0 to 28 kN/mm with steps of 2 kN/mm. The lowest stiffness gives the highest bending moments. The variation in displacement for the same case can be seen in Figure 32. The lowest stiffness gives the larges vertical displacement.

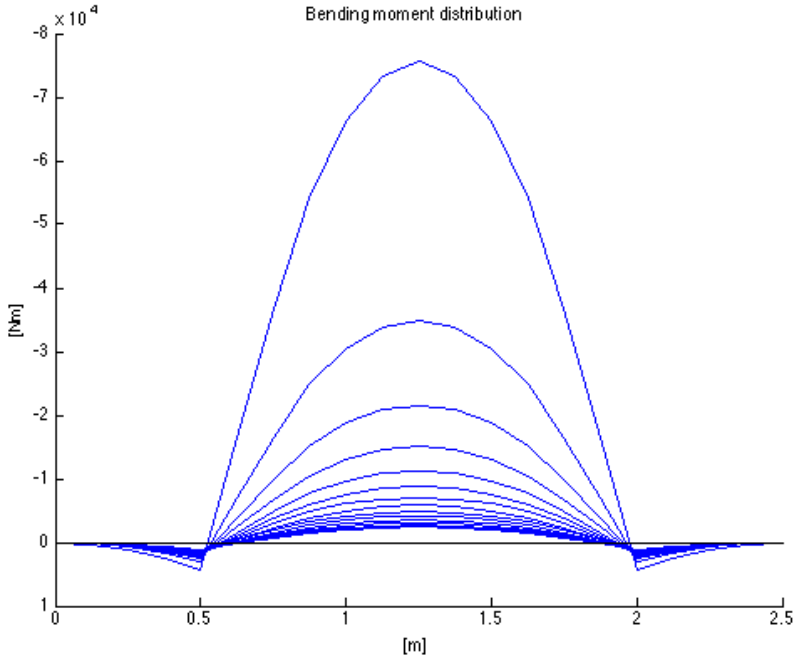

Figure 31 Bending moment variation for different stiffness values for Double Hanging to Full Support. The Stiffness per element varies from 0 to 28 kN/mm with steps of 2 kN/mm. The lowest stiffness gives the highest bending moments.

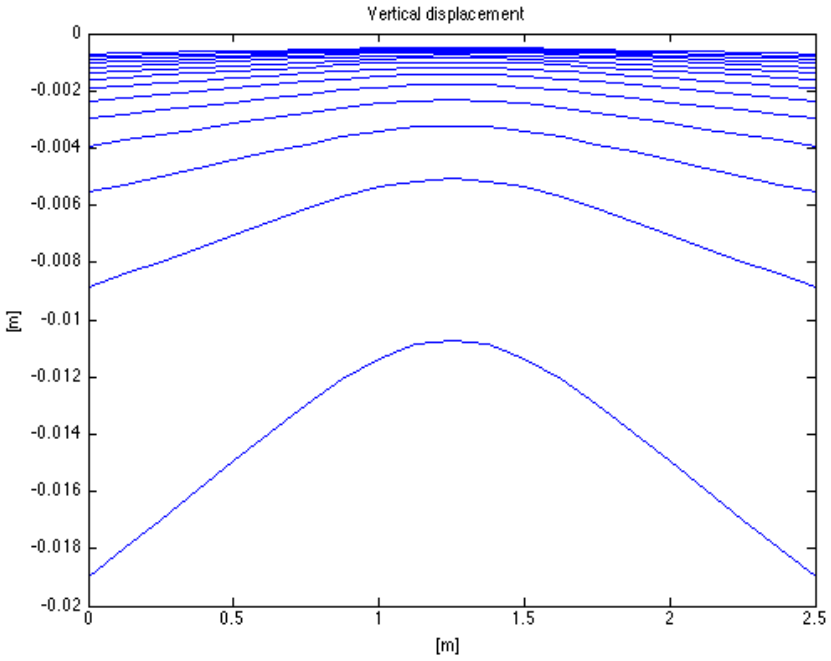

Figure 32 Vertical displacement variation for different stiffness for Double Hanging to Full Support. The Stiffness per element varies from 0 to 28 kN/mm with steps of 2 kN/mm.

Figure 33 and Figure 34 displays the bending moment distribution by stiffness over a sleeper with a central void with a support stiffness per element that varies between 0 and 28 kN/mm.

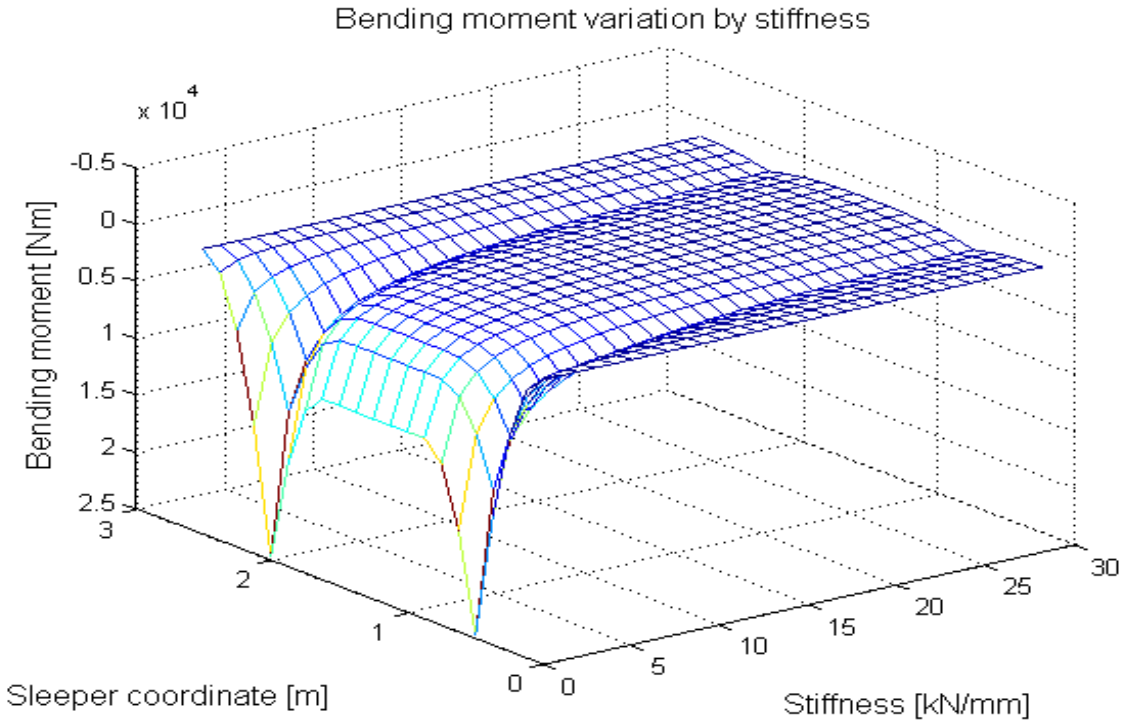

Figure 33 Bending moment variation caused by a variation in stiffness of a central void, view 1

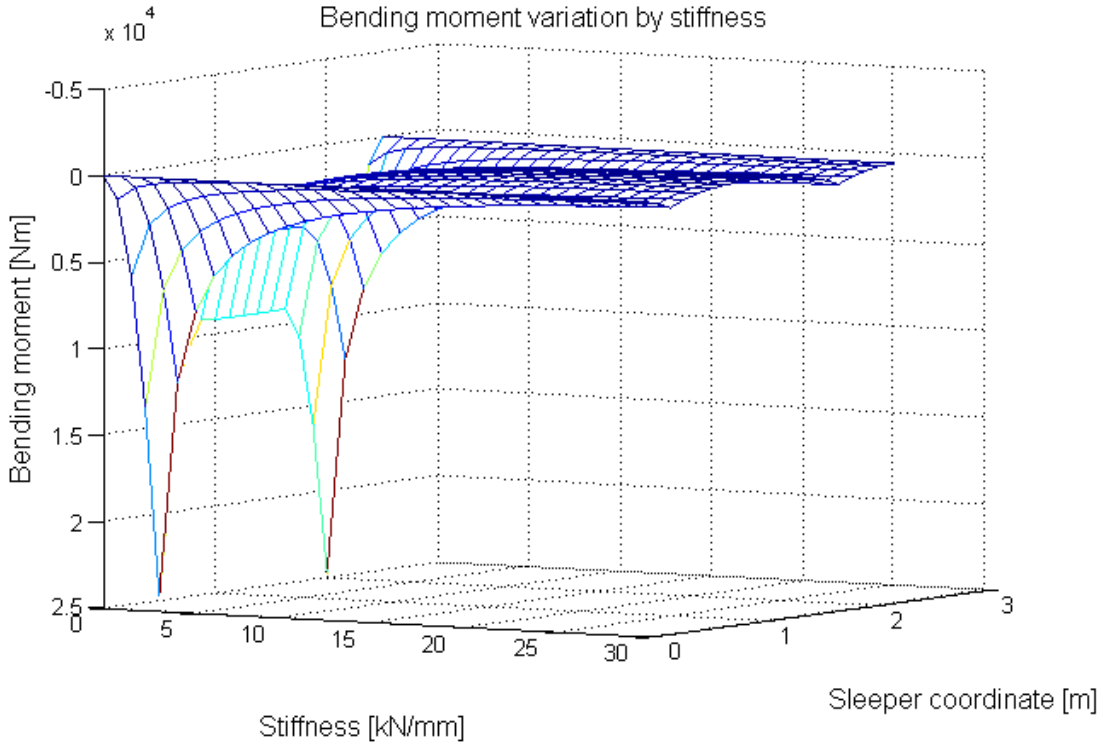

Figure 34 Bending moment variation caused by a variation in stiffness of a central void, view 2

The bending moment distribution for a double hanging sleeper where the support stiffness per element in the hanging areas varies from 0 to 28 kN/mm is presented in Figure 35 and Figure 36.

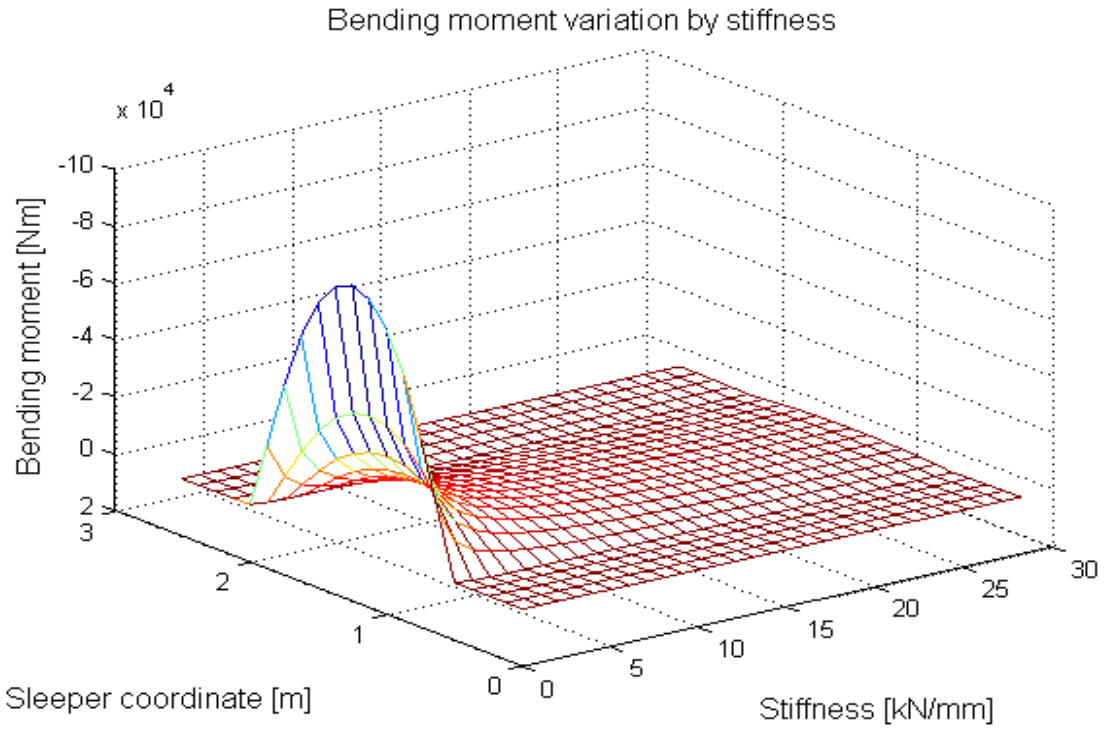

Figure 35 Bending moment variation caused by variation in stiffness in double hanging areas, view 1.

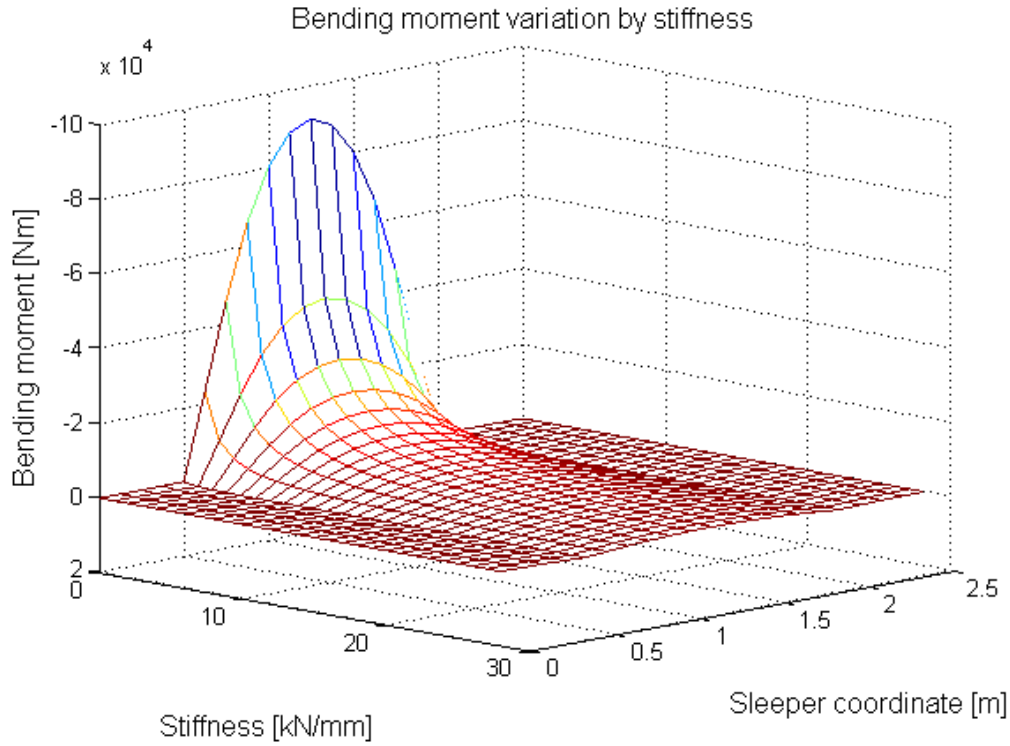

Figure 36 Bending moment variation caused by variation in stiffness in double hanging areas, view 2.

The bending moment distribution for a fully supported sleeper with varying support stiffness per element from 1 kN/mm to 28 kN/mm can be seen in Figure 37 and Figure 38.

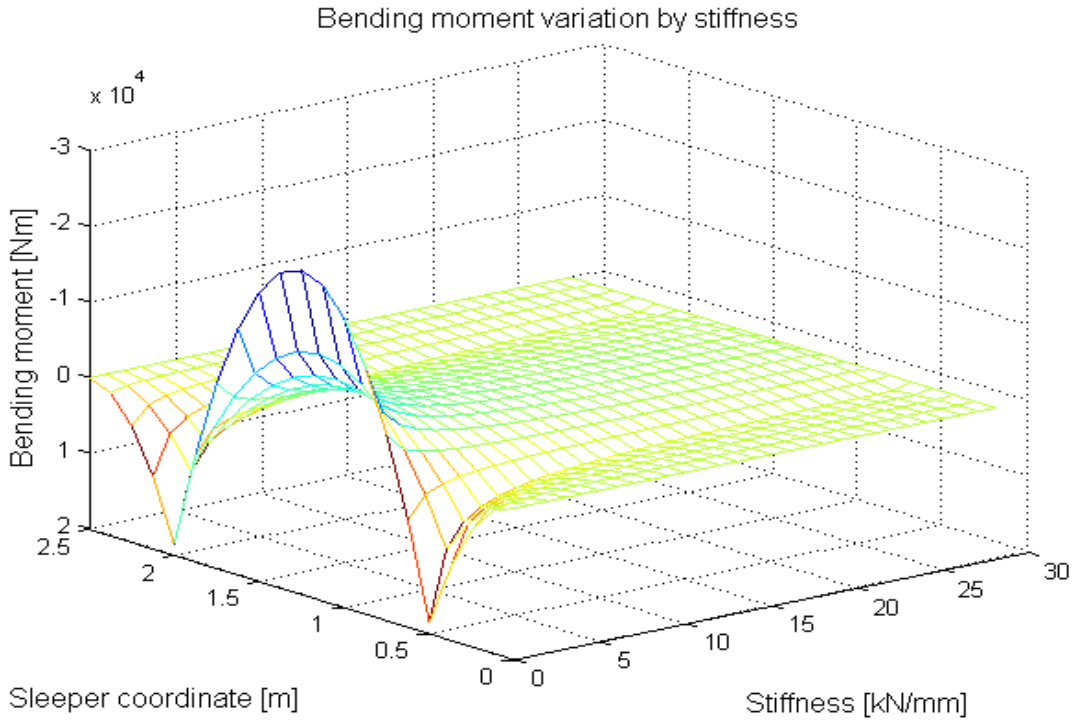

Figure 37 Bending moment variation caused by variation in stiffness for a fully supported sleeper, view 1.

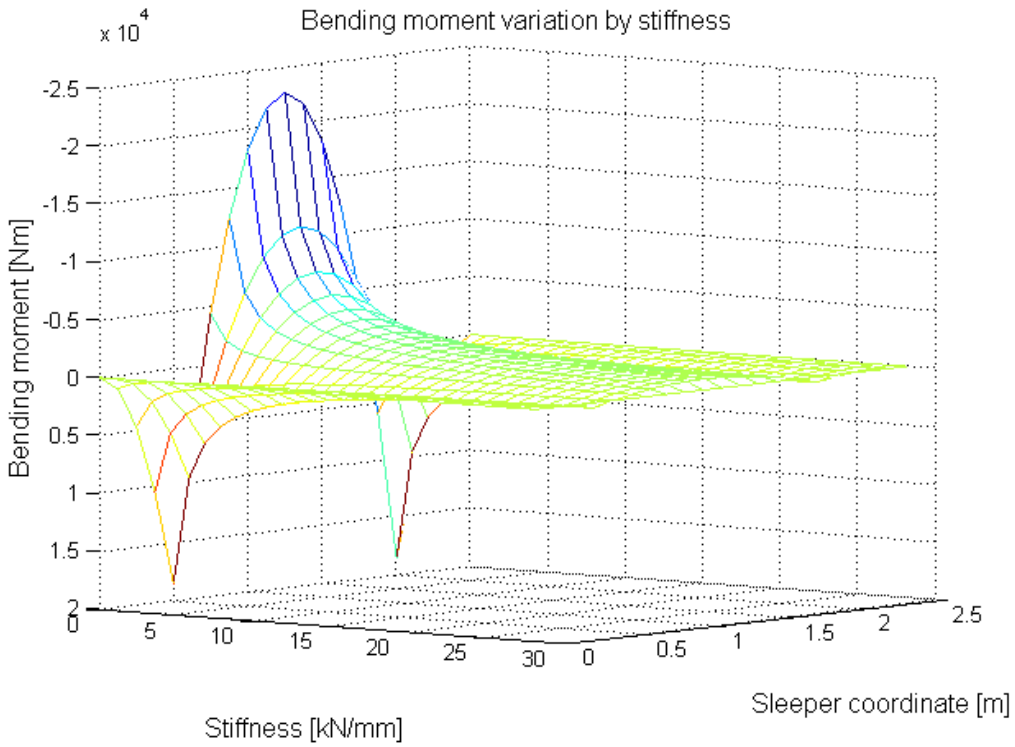

Figure 38 Bending moment variation caused by variation in stiffness for a fully supported sleeper, view 2.

The bending moment distribution for a sleeper with a central void where the stiffness is set to 0, and a support stiffness per element at the sides that varies from 0 kN/mm to 28 kN/mm, is presented in Figure 39. The lowest stiffness gives the highest bending moment.

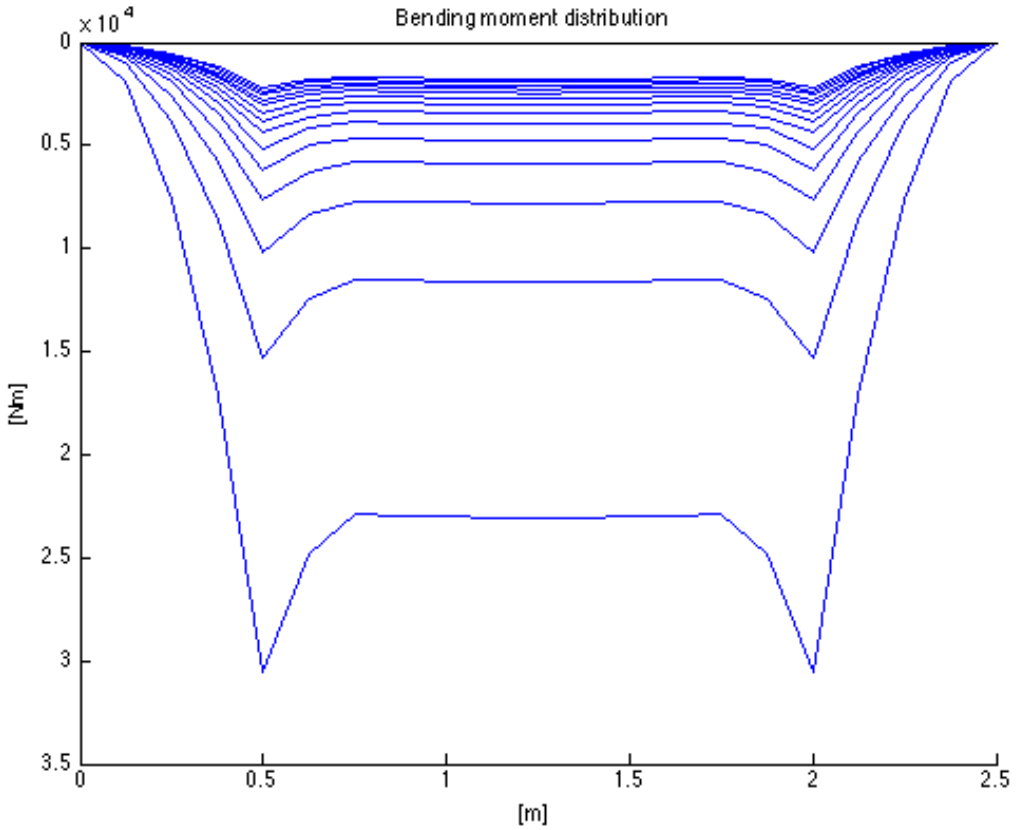

Figure 39 Bending moment distribution for a sleeper with zero support stiffness in the centre and varying stiffness at the sides of the sleeper. The lowest stiffness gives the highest bending moment.

Figure 40 shows the bending moment distribution for a double hanging sleeper where the stiffness at the sides is set to 0 and the centre stiffness varies from 0 kN/mm to 28 kN/mm per element. The lowest stiffness gives the highest bending moment.

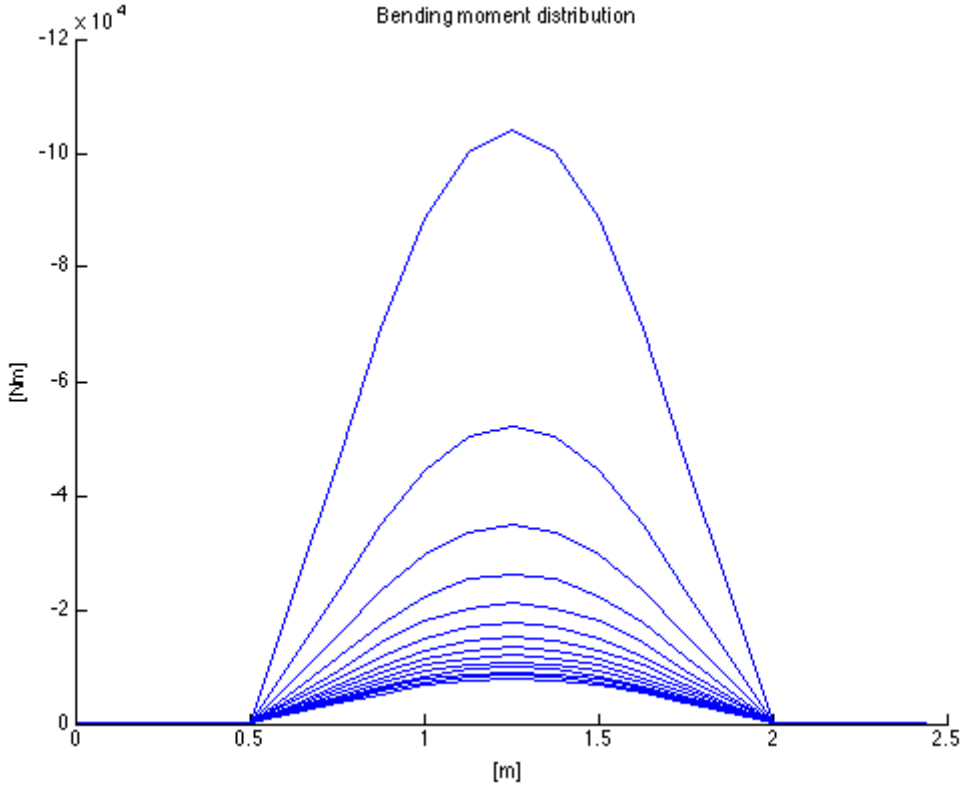

Figure 40 Bending moment distribution for a sleeper with zero support stiffness at the sides and declining stiffness at the centre of the sleeper. The lowest stiffness gives the highest bending moment.

5.4.3 Results from eigenfrequency analyses

Figure 41 presents result from an eigenvalue analysis of the first bending mode for a sleeper with a central void with variation in support stiffness. The figure shows that track stiffness has a large influence on the eigenfrequency. The curve is similar for the second and the third eigenfrequencies, see Appendix 5. The rigid body vibration modes (translation and rotation) are not considered.

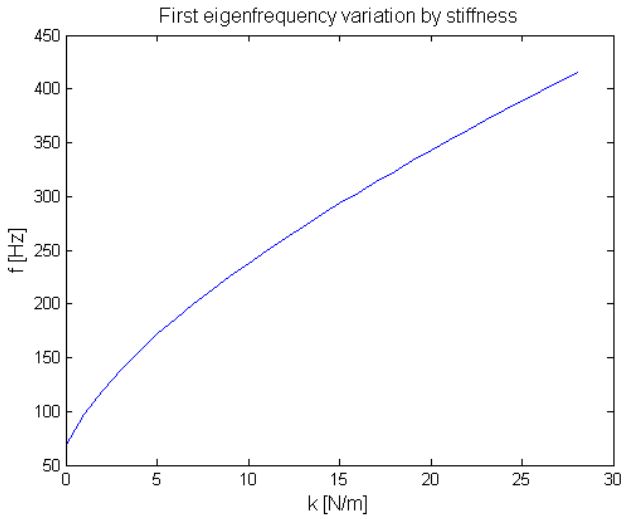

Figure 41 Variations in first eigenfrequency of a sleeper with a central void as the stiffness of the hanging areas goes from zero to 28 kN/mm for each element.

The relation between stiffness and eigenfrequency for a sleeper which is fully supported is shown in Figure 42.

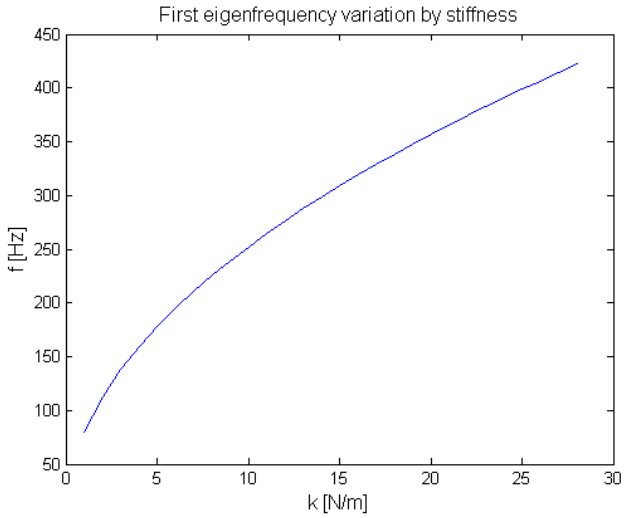

Figure 42 Variation in the eigenfrequency of the first bending mode as the stiffness of all elements goes from 1 to 28 kN/mm

Figure 41 and Figure 42 shows that a specific ballast stiffness value gives the same corresponding eigenfrequency for both a fully supported sleeper and a sleeper with a central void.

Figure 44 – 46 shows the eigenfrequencies of the first, second and third bending modes as support stiffness increases and changes from double hanging to fully supported. The correlation for the first two bending modes seems to be almost linear but the third is not. This trend does not appear for a fully supported sleeper or a sleeper with a central void.

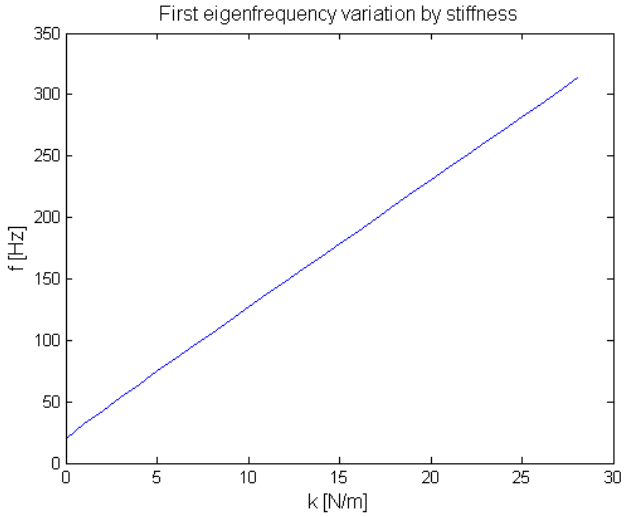

Figure 43 Variation in the eigenfrequency of the first bending mode as the stiffness of the hanging areas goes from zero to 28 kN/mm for each element

The eigenfrequency for a ballast stiffness of 28 kN/mm for all elements should be the same for all three cases. According to Figure 43 the maximum value of the first eigenfrequency for a double hanging sleeper is around 325 Hz compared to 425 Hz for the cases with full support and central void.

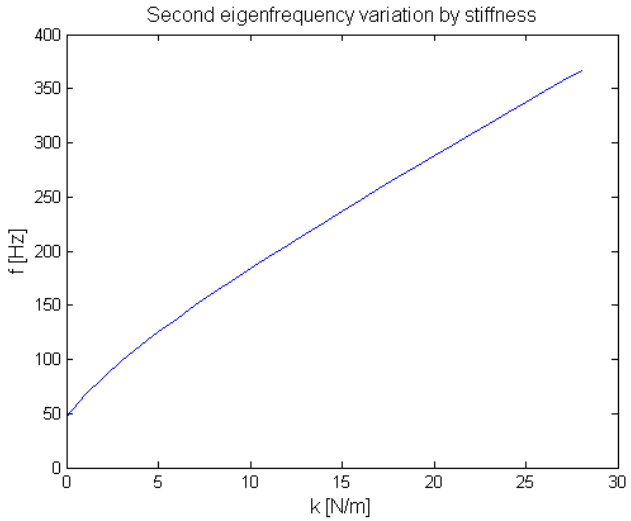

Figure 44 Variation in the eigenfrequency of the second bending mode as the stiffness of the hanging areas goes from zero to 28 kN/mm for each element

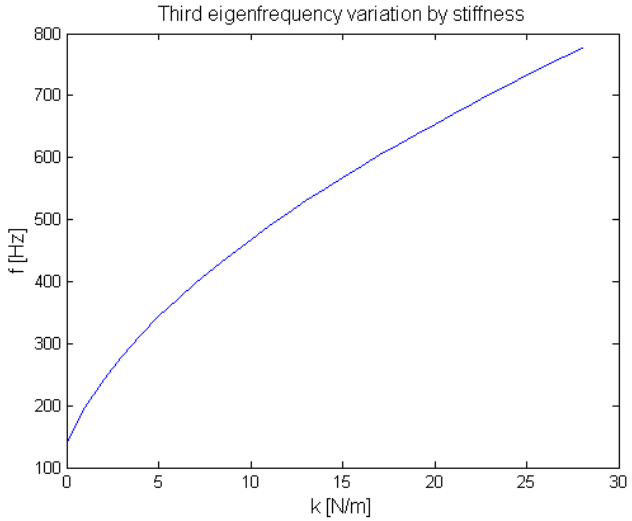

Figure 45 Variation in the eigenfrequency of the third bending mode as the stiffness of the hanging areas goes from zero to 28 kN/mm for each element

5.5 Discussion

The model does not give accurate results for calculations when the track stiffness, k, is equal to zero beneath the whole sleeper. Therefore the start value is set to 1 kN/mm per element for the simulation where the support condition is fully supported.

The results show that the case of a double hanging sleeper gives the largest bending moments, which is in accordance to the study by Bolmsvik and Nielsen (2006). The case where only half of the sleeper is supported also results in large moments. Cases of double side central void and fully supported sleepers differs from the general trend since the bending moment in the sleeper increases with increasing stiffness for these cases.

The simulations in this report indicate double hanging sleepers to be worse. This is in contrast to Li (2012), who states that a double side central void is the worst case scenario. Double hanging sleepers are however not a case studied in Li (2012). The comparison between the models may not be accurate as the elements that are supported could vary for the same support condition.

Analyses show that the largest displacements under the rails arise when a sleeper is single hanging or double hanging. These cases should according to the argumentation in 4.2 give considerable negative effects on the whole track.

The analyses show that higher stiffness results in smaller displacements. The general trend shows that the relation between stiffness and displacement is exponentially decreasing with increasing stiffness. Large displacements for the sleeper leads to high bending moments in the rails and it also induce high dynamic loads.

The largest displacements seen in Figure 30 and Figure 32 may not happen in reality. If the distance between sleeper and ballast is smaller than the deflection the sleeper will hit the ballast surface instead and the support condition and support stiffness will change.

Conclusions can be made from Figure 34 – 39 that when studying how the maximum bending moment is affected by support stiffness the relation between the moment and stiffness is

exponential and the relation between moment and change in stiffness is linear. This is also stated by Lilja (2006).

From Figure 34 – 39 it can be concluded that ballast stiffness over 120 kN/mm does not have a large influence on the bending moment of a sleeper.

It can also be concluded from the simulations that low track stiffness results in a high corresponding bending moment. To choose an optimal stiffness is complicated and cannot be done based only on the bending moment in one sleeper. Other parameters worth considering are for example damages on train components which should be larger because of harder track stiffness. Harder track stiffness should also have a negative effect on passenger comfort and give higher compression loads on the sleeper. On the other hand, with softer track stiffness the dissipated energy for trains should be larger than for a hard track. Different stiffness should also result in different bending moments in the rails. For further investigations all these parameters and more needs to be considered.

Modal analysis shows that the first three eigenfrequencies of a concrete sleeper is largely influenced by the ballast stiffness.

Local weaknesses along the track will generate large variations in track stiffness. Instead of aiming for an optimum stiffness value the intention should be to retain a constant stiffness along the track.

The results from the simulations, presented in Figure 39 and Figure 40 show that a softer track is more sensitive to variations in support conditions than a stiff track, when only looking into the bending moments and displacements of the sleeper. This should also be considered when choosing track stiffness and maintenance strategies

In addition to the current study of stiffness variations under a sleeper, there are literature studies on the influence of support conditions and stiffness along the track, see section 4. Combined analyses where support variation along one sleeper in models with support variations along the track would be interesting. This would lead to a more accurate response and might give a better understanding of how stiffness variations affect track and train dynamics.

6 Conclusions

Differences in ballast stiffness beneath the sleeper and along the track will cause higher contact forces, larger deflections and larger vibrations. This will induce an increased settlement of the ballast bed and create an even larger variation in ballast stiffness. The loss of homogenous track geometry is thereby accelerated. Further, the risk of failure of track components increases.

According to the simulations conducted in this study the track stiffness, and track stiffness variations along a sleeper, have a high impact on the bending moments, displacements and eigenfrequencies of the sleeper. It can therefore be concluded that track stiffness is an important parameter concerning track durability.

To choose an ultimate stiffness is complicated and cannot be done based solely on the results in this report. The priority should be to retain a constant stiffness along the track. If stiffness is evaluated for a track, it could be used as a parameter to optimize the maintenance e.g. by identifying local weaknesses along the track and detect hanging sleepers.

Due to the current short-term maintenance contracts of today, the whole lifespan of the railway track is seldom considered when maintenance is planned. Further, most maintenance performed today address acute problems and preventative measures, e.g. shoulder cleaning, are not regularly performed.

Given the circumstances, to implement track stiffness as a parameter when maintenance is planned would initially require more resources but in the long-term perspective this would probably lead to reduce costs due to less degradation of track. Before implementation, an economic calculation should be performed.

A new interesting maintenance method available is stoneblowing. It is motivated to investigate the sustainability of this method.

Additional preventive measures, e.g. ballast and shoulder cleaning, should be made to reduce the need of tamping and track lining and to raise the quality of the track. Stiffness measurements should be performed regularly and used as a tool when maintenance is planned.

References

Andersson E. and Berg M. (2007) *Spårtrafiksystem och spårfordon.* Stockholm (Del 1: Spårtrafiksystem)

Aursudkij B. (2007) *A Laboratory Study of Railway Ballast Behaviour under Traffic Loading and Tamping Maintenance.* Nottingham

Banverket (2002) *Typsektioner för banan.* (Handbook BVH 585.31)

Berggren E. (2009) *Railway Track Stiffness Dynamic Measurements and Evaluation for Efficient Maintenance*. Stockholm: Royal Institute of Technology (PhD thesis, Report TRITA AVE 2009:17, Aeronautical and Vehicle Engineering)

Berggren E. Jahlénius Å. Bengtsson B E. and Berg M (2005) Simulation, Development and Field Testing of a Track Stiffness Measurement Vehicle. *Proceedings of 8th Int. Heavy Haul Conference*. Rio de Janeiro

Bolmsvik R. and Nielsen J. (2006) *Dimensionerande böjmoment i sliprar vid 35 tons axellast.* Göteborg: Chalmers University of Technology (Research report 2006:09)

Brough M. Stirling A. Ghataora G. and Madelin K. (2003) Evaluation of railway trackbed and formation: a case study. *NDT & E International,* vol. 36, no. 3, pp. 145-156.

Dahlberg T. (2010) Railway Track Stiffness Variations – Consequences and Countermeasures. *International Journal of Civil Engineering*, vol. 8, no. 1

Fair P. (2003) *The geotechnical behaviour of ballast materials for railway track maintenance.* University of Sheffield (PhD thesis)

Hedström R. (2002) *Banretur: Återvinning av banvallsmassor och betongsliprar – en förstudie*. Linköping: Väg- och transportforskningsinstitutet (VTI meddelande 935)

Hon P. (2010) *Utvärdering av kontrollmetoder för obundna granulära material*. Lund: Lund University (MSc Degree Project, Department of Technology and Society)

Infranord (2012) *Mekanisk Vegetationsreglering,* http://www.infranord.se/Documents/projektblad/Mekanisk_Vegetationsreglering_INFRANORD_120411.pdf [15 feb 2013]

Innotrack (2006) *Recommentation of, and scientific basis for, minimum action rules and maintenance limits* (Project No. TIP5-CT-2006-031415)

Kabo E. (2004) *Förstudie Isolerskarvars inverkan på spårets mekaniska egenskaper: en finit elementanalys.* Göteborg: Chalmers University of Technology (Research report 2004:14)

Kaewunruen S. and Remennikov A. M. (2007) Effect of improper ballast packing/tamping on dynamic behaviors of on-track railway concrete sleeper. *International Journal of Structural Stability and Dynamics*, vol. 7, no. 1, pp. 167-177.

Kumaran G. Menon D. and Nair Krishnan K. (2003) Dynamic studies of railtrack sleepers in a track structure system. *Journal of Sound and Vibration*, vol. 268, issue 3, pp. 485-501.

Li S. (2012) *Railway Sleeper Modelling with Deterministic and Non-deterministic Support Conditions.* Stockholm: Royal Institute of Technology (Master degree project, Report TSC-MT 12-001, Department of Transport Science)

Li M. X. D. and Berggren E. G. (2010) A study of the effect of global track stiffness and its variations on track performance: simulation and measurement. *Proceedings of the Institution of Mechanical Engineers, Part F: Journal of Rail and Rapid Transit*, vol. 224, F5, pp. 375-382.

Lilja J. (2006) *Preliminaries for probabilistic railway sleeper design*. Göteborg: Chalmers University of Technology. (Lic thesis 2006:20)

Lopez Pita A., Teixeira P F. and Robuste F. (2004) High Speed and Track Deterioration: the Role of Vertical Stiffness on the Track. *Proceedings of the Institution of Mechanical Engineers.* Vol 218, no. 1, pp. 31-40.

Lundqvist A. and Dahlberg T. (2005) Load impact on railway track due to unsupported sleepers. *Proceedings of the Institution of Mechanical Engineers, Part F: Journal of Rail and Rapid Transit*, vol. 219, F2 , pp. 67-77.

Newman G.R. and Zarembski A.M. (2008) *Comparative Technical and Economic Analysis of Stoneblowing vs Tamping.* (AREMA)

Olsson E-L. and Zackrisson P (2002) *Longt-term measurement results, final report.* Borlänge: Banverket (Technical report 2B/000120/T2/DA) Cited in Load impact on railway track due to unsupported sleepers. *Proceedings of the Institution of Mechanical Engineers, Part F: Journal of Rail and Rapid Transit*, vol. 219, F2 , (2005) pp. 67-77.

Oscarsson J. and Dahlberg T. (1998) Dynamic Train/Track/Ballast Interaction – Computer Models and Full-Scale Experiments. *Vehicle System Dynamics: International Journal of Vehicle Mechanics and Mobility,* vol. 29, S1, pp. 73-84.

Plasser & Theurer (2012) *Tamping*
http://www.plassertheurer.com/en/machines-systems/tamping.html [21 feb 2013]

Recuero A M. Escalona J L. and Shabana A A. (2011) Finite-element analysis of unsupported sleepers using three-dimensional wheel-rail contact formulation. *Proceedings of the Institution of Mechanical Engineers, Part K: Journal of Multi-body Dynamics*, vol. 225, no. 2, pp. 153-165.

Rezaei E. (2010) *Vibrations of partly supported concrete railway sleeper*. Linköping: University of Linköping (Degree Project, Report LIU-IEI-TEK-A 10/00835-SE, Department of Management and Engineering)

Rezaei E. and Dahlberg T. (2010) Dynamic behaviour of an in situ partially supported concrete railway sleeper. *Proceedings of the Institution of Mechanical Engineere, Part F: Journal of Rail and Rapid Transit*, vol. 225, pp. 501-508.

Sundvall M. (2005) *Finjordsfläckar i överballast.* Luleå: University of Luleå (Degree Project, Report LTU-EX--05/133--SE, Department of Geotechnics)

Trafikverket (2012a) *Trafikverkets årsredovisning 2011*. Borlänge: Elanders (2012:082)

Trafikverket (2012b) Säkerhetsbesiktning av fasta järnvägsanläggningar. Version 2.0 (Föreskrift BVF 807.2)

UIC (2004) *UIC Leaflet 713 R Design of monobloc concrete sleepers*

Åström M. (2011) *Järnvägsteknik*. Stockholm: Liber

Appendix

Appendix 1 – MATLAB basis of calculations

Models and cross section values

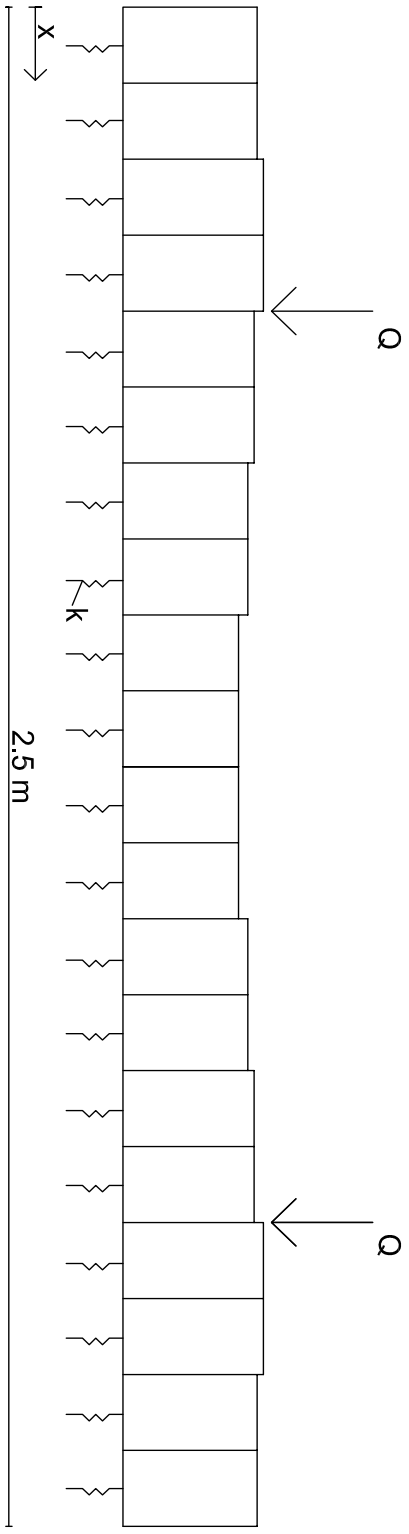

Figure 1 Model of sleeper on elastic foundation

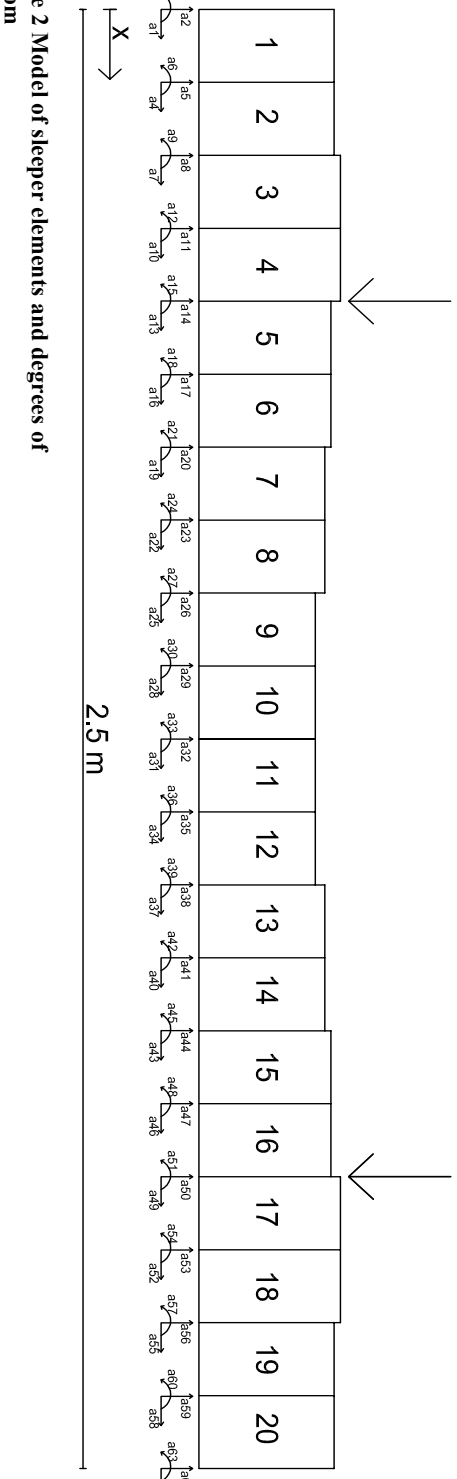

Figure 2 Model of sleeper elements and degrees of freedom

Table 6 Supported elements for each support condition

Support condition	**1**	**2**	**3**	**4**	**5**	**6**	**7**	**8**	**9**	**10**	**11**	**12**	**13**	**14**	**15**	**16**	**17**	**18**	**19**	**20**
a) Central void	X	X	X	X	X	X	X							X	X	X	X	X	X	X
b) Single hanging							X	X	X	X	X	X	X	X	X	X	X	X	X	X
c) Double hanging							X	X	X	X	X	X	X	X						
d) Side-central void			X	X	X	X	X							X	X	X	X	X	X	X
e) Double side-central void			X	X	X	X	X							X	X	X	X	X		
f) Full support	X	X	X	X	X	X	X	X	X	X	X	X	X	X	X	X	X	X	X	X

X Supported element

Table 7 Cross section values

	Section 1	**Section 2**	**Section 3**	**Section 4**	**Section 5**
Module of elasticity, E (GPa)	40	40	40	40	40
Density, ρ (kg/m^3)	2400	2400	2400	2400	2400
Cross section area, A (m^2)	4.71×10^{-2}	4.83×10^{-2}	4.46×10^{-2}	3.78×10^{-2}	3.32×10^{-2}
Moment of inertia, I (m^4)	2.54×10^{-4}	2.75×10^{-4}	2.16×10^{-4}	1.31×10^{-4}	8.92×10^{-5}

Appendix 2 – MATLAB Bending moment and vertical displacement for different stiffness values

MATLAB Code

```
% Values

Q=25e3*9.81*1.5/2;          % 50% dynamical effect, [N]
L=2.5;                      % Length of a sleeper, [m]
E=40e9;                     % Pre-stressed concrete (uncracked cross-
                            % section), [Pa]
Le=L/20;                    % Length of one element, [m]
q=250/L*9.81;               % Characteristic load of sleeper, [N/m]
d=2400;                     % Density concrete [kg/m^3]


% Stiffness values [N/m]

s0=2*100/20;
s1=2*40e6/20;
s2=2*78e6/20;
s3=2*120e6/20;
s4=2*186e6/20;
s5=2*252e6/20;

% Spring stiffness for each element, [N/m]

k1=s5;
k2=s5;
k3=s5;
k4=s5;
k5=s5;
k6=s5;
k7=s5;
k8=s5;
k9=s5;
k10=s5;
k11=s5;
k12=s5;
k13=s5;
k14=s5;
k15=s5;
k16=s5;
k17=s5;
k18=s5;
k19=s5;
k20=s5;

% Cross-section variables

% Area for each element, [m^2]

A1=4.71e-2;
A2=A1;
A3=4.83e-2;
A4=A3;
A5=4.46e-2;
A6=A5;
A7=3.78e-2;
A8=A7;
A9=3.32e-2;
```

```
A10=A9;
A11=A9;
A12=A9;
A13=A7;
A14=A7;
A15=A5;
A16=A5;
A17=A3;
A18=A3;
A19=A1;
A20=A1;

% Moment of inertia for each element, [m^4]

I1=2.54e-4;
I2=I1;
I3=2.75e-4;
I4=I3;
I5=2.16e-4;
I6=I5;
I7=1.31e-4;
I8=I7;
I9=8.92e-5;
I10=I9;
I11=I9;
I12=I9;
I13=I7;
I14=I7;
I15=I5;
I16=I5;
I17=I3;
I18=I3;
I19=I1;
I20=I1;

% Calculates if the length of the element is short enough

if Le>4*(I9*E/s5)^(1/4);
    disp('Element length to long')
end

% Topology matrix

edof=[1 1 2 3 4 5 6
    2 4 5 6 7 8 9
    3 7 8 9 10 11 12
    4 10 11 12 13 14 15
    5 13 14 15 16 17 18
    6 16 17 18 19 20 21
    7 19 20 21 22 23 24
    8 22 23 24 25 26 27
    9 25 26 27 28 29 30
    10 28 29 30 31 32 33
    11 31 32 33 34 35 36
    12 34 35 36 37 38 39
    13 37 38 39 40 41 42
    14 40 41 42 43 44 45
    15 43 44 45 46 47 48
    16 46 47 48 49 50 51
    17 49 50 51 52 53 54
    18 52 53 54 55 56 57
    19 55 56 57 58 59 60
```

```
    20 58 59 60 61 62 63];

% Geometrical data

ex1=[0 Le];
ex2=[Le 2*Le];
ex3=[2*Le 3*Le];
ex4=[3*Le 4*Le];
ex5=[4*Le 5*Le];
ex6=[5*Le 6*Le];
ex7=[6*Le 7*Le];
ex8=[7*Le 8*Le];
ex9=[8*Le 9*Le];
ex10=[9*Le 10*Le];
ex11=[10*Le 11*Le];
ex12=[11*Le 12*Le];
ex13=[12*Le 13*Le];
ex14=[13*Le 14*Le];
ex15=[14*Le 15*Le];
ex16=[15*Le 16*Le];
ex17=[16*Le 17*Le];
ex18=[17*Le 18*Le];
ex19=[18*Le 19*Le];
ex20=[19*Le 20*Le];

% Assemble in to one matrix

ex=[ex1;ex2;ex3;ex4;ex5;ex6;ex7;ex8;ex9;ex10
    ex11;ex12;ex13;ex14;ex15;ex16;ex17;ex18;ex19;ex20];

ey1=[0 0];
ey2=[0 0];
ey3=[0 0];
ey4=[0 0];
ey5=[0 0];
ey6=[0 0];
ey7=[0 0];
ey8=[0 0];
ey9=[0 0];
ey10=[0 0];
ey11=[0 0];
ey12=[0 0];
ey13=[0 0];
ey14=[0 0];
ey15=[0 0];
ey16=[0 0];
ey17=[0 0];
ey18=[0 0];
ey19=[0 0];
ey20=[0 0];

% Create a matrix of zeroes instead of assembling

ey=zeros(20,2);

% Element properties for each element

ep1=[E A1 I1 0 k1];
ep2=[E A2 I2 0 k2];
ep3=[E A3 I3 0 k3];
ep4=[E A4 I4 0 k4];
```

```
ep5=[E A5 I5 0 k5];
ep6=[E A6 I6 0 k6];
ep7=[E A7 I7 0 k7];
ep8=[E A8 I8 0 k8];
ep9=[E A9 I9 0 k9];
ep10=[E A10 I10 0 k10];
ep11=[E A11 I11 0 k11];
ep12=[E A12 I12 0 k12];
ep13=[E A13 I13 0 k13];
ep14=[E A14 I14 0 k14];
ep15=[E A15 I15 0 k15];
ep16=[E A16 I16 0 k16];
ep17=[E A17 I17 0 k17];
ep18=[E A18 I18 0 k18];
ep19=[E A19 I19 0 k19];
ep20=[E A20 I20 0 k20];

% Assemble data into one matrix

ep=[ep1;ep2;ep3;ep4;ep5;ep6;ep7;ep8;ep9;ep10
    ep11;ep12;ep13;ep14;ep15;ep16;ep17;ep18;ep19;ep20];

% Distributed loads

eq=[0 -q];          % Load in negative y-direction

% Preallocate stiffness matrix, K, and load vector, f

K=zeros(63);
f=zeros(63,1);

% Define the position of the point loads

f(14)=f(14)-Q;
f(50)=f(50)-Q;

% Compute stiffness matrix, K, and load vector, f

for i=1:20;
    [Ke,fe]=beam2w(ex(i,:),ey(i,:),ep(i,:),eq);
    [K,f]=assem(edof(i,:),K,Ke,f,fe);
end


% Boundary conditions

bc=[1 0
    4 0
    7 0
    10 0
    13 0
    16 0
    19 0
    22 0
    25 0
    28 0
    31 0
    34 0
    37 0
    40 0
```

```
    43 0
    46 0
    49 0
    52 0
    55 0
    58 0
    61 0];


% Compute displacements, a, and reaction forces, r

[a,r]=solveq(K,f,bc);

% Element displacements

ed=extract(edof,a);

% Compute section forces [N V M]

es=zeros(40,3);

for i=1:20
    ese=beam2ws(ex(i,:),ey(i,:),ep(i,:),ed(i,:),eq);
    es(i*2-1,:)=ese(1,:);
    es(i*2,:)=ese(2,:);
end


% Compute size and location of maximum moment

[Mmax,Position]=max(abs(es(:,3)));
Mmax

xM=ceil((Position-1)/2)*Le

% Compute size and location of maximum displacement

for i=1:21
    a_vertical(i,1)=a(3*i-1,:);
end

[a_max,Position_a]=max(abs(a_vertical));
a_max

xa=ceil(Position_a-1)*Le

% Create a moment vector, M

M=es(:,3);

% Create x-vector

x=zeros(21,1);
x(2:21,1)=ex(:,2);

% Preallocate and create bending moment vector to plot

Mplot=zeros(21,1);
```

```
for i=1:19;
    Mplot(i+1,:)=M(2*i+1,:);

end

% Plot bending moment distribution

figure (1)
plot(x,Mplot)
hold on
set(gca,'YDir','reverse');
plot(linspace(0,2.5,1000),0,'k','LineWidth',2);
title('Bending moment distribution');
xlabel('m');
ylabel('Nm');
hold off

% Plot vertical displacement

figure (2)
plot(x,a_vertical)
hold on
plot(linspace(0,2.5,1000),0,'k','LineWidth',2);
title('Vertical displacement');
xlabel('m');
ylabel('m');
axis([0 2.5 -a_max*1.3 0.002])
hold off
%
% echo off
% diary off
```

Results

Table 8 Maximum moment and position of maximum moment for the different support conditions and stiffness values

Stiffness	40 kN/mm		78 kN/mm		120 kN/mm		186 kN/mm		252 kN/mm	
Support condition	Maximum moment [kNm]	Position [m]	Maximum moment [kNm]	Position [m]	Maximum moment [kNm]	Position [m]	Maximum moment [kNm]	Position [m]	Maximum moment [kNm]	Position [m]
a) Central void	29.5	0.5, 2	29.2	0.5, 2	28.9	0.5, 2	28.4	0.5, 2	28.0	0.5, 2
b) Single hanging	83.9	1.25	83.1	1.125	82.5	1.125	81.6	1.125	80.7	1.125
c) Double hanging	92.2	1.25	92.0	1.25	91.7	1.25	91.3	1.25	90.9	1.25
d) Side-central void	22.0	0.5, 2	22.0	0.5, 2	22.0	0.5, 2	21.9	0.5, 2	21.9	0.5, 2
e) Double side-central void	11.4	0.875	11.3	1.625	11.2	0.875	11.0	1.625	10.8	0.5, 2
f) Full support	21.9	1.25	21.0	1.25	20.1	1.25	19.8	2	20.2	0.5, 2

Figures

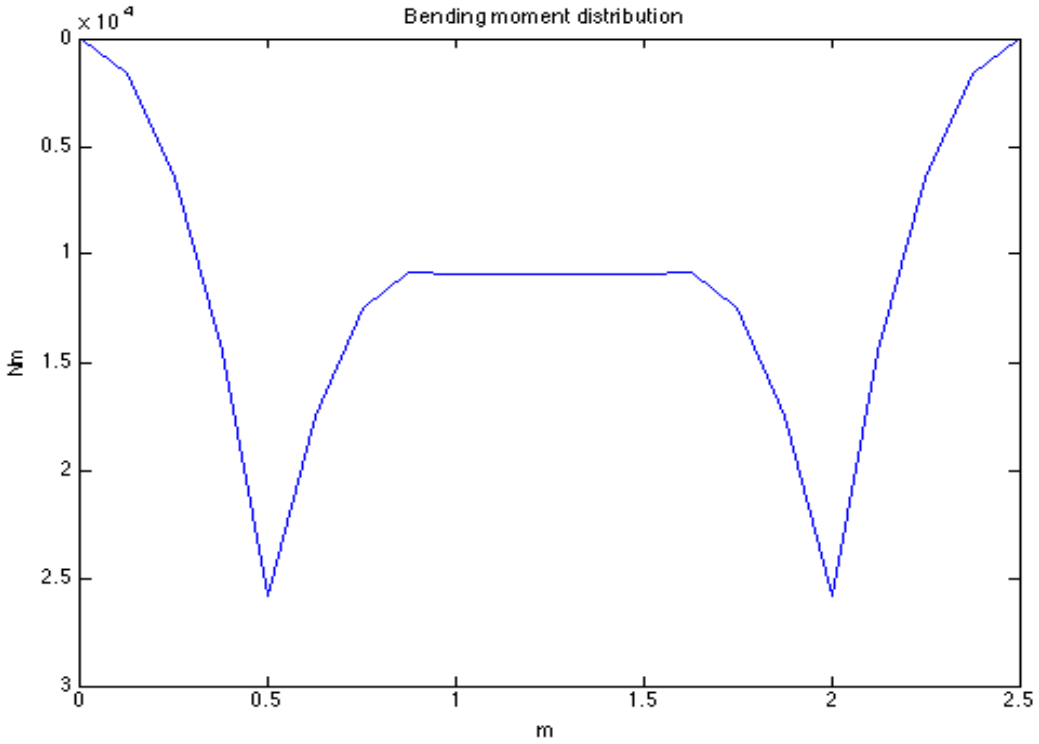

Figure 46 Bending moment distribution for case a) Central void with element support stiffness k=7.8 kN/mm

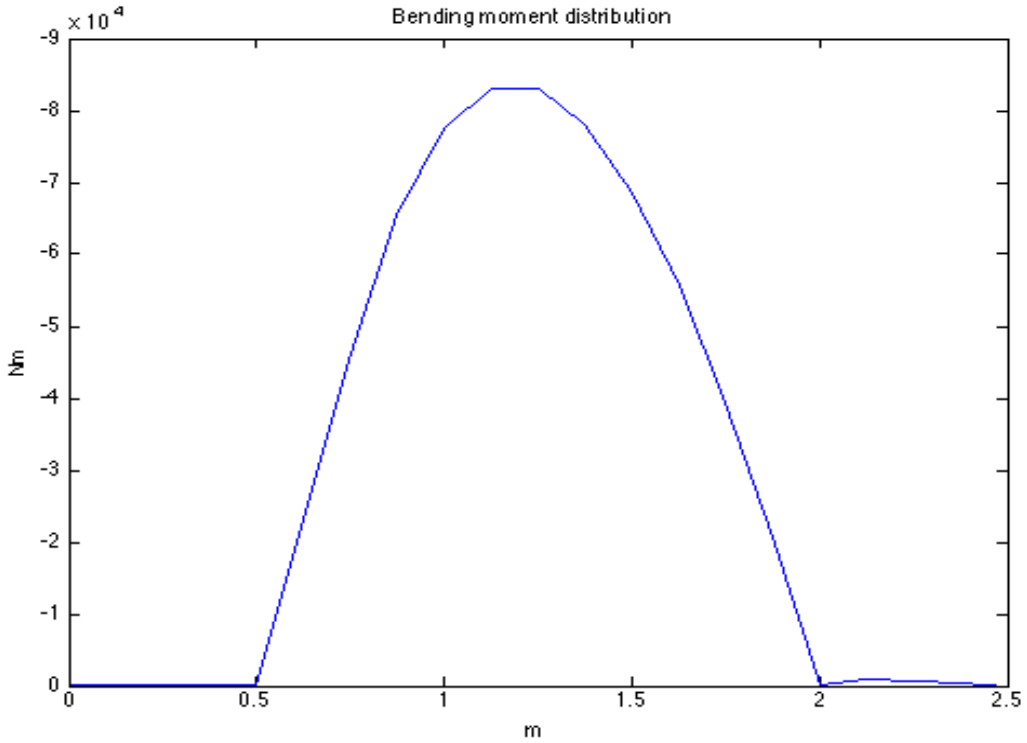

Figure 47 Bending moment distribution for case b) Single hanging with element support stiffness k=7.8 kN/mm

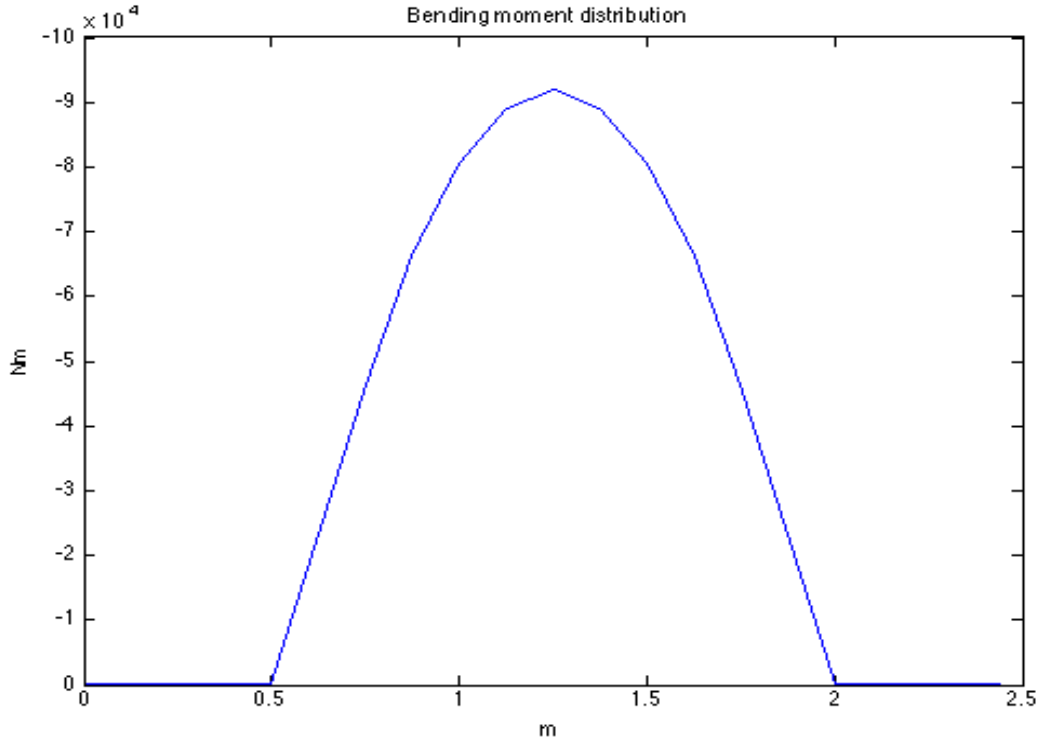

Figure 48 Bending moment distribution for case c) Double hanging with element support stiffness k=7.8 kN/mm

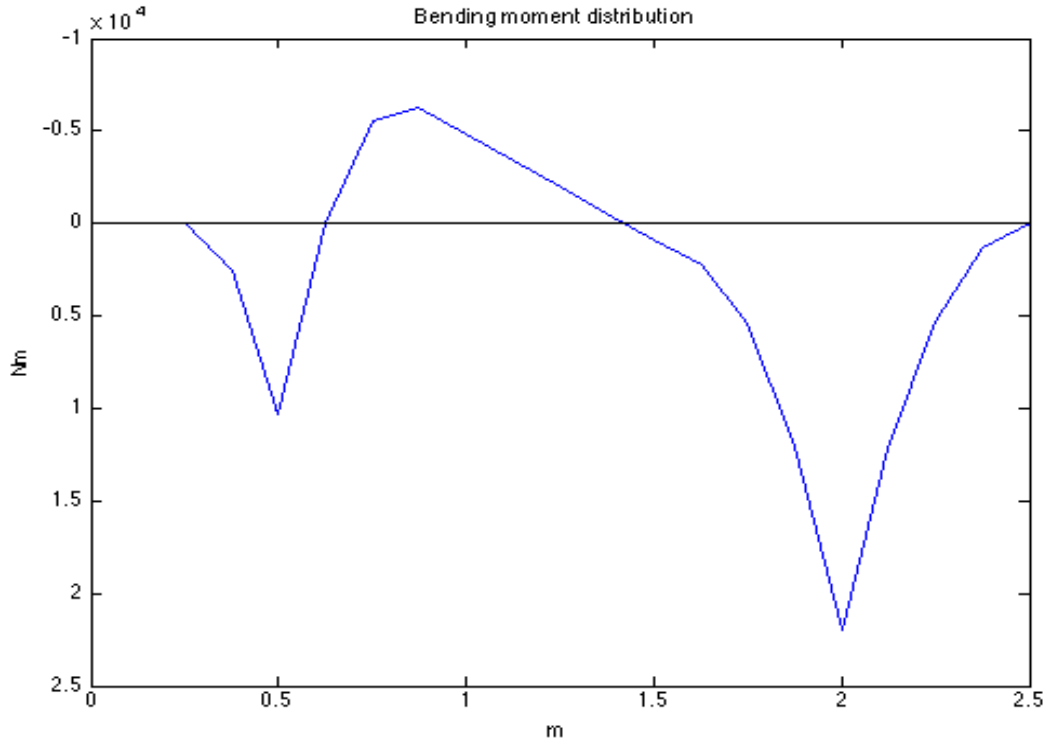

Figure 49 Bending moment distribution for case d) Side- central void with element support stiffness k=7.8 kN/mm

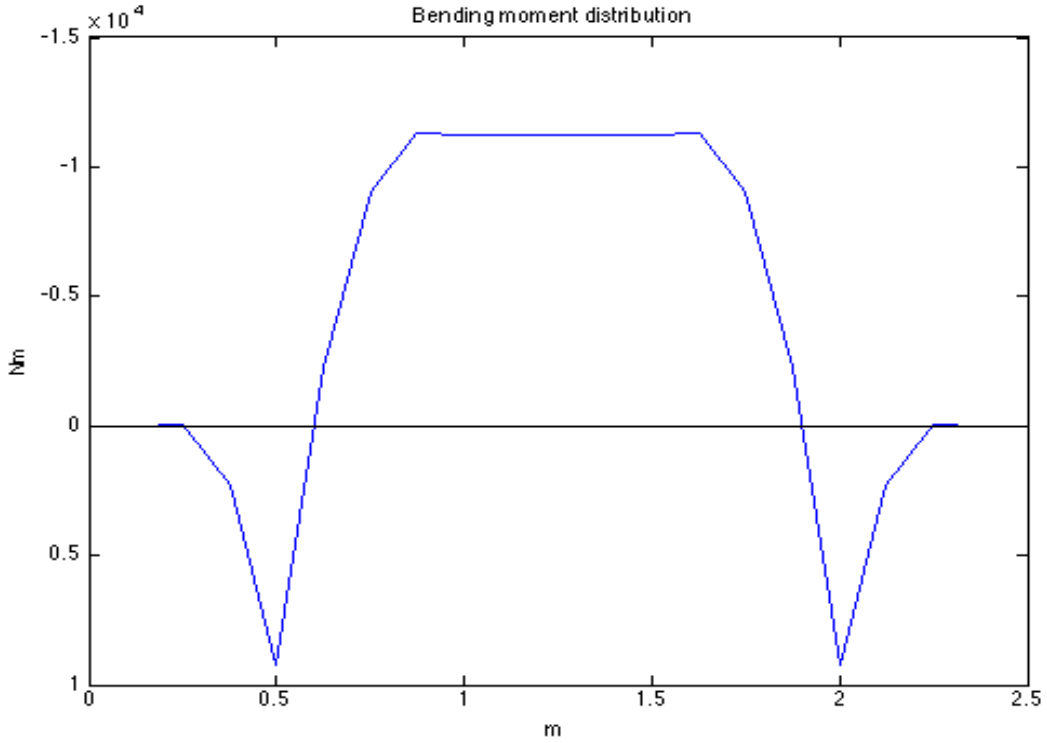

Figure 50 Bending moment distribution for case e) Double side- central void with element support stiffness k=7.8 kN/mm

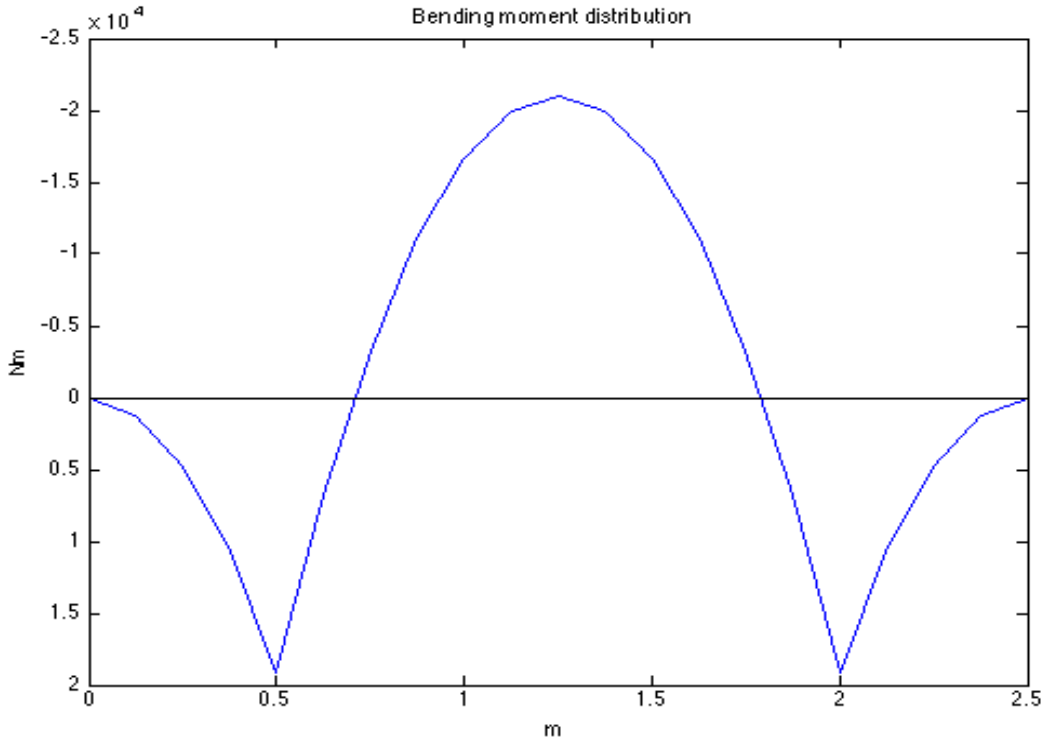

Figure 51 Bending moment distribution for case f) fully supported with element support stiffness k=7.8 kN/mm

Appendix 3 – MATLAB Bending moment and vertical displacement variation by stiffness (2D)

MATLAB Code

```
% Values

Q=25e3*9.81*1.5/2;          % 50% dynamical effect, [N]
L=2.5;                      % Length of a sleeper, [m]
E=40e9;                     % Pre-stressed concrete (uncracked cross-
                            % section), [Pa]
Le=L/20;                    % Length of one element, [m]
q=250/L*9.81;               % Characteristic load of sleeper, [N/m]
d=2400;                     % Density concrete [kg/m^3]


% Stiffness values [N/m]
s5=2*280e6/20;

% Cross-section variables

% Area for each element, [m^2]

A1=4.71e-2;
A2=A1;
A3=4.83e-2;
A4=A3;
A5=4.46e-2;
A6=A5;
A7=3.78e-2;
A8=A7;
A9=3.32e-2;
A10=A9;
A11=A9;
A12=A9;
A13=A7;
A14=A7;
A15=A5;
A16=A5;
A17=A3;
A18=A3;
A19=A1;
A20=A1;

% Moment of inertia for each element, [m^4]

I1=2.54e-4;
I2=I1;
I3=2.75e-4;
I4=I3;
I5=2.16e-4;
I6=I5;
I7=1.31e-4;
I8=I7;
I9=8.92e-5;
I10=I9;
I11=I9;
I12=I9;
I13=I7;
I14=I7;
I15=I5;
I16=I5;
I17=I3;
I18=I3;
```

```
I19=I1;
I20=I1;

% Calculates if the length of the element is short enough

if Le>4*(I9*E/s5)^(1/4);
    disp('Element length to long')
end

% Topology matrix

edof=[1 1 2 3 4 5 6
    2 4 5 6 7 8 9
    3 7 8 9 10 11 12
    4 10 11 12 13 14 15
    5 13 14 15 16 17 18
    6 16 17 18 19 20 21
    7 19 20 21 22 23 24
    8 22 23 24 25 26 27
    9 25 26 27 28 29 30
    10 28 29 30 31 32 33
    11 31 32 33 34 35 36
    12 34 35 36 37 38 39
    13 37 38 39 40 41 42
    14 40 41 42 43 44 45
    15 43 44 45 46 47 48
    16 46 47 48 49 50 51
    17 49 50 51 52 53 54
    18 52 53 54 55 56 57
    19 55 56 57 58 59 60
    20 58 59 60 61 62 63];

% Geometrical data

ex1=[0 Le];
ex2=[Le 2*Le];
ex3=[2*Le 3*Le];
ex4=[3*Le 4*Le];
ex5=[4*Le 5*Le];
ex6=[5*Le 6*Le];
ex7=[6*Le 7*Le];
ex8=[7*Le 8*Le];
ex9=[8*Le 9*Le];
ex10=[9*Le 10*Le];
ex11=[10*Le 11*Le];
ex12=[11*Le 12*Le];
ex13=[12*Le 13*Le];
ex14=[13*Le 14*Le];
ex15=[14*Le 15*Le];
ex16=[15*Le 16*Le];
ex17=[16*Le 17*Le];
ex18=[17*Le 18*Le];
ex19=[18*Le 19*Le];
ex20=[19*Le 20*Le];

% Assemble in to one matrix

ex=[ex1;ex2;ex3;ex4;ex5;ex6;ex7;ex8;ex9;ex10
    ex11;ex12;ex13;ex14;ex15;ex16;ex17;ex18;ex19;ex20];

ey=zeros(20,2);
```

```
% Distributed loads

eq=[0 -q];          % Load in negative y-direction

% Preallocate stiffness matrix, K, and load vector, f

K=zeros(63);
f=zeros(63,1);

% Define the position of the point loads

f(14)=f(14)-Q;
f(50)=f(50)-Q;

% Calculating displacements an bending moments for a decreasing stiffness

for s=0:4:28

% Spring stiffness for each element, [N/m]

k1=s5;
k2=s5;
k3=s5;
k4=s5;
k5=s5;
k6=s5;
k7=s5;
k8=s*10^6;
k9=s*10^6;
k10=s*10^6;
k11=s*10^6;
k12=s*10^6;
k13=s*10^6;
k14=s5;
k15=s5;
k16=s5;
k17=s5;
k18=s5;
k19=s5;
k20=s5;

% Element properties for each element

ep1=[E A1 I1 0 k1];
ep2=[E A2 I2 0 k2];
ep3=[E A3 I3 0 k3];
ep4=[E A4 I4 0 k4];
ep5=[E A5 I5 0 k5];
ep6=[E A6 I6 0 k6];
ep7=[E A7 I7 0 k7];
ep8=[E A8 I8 0 k8];
ep9=[E A9 I9 0 k9];
ep10=[E A10 I10 0 k10];
ep11=[E A11 I11 0 k11];
ep12=[E A12 I12 0 k12];
ep13=[E A13 I13 0 k13];
ep14=[E A14 I14 0 k14];
ep15=[E A15 I15 0 k15];
ep16=[E A16 I16 0 k16];
ep17=[E A17 I17 0 k17];
```

```
ep18=[E A18 I18 0 k18];
ep19=[E A19 I19 0 k19];
ep20=[E A20 I20 0 k20];

% Assemble data into one matrix

ep=[ep1;ep2;ep3;ep4;ep5;ep6;ep7;ep8;ep9;ep10
    ep11;ep12;ep13;ep14;ep15;ep16;ep17;ep18;ep19;ep20];

% Compute stiffness matrix, K, and load vector, f

for i=1:20;
    [Ke,fe]=beam2w(ex(i,:),ey(i,:),ep(i,:),eq);
    [K,f]=assem(edof(i,:),K,Ke,f,fe);
end

% Boundary conditions

bc=[1 0;4 0;7 0;10 0;13 0;16 0;19 0;22 0;25 0;28 0;31 0;34 0;37 0;40 0
    43 0;46 0;49 0;52 0;55 0;58 0;61 0];

% Compute displacements, a, and reaction forces, r

[a,r]=solveq(K,f,bc);

% Element displacements

ed=extract(edof,a);

% Compute section forces [N V M]

es=zeros(40,3);

for j=1:20
    ese=beam2ws(ex(j,:),ey(j,:),ep(j,:),ed(j,:),eq);
    es(j*2-1,:)=ese(1,:);
    es(j*2,:)=ese(2,:);
end

% Create a moment vector, M

M=es(:,3);

% Create x-vector

x=zeros(21,1);
x(2:21,1)=ex(:,2);

% Preallocate and create bending moment vector to plot

Mplot=zeros(21,1);

for k=1:19;
    Mplot(k+1,:)=M(2*k+1,:);

end

% Plot bending moment distribution
```

```
figure (1)
hold on
plot(x,Mplot)
set(gca,'YDir','reverse');
plot(linspace(0,2.5,1000),0,'k','LineWidth',2);
title('Bending moment distribution');
xlabel('m');
ylabel('Nm');

% Compute size and location of maximum displacement

for l=1:21
    a_vertical(l,1)=a(3*l-1,:);
end

% Plot vertical displacement

figure (2)
plot(x,a_vertical)
hold on
plot(linspace(0,2.5,1000),0,'k','LineWidth',2);
title('Vertical displacement');
xlabel('m');
ylabel('m');
axis([0 2.5 -0.0015 0.0005])

end
```

Figures

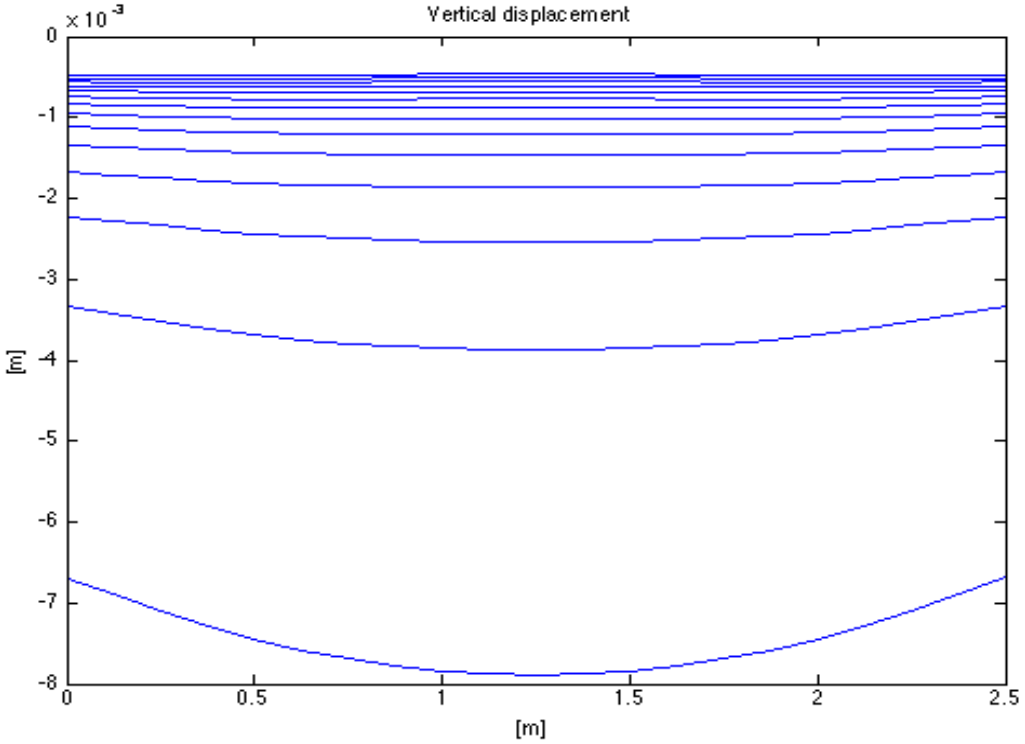

Figure 52 Vertical displacement variation for different stiffness values for Central Void to Full Support. Stiffness per element varies from 0-28 kN/mm with steps of 2 kN/mm

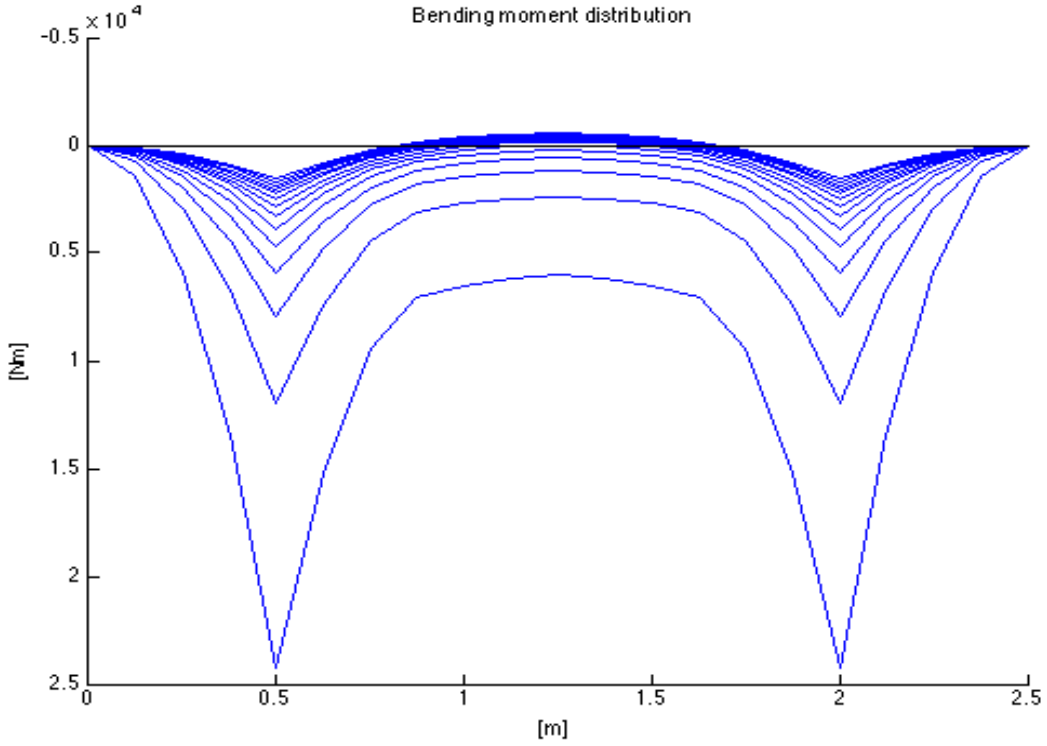

Figure 53 Bending moment variation for different stiffness for Central Void to Full Support. Stiffness per sleeper varies from 0-28 kN/mm with steps of 2 kN/mm. The lowest stiffness gives the highest bending moments.

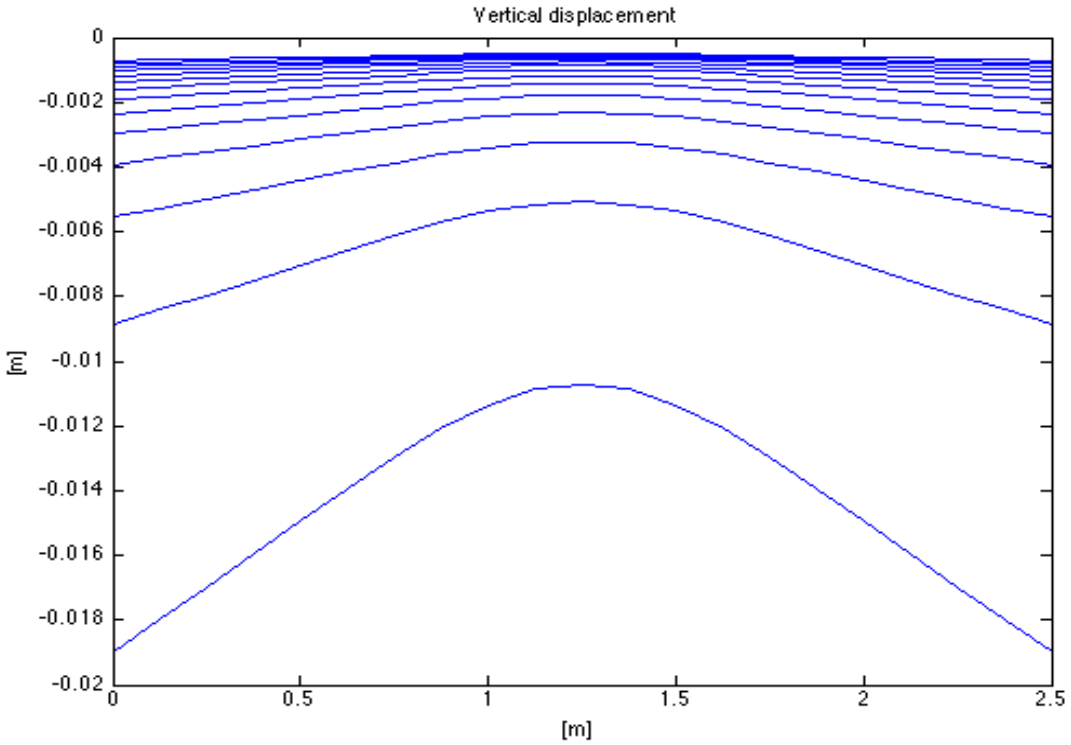

Figure 54 Vertical displacement variation for different stiffness values for Central Void to Full Support. Stiffness per sleeper varies from 0-28 kN/mm with steps of 2 kN/mm

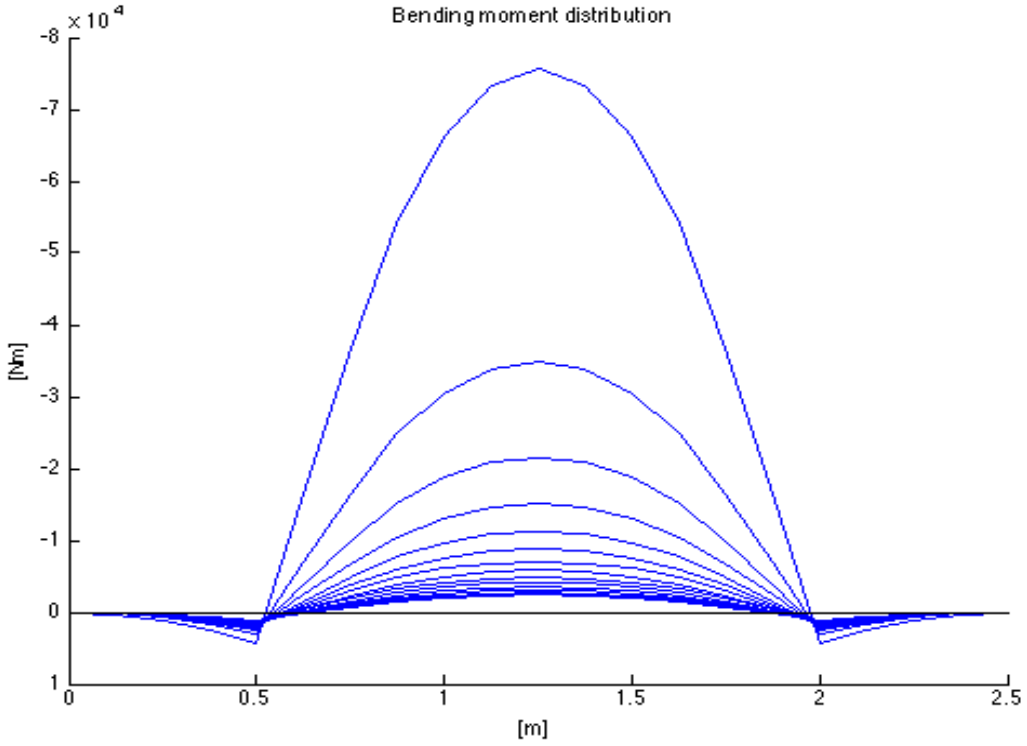

Figure 55 Bending moment variation for different stiffness for Double Hanging to Full Support. Stiffness per sleeper varies from 0-28 kN/mm with steps of 2 kN/mm. The lowest stiffness gives the highest bending moments.

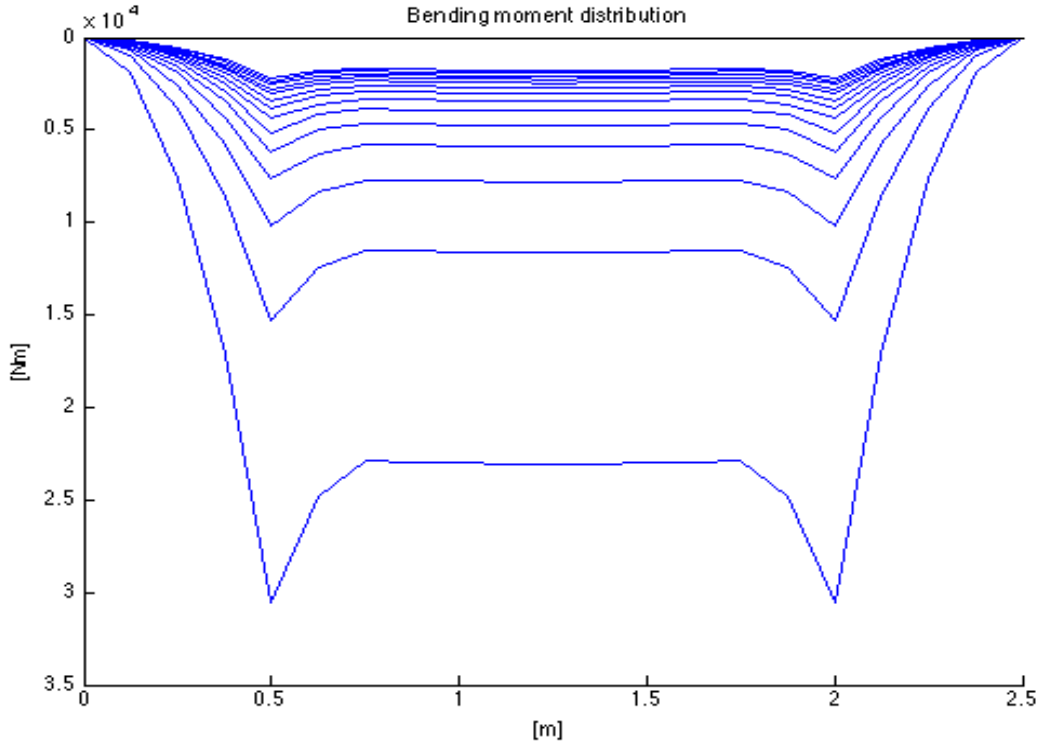

Figure 56 Bending moment distribution for central void with zero stiffness in the centre and declining stiffness at the sides of the sleeper. The lowest stiffness gives the highest bending moment.

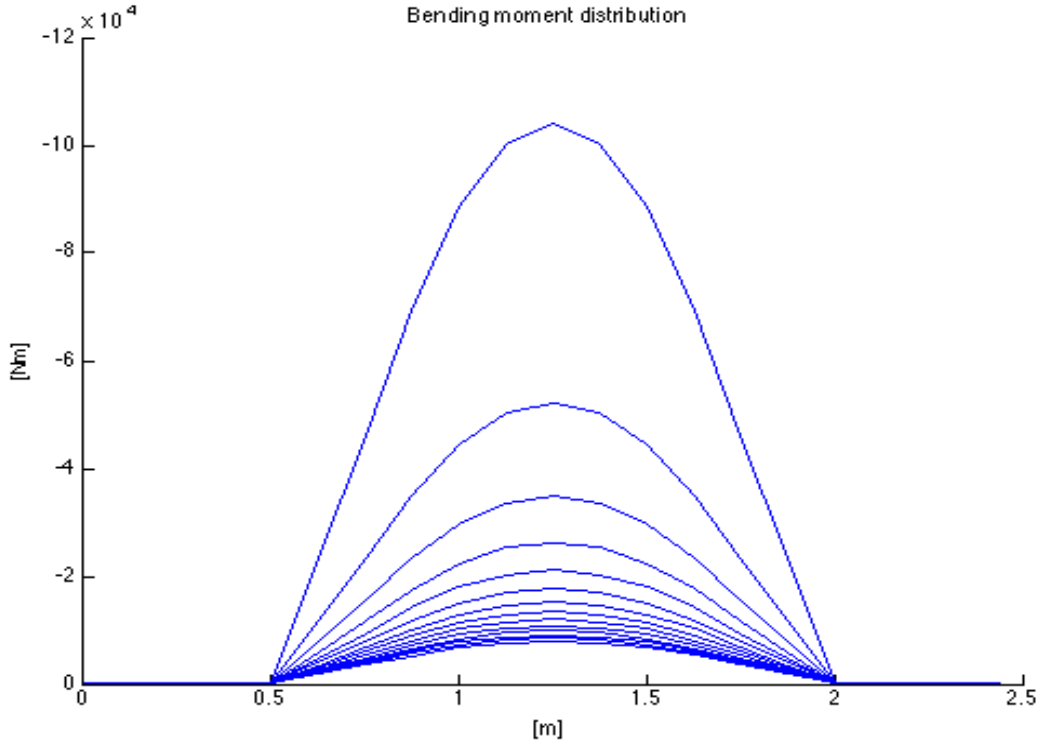

Figure 57 Bending moment distribution for double hanging with zero stiffness at the sides and declining stiffness at the centre of the sleeper. The lowest stiffness gives the highest bending moment.

Appendix 4 – MATLAB Bending moment variation by stiffness (3D)

MATLAB Code

```
% Values

Q=25e3*9.81*1.5/2;          % 50% dynamical effect, [N]
L=2.5;                      % Length of a sleeper, [m]
E=40e9;                     % Pre-stressed concrete (uncracked cross-
                            % section), [Pa]
Le=L/20;                    % Length of one element, [m]
q=250/L*9.81;               % Characteristic load of sleeper, [N/m]
d=2400;                     % Density concrete [kg/m^3]

% Stiffness values [N/m]
s5=2*280e6/20;
s1=2*280/20;

% Cross-section variables

% Area for each element, [m^2]

A1=4.71e-2;
A2=A1;
A3=4.83e-2;
A4=A3;
A5=4.46e-2;
A6=A5;
A7=3.78e-2;
A8=A7;
A9=3.32e-2;
A10=A9;
A11=A9;
A12=A9;
A13=A7;
A14=A7;
A15=A5;
A16=A5;
A17=A3;
A18=A3;
A19=A1;
A20=A1;

% Moment of inertia for each element, [m^4]

I1=2.54e-4;
I2=I1;
I3=2.75e-4;
I4=I3;
I5=2.16e-4;
I6=I5;
I7=1.31e-4;
I8=I7;
I9=8.92e-5;
I10=I9;
I11=I9;
I12=I9;
I13=I7;
I14=I7;
I15=I5;
I16=I5;
I17=I3;
I18=I3;
```

```
I19=I1;
I20=I1;

% Calculates if the length of the element is short enough

if Le>4*(I9*E/s5)^(1/4);
    disp('Element length to long')
end

% Topology matrix

edof=[1 1 2 3 4 5 6
    2 4 5 6 7 8 9
    3 7 8 9 10 11 12
    4 10 11 12 13 14 15
    5 13 14 15 16 17 18
    6 16 17 18 19 20 21
    7 19 20 21 22 23 24
    8 22 23 24 25 26 27
    9 25 26 27 28 29 30
    10 28 29 30 31 32 33
    11 31 32 33 34 35 36
    12 34 35 36 37 38 39
    13 37 38 39 40 41 42
    14 40 41 42 43 44 45
    15 43 44 45 46 47 48
    16 46 47 48 49 50 51
    17 49 50 51 52 53 54
    18 52 53 54 55 56 57
    19 55 56 57 58 59 60
    20 58 59 60 61 62 63];

% Geometrical data

ex1=[0 Le];
ex2=[Le 2*Le];
ex3=[2*Le 3*Le];
ex4=[3*Le 4*Le];
ex5=[4*Le 5*Le];
ex6=[5*Le 6*Le];
ex7=[6*Le 7*Le];
ex8=[7*Le 8*Le];
ex9=[8*Le 9*Le];
ex10=[9*Le 10*Le];
ex11=[10*Le 11*Le];
ex12=[11*Le 12*Le];
ex13=[12*Le 13*Le];
ex14=[13*Le 14*Le];
ex15=[14*Le 15*Le];
ex16=[15*Le 16*Le];
ex17=[16*Le 17*Le];
ex18=[17*Le 18*Le];
ex19=[18*Le 19*Le];
ex20=[19*Le 20*Le];

% Assemble in to one matrix

ex=[ex1;ex2;ex3;ex4;ex5;ex6;ex7;ex8;ex9;ex10
    ex11;ex12;ex13;ex14;ex15;ex16;ex17;ex18;ex19;ex20];

ey=zeros(20,2);
```

```
% Distributed loads

eq=[0 -q];          % Load in negative y-direction

% Preallocate stiffness matrix, K, and load vector, f

K=zeros(63);
f=zeros(63,1);

% Define the position of the point loads

f(14)=f(14)-Q;
f(50)=f(50)-Q;

% Preallocate bending moment matrix

Mmesh=zeros(21,28);

% Calculating displacements an bending moments for a decreasing stiffness

for s=1:1:28

% Spring stiffness for each element, [N/m]

k1=s*10^6;
k2=s*10^6;
k3=s*10^6;
k4=s*10^6;
k5=s*10^6;
k6=s*10^6;
k7=s*10^6;
k8=s*10^6;
k9=s*10^6;
k10=s*10^6;
k11=s*10^6;
k12=s*10^6;
k13=s*10^6;
k14=s*10^6;
k15=s*10^6;
k16=s*10^6;
k17=s*10^6;
k18=s*10^6;
k19=s*10^6;
k20=s*10^6;

% Element properties for each element

ep1=[E A1 I1 0 k1];
ep2=[E A2 I2 0 k2];
ep3=[E A3 I3 0 k3];
ep4=[E A4 I4 0 k4];
ep5=[E A5 I5 0 k5];
ep6=[E A6 I6 0 k6];
ep7=[E A7 I7 0 k7];
ep8=[E A8 I8 0 k8];
ep9=[E A9 I9 0 k9];
ep10=[E A10 I10 0 k10];
ep11=[E A11 I11 0 k11];
ep12=[E A12 I12 0 k12];
```

```
ep13=[E A13 I13 0 k13];
ep14=[E A14 I14 0 k14];
ep15=[E A15 I15 0 k15];
ep16=[E A16 I16 0 k16];
ep17=[E A17 I17 0 k17];
ep18=[E A18 I18 0 k18];
ep19=[E A19 I19 0 k19];
ep20=[E A20 I20 0 k20];

% Assemble data into one matrix

ep=[ep1;ep2;ep3;ep4;ep5;ep6;ep7;ep8;ep9;ep10
    ep11;ep12;ep13;ep14;ep15;ep16;ep17;ep18;ep19;ep20];

% Compute stiffness matrix, K, and load vector, f

for i=1:20;
    [Ke,fe]=beam2w(ex(i,:),ey(i,:),ep(i,:),eq);
    [K,f]=assem(edof(i,:),K,Ke,f,fe);
end

% Boundary conditions

bc=[1 0;4 0;7 0;10 0;13 0;16 0;19 0;22 0;25 0;28 0;31 0;34 0;37 0;40 0
    43 0;46 0;49 0;52 0;55 0;58 0;61 0];

% Compute displacements, a, and reaction forces, r

[a,r]=solveq(K,f,bc);

% Element displacements

ed=extract(edof,a);

% Compute section forces [N V M]

es=zeros(40,3);

for j=1:20
    ese=beam2ws(ex(j,:),ey(j,:),ep(j,:),ed(j,:),eq);
    es(j*2-1,:)=ese(1,:);
    es(j*2,:)=ese(2,:);
end

% Create a moment vector, M

M=es(:,3);

% Create x-vector

x=zeros(21,1);
x(2:21,1)=ex(:,2);

% Preallocate and create bending moment vector to plot

Mplot=zeros(21,1);

for k=1:19;
    Mplot(k+1,:)=M(2*k+1,:);
```

```
end

Mmesh(:,s+1)=Mplot;

end

k=(1:1:28);

figure (1)
mesh(k,x,Mmesh);
set(gca,'ZDir','reverse');
xlabel('Stiffness [N/m]','FontSize',12)
ylabel('Sleeper [m]','FontSize',12)
zlabel('Bending moment [Nm]','FontSize',12)
title('Bending moment variation by stiffness','FontSize',12)
```

Figures

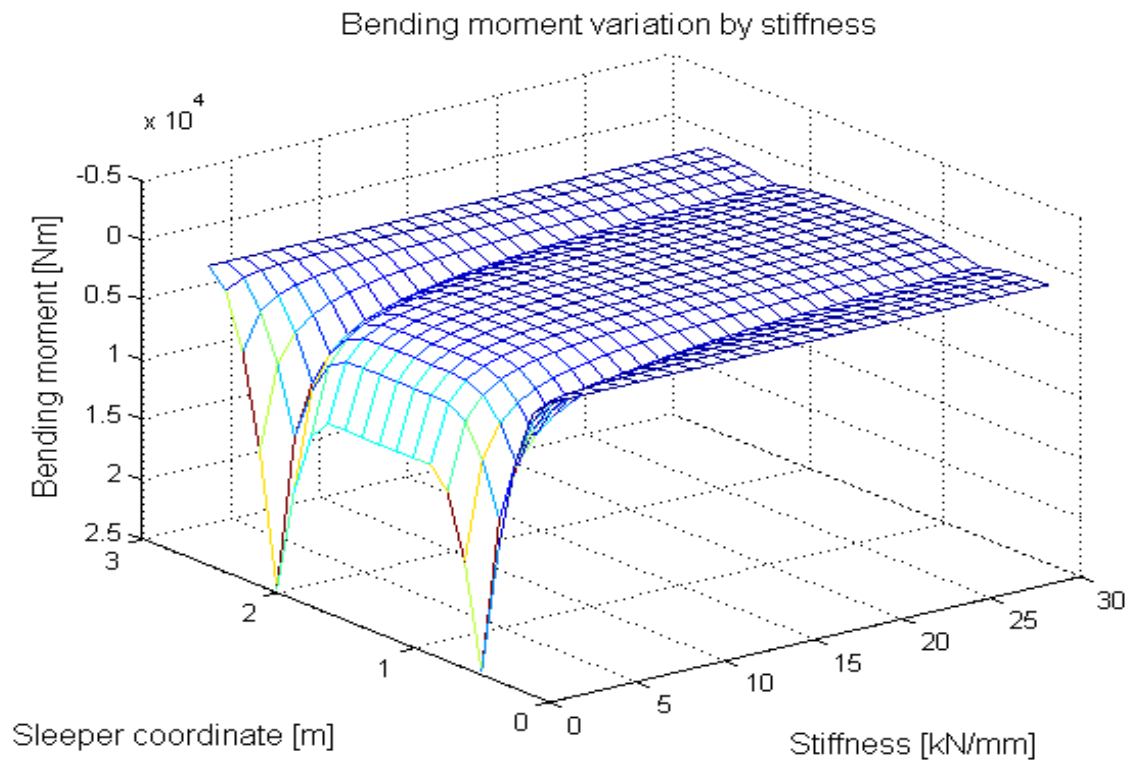

Figure 58 Bending moment variation by stiffness for Central Void to Full Support

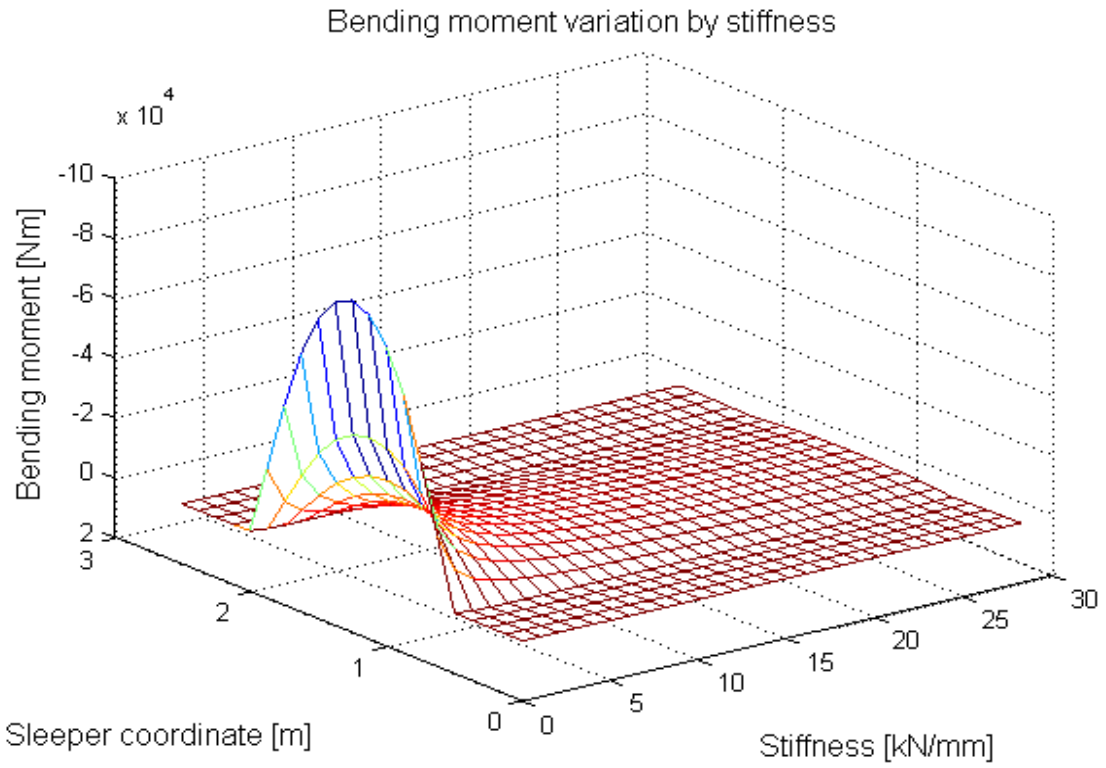

Figure 59 Bending moment variation by stiffness for Double Hanging to Full Support

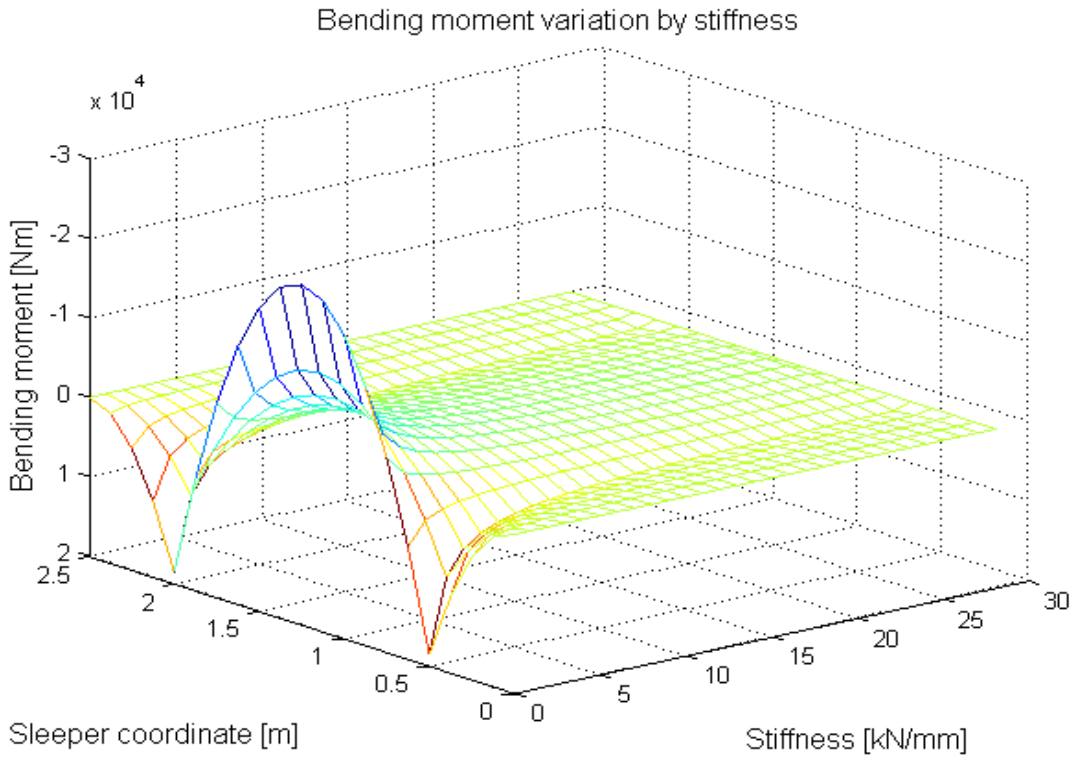

Figure 60 Bending moment variation by stiffness for Fully Hanging to Full Support

Appendix 5 – MATLAB Simulations of Eigenfrequencies

MATLAB Code

```
% Values

Q=25e3*9.81*1.5/2;          % 50% dynamical effect, [N]
L=2.5;                      % Length of a sleeper, [m]
E=40e9;                     % Pre-stressed concrete (uncracked cross-
                            % section), [Pa]
Le=L/20;                    % Length of one element, [m]
q=250/L*9.81;               % Characteristic load of sleeper, [N/m]
d=2400;                     % Density concrete [kg/m^3]


% Stiffness values [N/m]
s5=2*280e6/20;
s1=2*280/20;

% Cross-section variables

% Area for each element, [m^2]

A1=4.71e-2;
A2=A1;
A3=4.83e-2;
A4=A3;
A5=4.46e-2;
A6=A5;
A7=3.78e-2;
A8=A7;
A9=3.32e-2;
A10=A9;
A11=A9;
A12=A9;
A13=A7;
A14=A7;
A15=A5;
A16=A5;
A17=A3;
A18=A3;
A19=A1;
A20=A1;

% Moment of inertia for each element, [m^4]

I1=2.54e-4;
I2=I1;
I3=2.75e-4;
I4=I3;
I5=2.16e-4;
I6=I5;
I7=1.31e-4;
I8=I7;
I9=8.92e-5;
I10=I9;
I11=I9;
I12=I9;
I13=I7;
I14=I7;
I15=I5;
I16=I5;
I17=I3;
```

```
I18=I3;
I19=I1;
I20=I1;

% Calculates if the length of the element is short enough

if Le>4*(I9*E/s5)^(1/4);
    disp('Element length to long')
end

% Topology matrix

edof=[1 1 2 3 4 5 6
    2 4 5 6 7 8 9
    3 7 8 9 10 11 12
    4 10 11 12 13 14 15
    5 13 14 15 16 17 18
    6 16 17 18 19 20 21
    7 19 20 21 22 23 24
    8 22 23 24 25 26 27
    9 25 26 27 28 29 30
    10 28 29 30 31 32 33
    11 31 32 33 34 35 36
    12 34 35 36 37 38 39
    13 37 38 39 40 41 42
    14 40 41 42 43 44 45
    15 43 44 45 46 47 48
    16 46 47 48 49 50 51
    17 49 50 51 52 53 54
    18 52 53 54 55 56 57
    19 55 56 57 58 59 60
    20 58 59 60 61 62 63];

% Geometrical data

ex1=[0 Le];
ex2=[Le 2*Le];
ex3=[2*Le 3*Le];
ex4=[3*Le 4*Le];
ex5=[4*Le 5*Le];
ex6=[5*Le 6*Le];
ex7=[6*Le 7*Le];
ex8=[7*Le 8*Le];
ex9=[8*Le 9*Le];
ex10=[9*Le 10*Le];
ex11=[10*Le 11*Le];
ex12=[11*Le 12*Le];
ex13=[12*Le 13*Le];
ex14=[13*Le 14*Le];
ex15=[14*Le 15*Le];
ex16=[15*Le 16*Le];
ex17=[16*Le 17*Le];
ex18=[17*Le 18*Le];
ex19=[18*Le 19*Le];
ex20=[19*Le 20*Le];

% Assemble in to one matrix

ex=[ex1;ex2;ex3;ex4;ex5;ex6;ex7;ex8;ex9;ex10
    ex11;ex12;ex13;ex14;ex15;ex16;ex17;ex18;ex19;ex20];
```

```
ey=zeros(20,2);

% Distributed loads

eq=[0 -q];          % Load in negative y-direction

% Preallocate stiffness matrix, K, and load vector, f

K=zeros(63);
f=zeros(63,1);

% Define the position of the point loads

f(14)=f(14)-Q;
f(50)=f(50)-Q;

% Preallocate fr vector

eig_fr=zeros(29,1);

% Calculating displacements and bending moments for a decreasing stiffness


for s=0:1:28

% Spring stiffness for each element, [N/m]

k1=s*10^6;
k2=s*10^6;
k3=s*10^6;
k4=s*10^6;
k5=s*10^6;
k6=s*10^6;
k7=s*10^6;
k8=s1*10^6;
k9=s1*10^6;
k10=s1*10^6;
k11=s1*10^6;
k12=s1*10^6;
k13=s1*10^6;
k14=s*10^6;
k15=s*10^6;
k16=s*10^6;
k17=s*10^6;
k18=s*10^6;
k19=s*10^6;
k20=s*10^6;

% Element properties for each element

ep1=[E A1 I1 0 k1];
ep2=[E A2 I2 0 k2];
ep3=[E A3 I3 0 k3];
ep4=[E A4 I4 0 k4];
ep5=[E A5 I5 0 k5];
ep6=[E A6 I6 0 k6];
ep7=[E A7 I7 0 k7];
ep8=[E A8 I8 0 k8];
ep9=[E A9 I9 0 k9];
ep10=[E A10 I10 0 k10];
```

```
ep11=[E A11 I11 0 k11];
ep12=[E A12 I12 0 k12];
ep13=[E A13 I13 0 k13];
ep14=[E A14 I14 0 k14];
ep15=[E A15 I15 0 k15];
ep16=[E A16 I16 0 k16];
ep17=[E A17 I17 0 k17];
ep18=[E A18 I18 0 k18];
ep19=[E A19 I19 0 k19];
ep20=[E A20 I20 0 k20];

% Create mass matrix

m1=A1*d;
m2=A2*d;
m3=A3*d;
m4=A4*d;
m5=A5*d;
m6=A6*d;
m7=A7*d;
m8=A8*d;
m9=A9*d;
m10=A10*d;
m11=A11*d;
m12=A12*d;
m13=A13*d;
m14=A14*d;
m15=A15*d;
m16=A16*d;
m17=A17*d;
m18=A18*d;
m19=A19*d;
m20=A20*d;

epm1=[E A1 I1 m1];
epm2=[E A2 I2 m2];
epm3=[E A3 I3 m3];
epm4=[E A4 I4 m4];
epm5=[E A5 I5 m5];
epm6=[E A6 I6 m6];
epm7=[E A7 I7 m7];
epm8=[E A8 I8 m8];
epm9=[E A9 I9 m9];
epm10=[E A10 I10 m10];
epm11=[E A11 I11 m11];
epm12=[E A12 I12 m12];
epm13=[E A13 I13 m13];
epm14=[E A14 I14 m14];
epm15=[E A15 I15 m15];
epm16=[E A16 I16 m16];
epm17=[E A17 I17 m17];
epm18=[E A18 I18 m18];
epm19=[E A19 I19 m19];
epm20=[E A20 I20 m20];

epm=[epm1;epm2;epm3;epm4;epm5;epm6;epm7;epm8;epm9;epm10
    epm11;epm12;epm13;epm14;epm15;epm16;epm17;epm18;epm19;epm20];

% Assemble data into one matrix

ep=[ep1;ep2;ep3;ep4;ep5;ep6;ep7;ep8;ep9;ep10
    ep11;ep12;ep13;ep14;ep15;ep16;ep17;ep18;ep19;ep20];
```

```
% Compute stiffness matrix, K, and load vector, f

for i=1:20;
    [Ke,fe]=beam2w(ex(i,:),ey(i,:),ep(i,:),eq);
    [K,f]=assem(edof(i,:),K,Ke,f,fe);
end

% Boundary conditions

bc=[1 0;4 0;7 0;10 0;13 0;16 0;19 0;22 0;25 0;28 0;31 0;34 0;37 0;40 0
    43 0;46 0;49 0;52 0;55 0;58 0;61 0];


M=zeros(63);
Kem=zeros(63);

for i=1:20;
    [Kem,Me]=beam2d(ex(i,:),ey(i,:),epm(i,:));
    M=assem(edof(i,:),M,Me);
end


[Ev Eu]=eigen(K,M,bc(:,1));

% Calculate eigenfrequency for all nodes

fr=sqrt(Ev)/2/pi;


if fr(1)>10
    eig_fr(s/10+1)=fr(3);
else
    if fr(2)>10
    eig_fr(s/10+1)=fr(4);
    else
            if fr(3)>10
            eig_fr(s/10+1)=fr(5);
            else
            eig_fr(s/10+1)=fr(6);
            end
    end
end


end


% Display first eigenvalue

eig_fr

% Create stiffness vector to plot

s_plot=[0:1:28];

% Plot eigenvalues for each stiffness

plot(s_plot',eig_fr)
```

```
hold on
title('Third eigenfrequency variation by stiffness','FontSize',20);
xlabel('k [N/m]','FontSize',20);
ylabel('f [Hz]','FontSize',20);
```

Figures

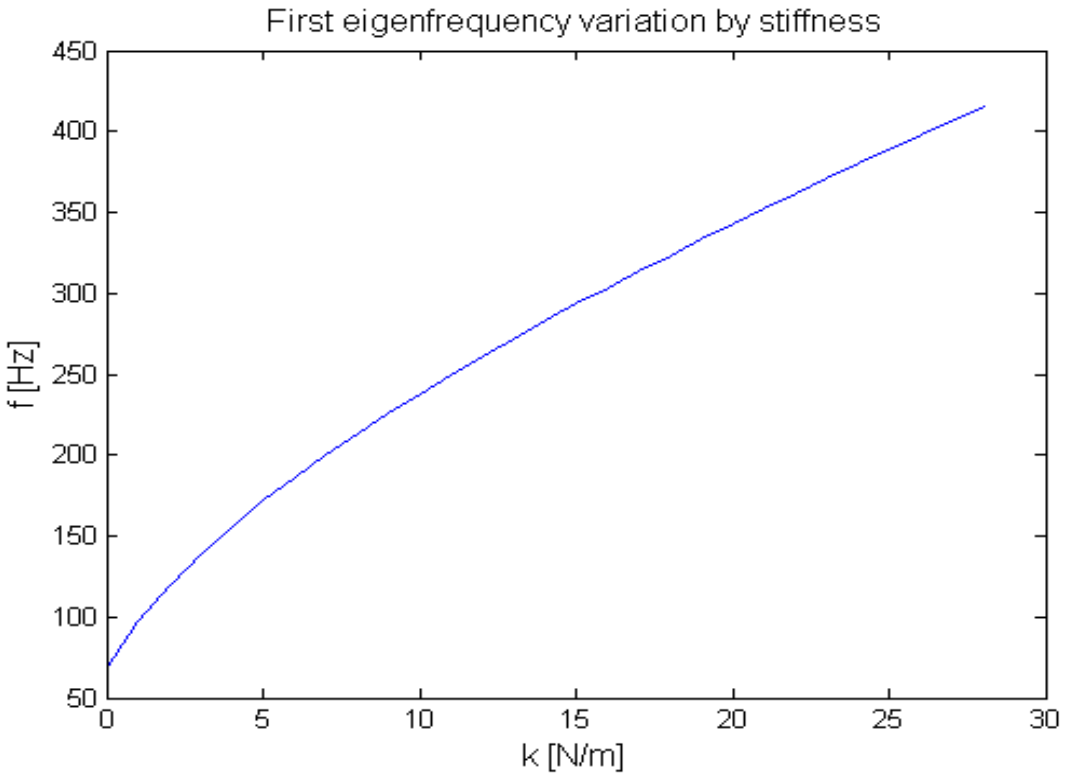

Figure 61 First eigenfrequency variation by stiffness for Central Void to Full Support

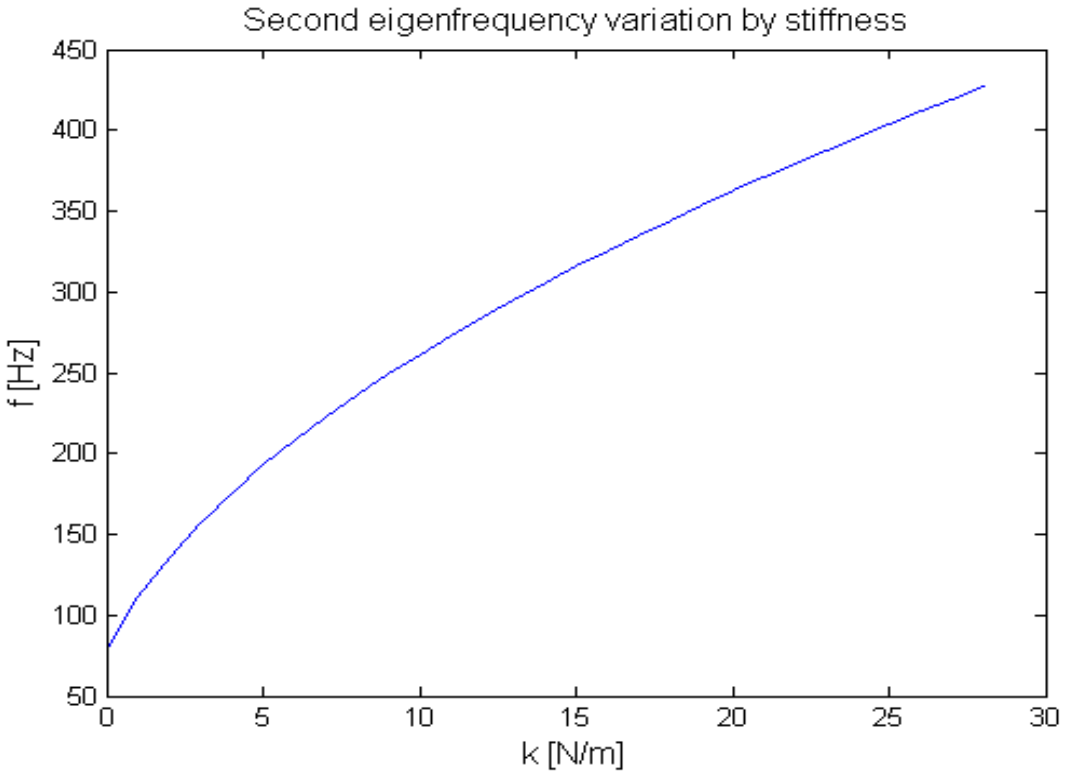

Figure 62 Second eigenfrequency variation by stiffness for Central Void to Full Support

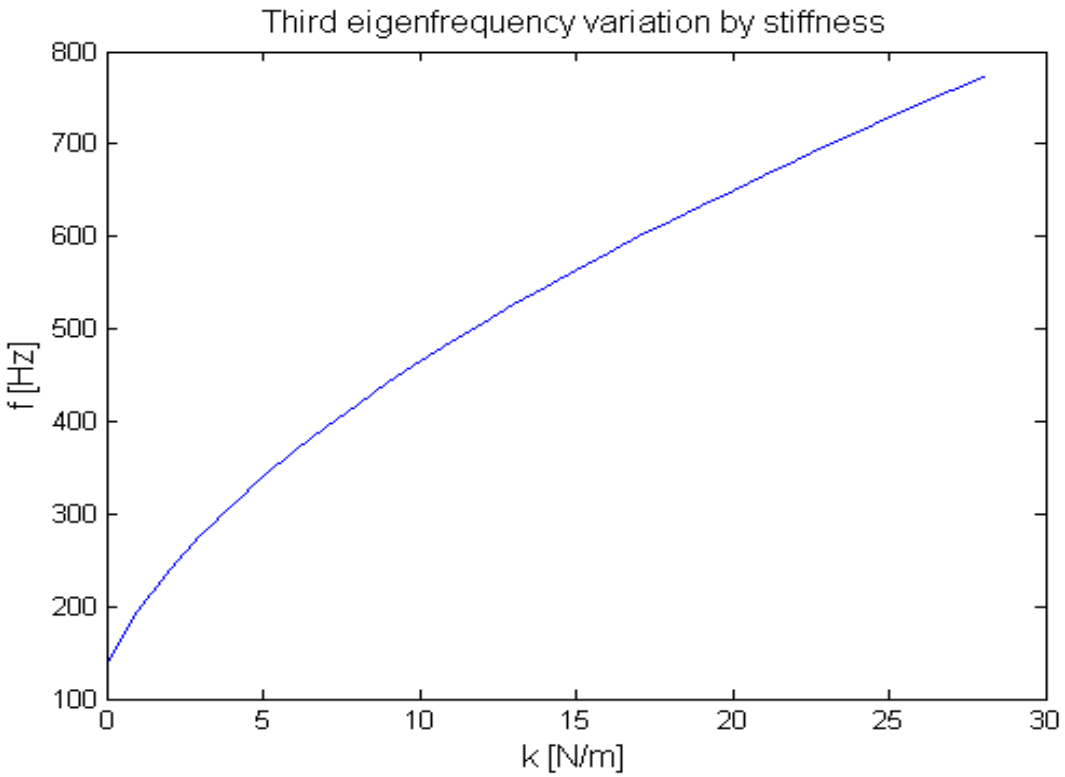

Figure 63 Third eigenfrequency variation by stiffness for Central Void to Full Support

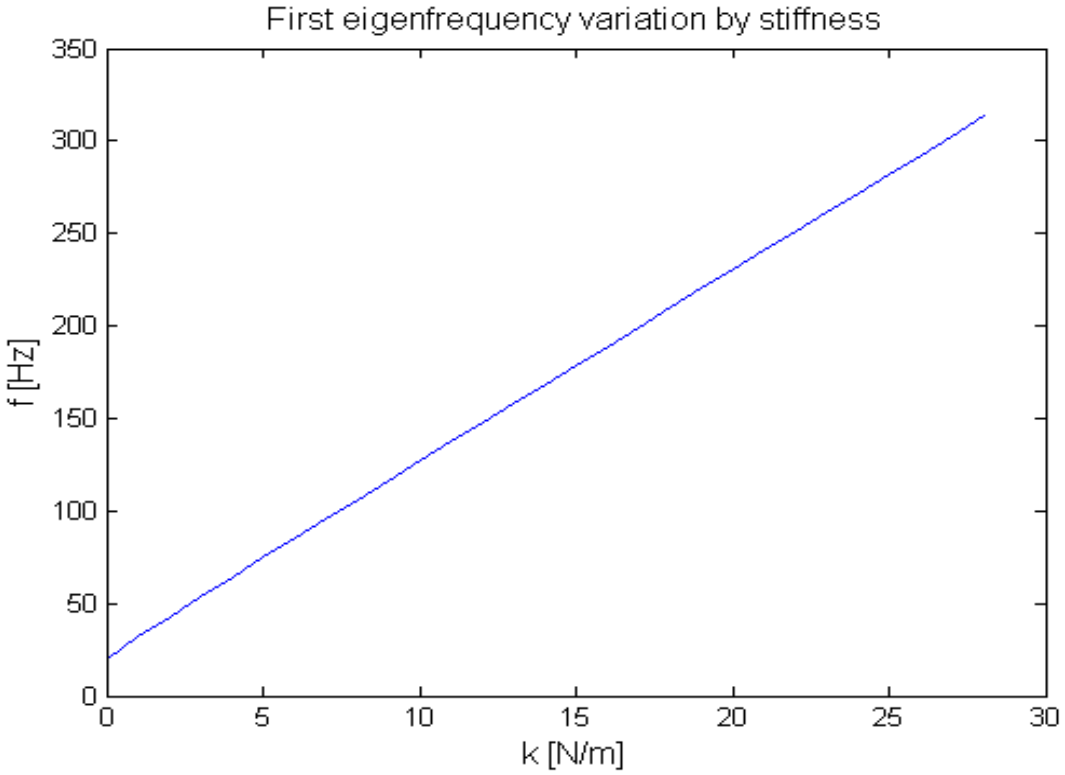

Figure 64 First eigenfrequency variation by stiffness for Double Hanging to Full Support

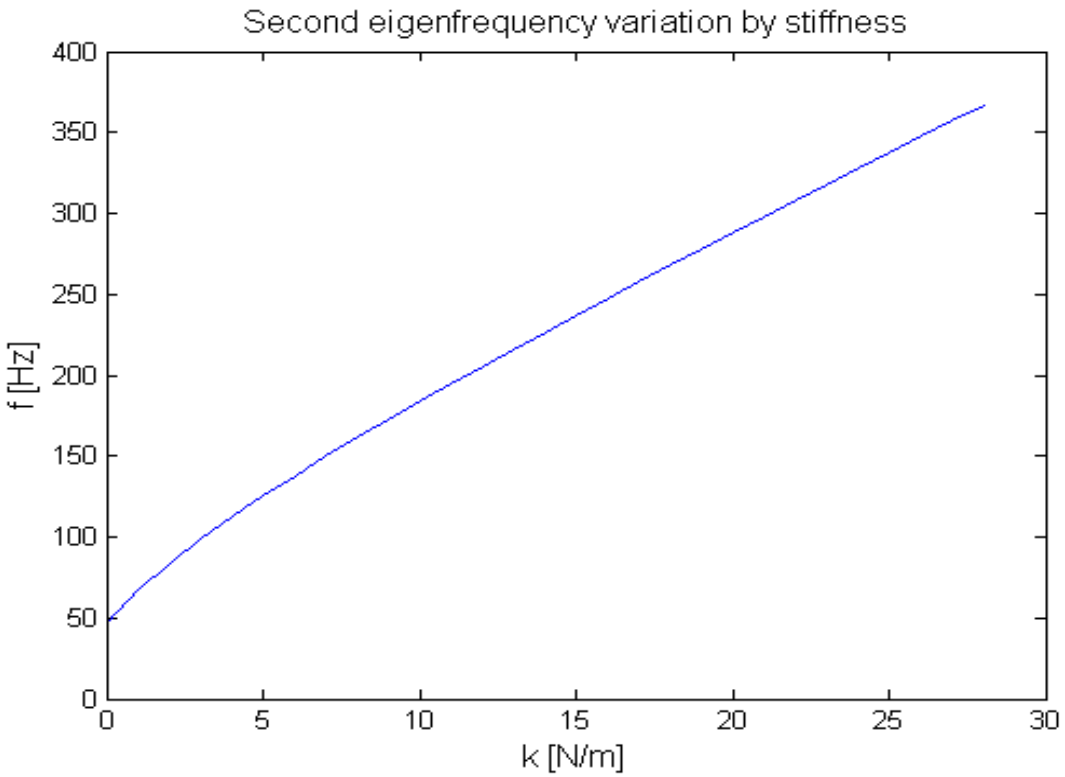

Figure 65 Second eigenfrequency variation by stiffness for Double Hanging to Full Support

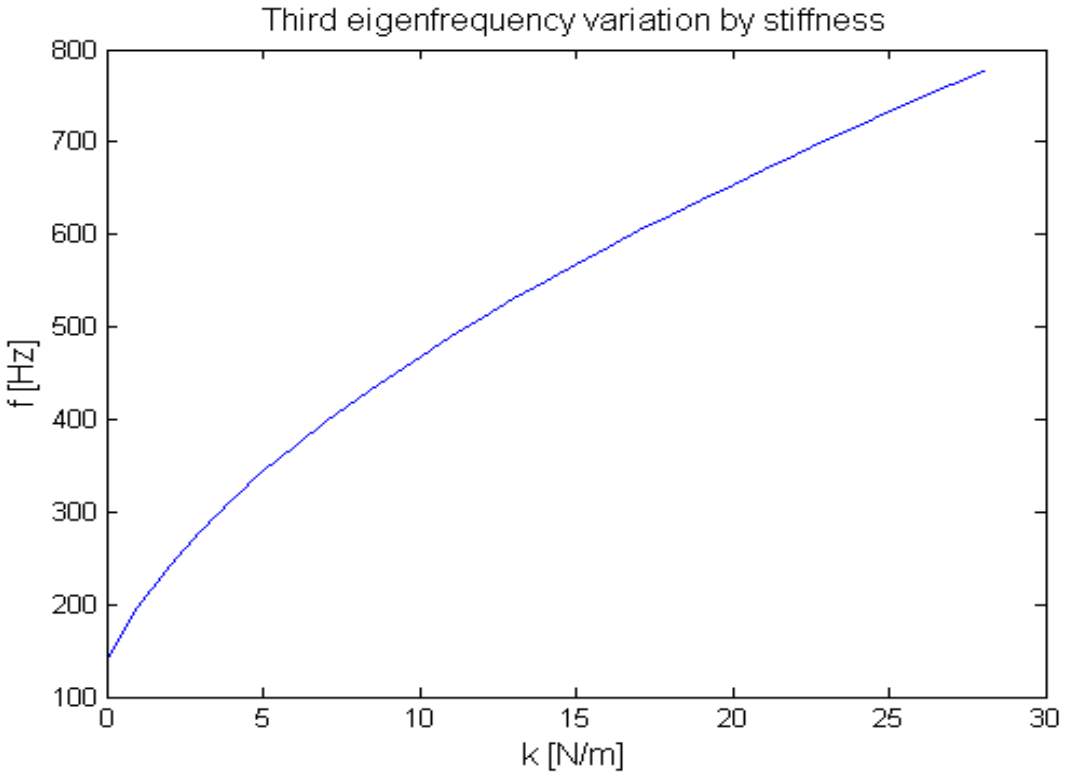

Figure 66 Third eigenfrequency variation by stiffness for Double Hanging to Full Support

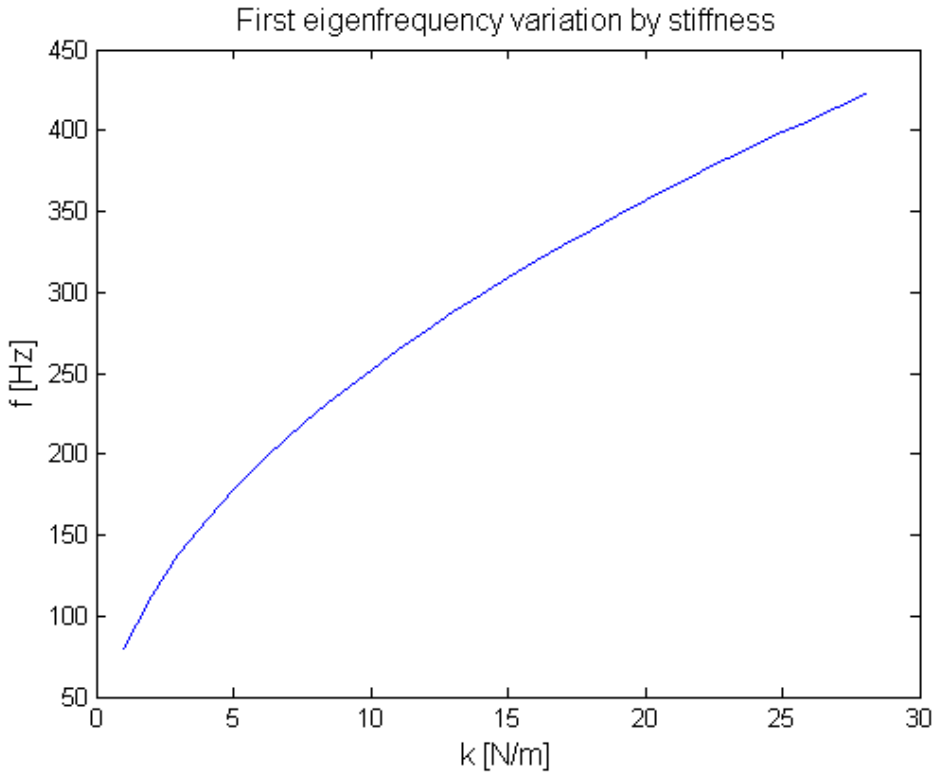

Figure 67 Variation in the eigenfrequency of the first bending mode as the stiffness of all elements goes from 1 to 28 kN/mm

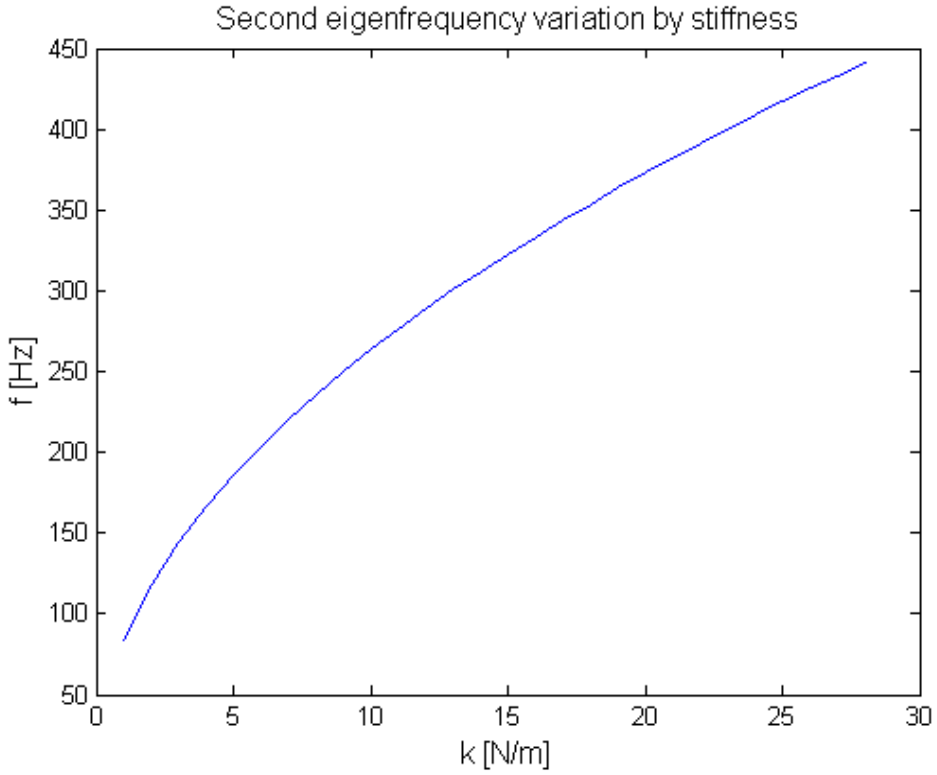

Figure 68 Variation in the eigenfrequency of the second bending mode as the stiffness of all elements goes from 1 to 28 kN/mm

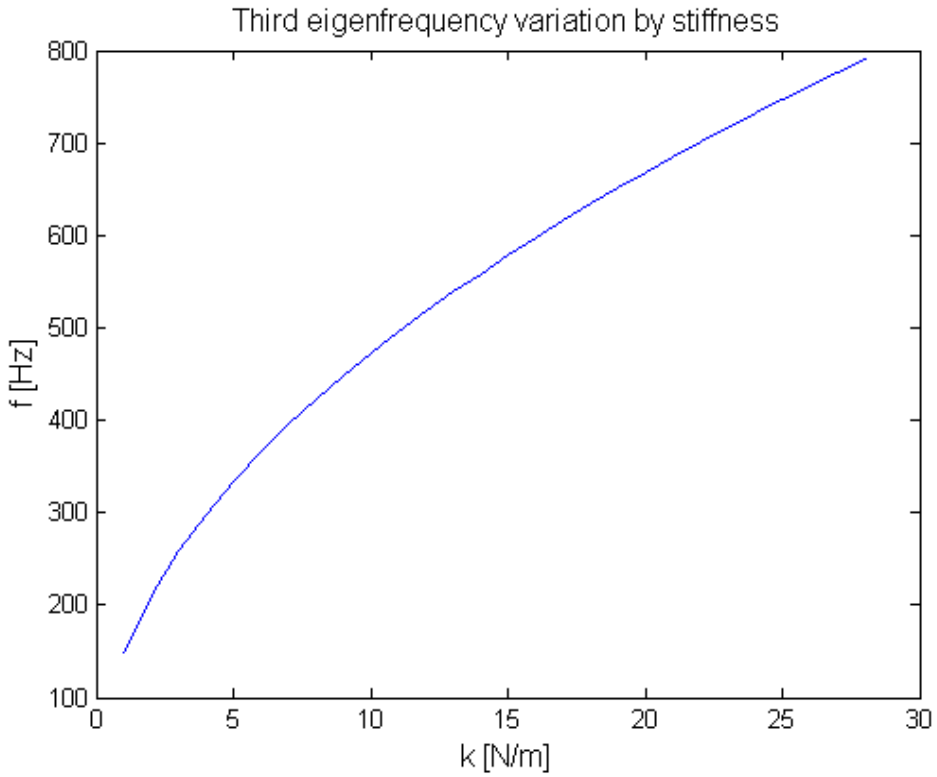

Figure 69 Variation in the eigenfrequency of the third bending mode as the stiffness of all elements goes from 1 to 28 kN/mm